Lawrence Berkeley National Laboratory

Lawrence Berkeley National Laboratory

Title

Development of a database for prompt gamma-ray neutron activation analysis: Summary report
of the third research coordination meeting

Permalink

https://escholarship.org/uc/item/65h613zr

Authors

Lindstrom, Richard M.
Firestone, Richard B.
Pavi, ???

Publication Date

2003-04-01

I N D C INTERNATIONAL NUCLEAR DATA COMMITTEE

Development of a Database for Prompt γ-ray Neutron Activation Analysis

Summary Report of the Third Research Coordination Meeting

IAEA Headquarters
Vienna, Austria
24 to 26 March 2003

Prepared by

Richard M. Lindstrom*, Richard B. Firestone** and R. Paviotti-Corcuera

* National Institute of Standards and Technology, Gaithersburg, MD, USA

**Lawrence Berkeley National Laboratory, Berkeley, CA, USA

April 2003

Development of a Database for Prompt γ-ray Neutron Activation Analysis

Summary Report of the Third Research Coordination Meeting

IAEA Headquarters
Vienna, Austria
24 to 26 March 2003

Prepared by

Richard M. Lindstrom*, Richard B. Firestone** and R. Paviotti-Corcuera

* National Institute of Standards and Technology, Gaithersburg, MD, USA
**Lawrence Berkeley National Laboratory, Berkeley, CA, USA

Abstract

The main discussions and conclusions from the Third Co-ordination Meeting on the Development of a Database for Prompt γ-ray Neutron Activation Analysis are summarised in this report. All results were reviewed in detail, and the final version of the TECDOC and the corresponding software were agreed upon and approved for preparation. Actions were formulated with the aim of completing the final version of the TECDOC and associated software by May 2003.

April 2003

Table of Contents

1. SUMMARY OF THE MEETING

1.1. Objectives

The Third Research Co-ordination Meeting (RCM) on Development of a Database for Prompt γ-ray Neutron Activation Analysis was held at the IAEA Headquarters in Vienna, Austria, from 24 to 26 March 2003. The primary purpose of this meeting was to review the results achieved in the development of the database, and to approve the final version of the TECDOC and corresponding software.

H.-D. Choi of the Seoul National University (R. Korea) was elected Chairman of the meeting; R.B. Firestone (LBNL, USA) and R.M. Lindstrom (NIST, USA) agreed to act as rapporteurs. The approved Agenda is attached (see Appendix 1). Other participating laboratories were represented by N. Canh Hai (VAEC, Vietnam), G.L. Molnár (CRC, Hungary), S.F. Mughabghab (BNL, USA) and C. Zhou (CNDC, P.R. China). Appendix 2 lists all of the participants attending the RCM, including their affiliations.

Alan Nichols (Head, IAEA Nuclear Data Section) welcomed the participants, and emphasized the significance of their role in the development and production of this improved database for the worldwide use and benefit of all Member States. The quality and credibility of the resulting database for subsequent adoption in conjunction with an extremely important analytical technique would be heavily dependent on their good efforts. R. Paviotti-Corcuera (Scientific Secretary of the RCM) summarized the status of the CRP and the purpose of the meeting (see Appendix 3).

Contributions to the meeting by various CRP participants are included in Appendix 4.

1.2. Discussions

The participants reviewed draft versions of the TECDOC and CD-ROM that are the primary products of the CRP. Modifications and corrections were made, and some additional contributions will be completed within the next two weeks and communicated to the Scientific Secretary for inclusion into the TECDOC. Changes were introduced to better reflect the actual results of the CRP, and to maintain consistency between the formulae and tables in the different chapters.

The responsibilities for the individual sections are as follows:

- Chapters 1, 2, 3, 4 and 8 are the overall responsibility of R. Paviotti-Corcuera;

- Table of definitions will be provided by H.-D. Choi for insertion after the list of Contents;

- List of acronyms will be supplied by R.M. Lindstrom, and will be inserted into Chapter 1;

- Chapter 2: Mughabghab table of resonance energies will be scanned and entered as Table 4 by R. Paviotti-Corcuera; H.-D. Choi will produce equations to be consistent with the table of definitions;

- Chapter 3: Table 5 to be added that compares k_0 factors obtained by the participants with other published data; this table will also have an explanatory text to be written as Section 3.6 by G.L. Molnár (his original table 2), and sent to R. Paviotti-Corcuera;

- Chapter 4: R.M. Lindstrom will number the equations, and will also provide table of comparative results from the analysis of the "unknown" test sample;

- Chapter 5: isotope-specific table with recommended data will be modified by R.B. Firestone and transferred to Chapter 7; table of inferred neutron binding energies and capture cross sections has been provided by G.L. Molnár (his original table 4) with associated text, and will be inserted into this chapter by R.B. Firestone;

- Chapter 6: R.B. Firestone will be responsible for modifications to this chapter - move the decay data table to Chapter 7, include a complete table of Budapest data (not available elsewhere), Table I in Chapter 5 will be moved to Chapter 6, and specific Budapest data will constitute an appendix to this table;

- Chapter 7: R.B. Firestone will be responsible for modifications to this chapter. Several tables are to be transferred to this chapter, and the headings will be modified to conform to the table of definitions;

- Chapter 8: description of the contents of the CD-ROM is the responsibility of R. Paviotti-Corcuera, with input from V. Zerkin and R.B. Firestone. R.B. Firestone will also collect useful Web links to include in the CD-ROM.

Current versions of both the TECDOC and CD-ROM will be made available by R. Paviotti-Corcuera on the IAEA web site as soon as the above additions and modifications are received and incorporated into both products. Participants will be expected to make their final comments to R. Paviotti-Corcuera and V. Zerkin within two weeks of being notified of their availability.

All contributions submitted to this RCM are included as appendices to this report.

2. CONCLUSIONS

An important outcome of the CRP is the determination of numerous Total Cross Sections from the sum of primary and/or ground state gamma-ray intensities. Surprising anomalies were found for ^{6}Li, ^{12}C and a limited number of other isotopes, while numerous confirmations of previous measurements were also observed. The IAEA-NDS should ensure that future CRPs incorporate these data into the thermal cross section data files (as recommended by R.B. Firestone).

Future updates to the PGAA database should be transmitted to the IAEA-NDS for further distribution both electronically and as INDC publications (R.B. Firestone).

A highly suitable topic for a future CRP would be "Averaged resonance capture gamma-ray intensities from individual resonances and filtered neutron beams". This topic is related to photon strength functions (S.F. Mughabghab).

The amount and completeness of the data tables prepared during the course of this CRP is impressive when compared to what was available before. There can be no doubt that these new data will extend to other areas of application and introduce fundamental changes to the traditional approaches previously adopted in PGAA. Scientists who specialise in gamma-ray and elemental analyses need to be made fully aware of the comprehensive contents of the resulting CRP database, whose satisfactory adoption and application represents further challenges in PGAA (H.-D. Choi and R. Paviotti-Corcuera). The question of the publication of this database in a scientific journal as suggested at the first RCM is deferred to a later date (R.M. Lindstrom).

APPENDICES

Appendix 1: Agenda

International Atomic Energy Agency
Third Research Co-ordination Meeting on
"Development of a Database for Prompt Gamma-ray Neutron Activation Analysis"

IAEA Headquarters, Vienna, Austria
24 to 26 March 2003

Meeting Room F 0125

AGENDA

Monday, 24 March

08:30 - 09:20   **Registration** (IAEA Registration desk, Gate 1)

09:30 - 10:30   **Opening Session**

Opening (A.L. Nichols, Head of the IAEA Nuclear Data Section)
Election of Chairman and Rapporteur
Discussion and Adoption of Agenda (Chairman)
Status of CRP - emphasis on the products (R. Paviotti–Corcuera, Scientific Secretary, IAEA/NDS)

10:30 - 10:45   **Coffee break**

10:45 - 12:35   **Session 1: Preparation of TECDOC**

1   INTRODUCTION: AN OVERVIEW OF DEVELOPMENT AND PGAA APPLICATIONS (R.M. Lindstrom).
2   NOMENCLATURES, NEUTRON SPECTRAL SHAPE DEPENDENT FORMULISM (H.-D. Choi and A. Trkov)

12:35 - 14:35   **Lunch and Administrative/Financial Matters Related to Participants**

14:35 - 17:00   **Session 1: Preparation of TECDOC (cont.)**

3   CHARACTERISTICS OF PGAA FACILITIES (H.-D. Choi).
4   BENCHMARKS AND REFERENCE MATERIALS (R.M. Lindstrom).
5   ISOTOPIC DATA: THERMAL NEUTRON CROSS SECTIONS, AND ATOMIC MASSES (R.B. Firestone).
6   EVALUATION METHODOLOGY (R.B. Firestone).

(Coffee break intervals as appropriate)

17:30   **Reception – A23 corridor**

Tuesday, 25 March

09:00 - 10:00   Session 1: Preparation of TECDOC (cont.)

  7 ADOPTED DATABASE AND USER TABLES (R.B. Firestone).
  8 RETRIEVAL SYSTEM (V. Zerkin and R.B. Firestone).

 10:00 - 18:00   Session 2:

  Database on CD-ROM (Demo) V. Zerkin
  Database on the Web NDS/IAEA V. Zerkin
  Contents of CD-ROM (information about the CRP, PGAA-IAEA database Viewer,
  database retrieval system, TECDOC, INDC report of Said, PGAA Database Files
  (other databases), PGAA Database Evaluation
  New Prompt Gamma-ray Data, G.L. Molnár
  Determination of the prompt k_0-factors for B, N, Si,, P and S, H.-D. Choi

  (Lunch and coffee break intervals as appropriate)

Wednesday, 26 March

09:00 - 18:00   Concluding Session: Approval of TECDOC and Meeting Report

  (Lunch and coffee break intervals as appropriate)

Appendix 2: Participants

International Atomic Energy Agency
Third Research Co-ordination Meeting on
"Development of a Database for Prompt Gamma-ray Neutron Activation Analysis"

IAEA Headquarters, Vienna, Austria
24 - 26 March 2003
Meeting Room F 0125

LIST OF PARTICIPANTS

CHINA
Mr. C. Zhou
China Nuclear Data Centre
China Institute of Atomic Energy
P.O. Box 275 (41)
102413 – Beijing
Tel: +86 10 6935 7830
Fax: +86 10 6935 7008
E-mail: zcm@iris.ciae.ac.cn

HUNGARY
Mr. G.L. Molnar
Department of Nuclear Research
Institute of Isotope and
Surface Chemistry
Chemical Research Centre, P.O. Box 77
Budapest H-1525
Tel: +36 1 3922 539
Fax: +36 1 3922 584
E-mail: molnar@alpha0.iki.kfki.hu

KOREA
Mr. H.-D. Choi
Department of Nuclear Engineering
Seoul National University
Seoul 151-742
Tel: +82 2 880 7205
Fax: +82 2 889 2688
E-mail: choihdg@snu.ac.kr

USA
Mr. R.B. Firestone
Isotopes Project, MS 88R0192
Lawrence Berkeley National Laboratory,
University of California,
1 Cyclotron Road,Berkeley, CA 94720
Tel: +1 510 486 7646
Fax: +1 510 486 5757
E-mail: rbf@lbl.gov

USA
Mr. R.M. Lindstrom
Analytical Chemistry Division
National Institute of Stanards and
Technology, Stop 8395
Gaithersburg - MD 20899
Tel: +1 301 975 6281
Fax: +1 301 208 9279
E-mail: richard.lindstrom@nist.gov

USA
Mr. S.F. Mughabghab
Building 197 D
Energy Technology Division
Brookhaven National Laboratory
P.O. Box 5000
Upton, NY 11973-5000
Tel: +1 531 344 5085
Fax: +1 531 344 3021
E-mail: mugabgab@bnl.gov

VIETNAM
Mr. Nguyen Canh Hai
Department of Nuclear Physics and
Techniques, Nuclear Research Institute
1 Nguyen Tu Luc, Dalat
Tel: +84 63 829 436
Fax: +84 63 821 107
E-mail: chai@hcm.vnn.vn

IAEA

Ms. R. Paviotti-Corcuera
Scientific Secretary
Nuclear Data Section
Division of Physical and
Chemical Sciences
Room A2319
Tel: +43 1 2600. ext. 21708
Fax: +43 1 26007
E-mail: R.Paviotti-Corcuera@iaea.org

Mr. A. Nichols
Head, Nuclear Data Section
Division of Physical and Chemical
Sciences
Room A2312
Tel: +43 1 2600 ext. 21709
Fax: +43 1 26007
E-mail: A.Nichols@iaea.org

Mr. A. Trkov
Deputy Head
Nuclear Data Section
Division of Physical and Chemical
Sciences
Room A2316
Tel: +43 1 2600 ext: 21712
Fax: +43 1 26007
E-mail: A.Trkov@iaea.org

Mr. V. Zerkin
Nuclear Data Section
Division of Physical and Chemical
Sciences
Room A2318
Tel: +43 1 2600 21714
Fax: +43 1 26007
E-mail: V.Zerkin@iaea.org

Appendix 3: Actions and Status

STATUS OF ACTIVITIES

(FEBRUARY 2003)

Deadlines (as agreed CRM in June 2001)	Action	Responsible	Status
15 June 2001 15 March 2002	S. Mughabghab and R. Firestone to exchange lists of isotopes with strongly discrepant published σ_o values. Lists will be concurrently sent to R. Paviotti-Corcuera for posting on the CRP WEB server. (Z from 1 to 60 by 15 June 2001; Z from 61 to 99 by 15 March 2002)	**Mughabghab and Firestone**	Postponed to April 2002 Received Dec. 2002
1 September 2001 15 December 2001 15 January 2002	G. Molnar to co-ordinate a benchmark of measurement of g-factors for ^{113}Cd and ^{157}Gd for thermal and cold beam facilities. Potential participants NIST (USA), Budapest, India, Japan and Korea. (Mr. Molnar to distribute samples by 1 Sept. 2001, measurements by 15 Dec. 2001, summary by 15 Jan. 2002)	Molnar+ participants (experimental) **NIST Korea India Japan**	No information received as of Jan. 2003
1 September 2001	S. Frankle to send thermal neutron capture gamma ray data compiled and evaluated at LANL to Firestone and R. Paviotti-Corcuera (by 1 Sept. 2001)	**Frankle**	Task completed Dec. 2001
15 October 2001	S. Mughabghab to compute Westcott g-factors for Maxwellian spectral shape at 30°K and 100°K using latest release of ENDF/B-6 for non-1/v isotopes (by 15 Oct. 2001)	**Mughabghab**	No information received as of Sept. 2002. Task done by Trkov, Oct. 2002
15 December 2001	Budapest to re-measure σ_o of ^{6}Li for thermal and cold neutron beams	**Molnar**	No information received as of Jan. 2003 (?)
15 December 2001	• Trkov to develop software for computation of generalized Westcott g-factors for non-Maxwellian sub-thermal to epithermal range neutron spectral shapes for 1/v and non-1/v nuclei. (Verification of the software).	**Trkov**	Verification of software (completed) Jan. 2002

	• Compute g-factor for cold beam shape (Maxwellian modified with λ^2 weighting factor for guided beam tubes) • Compute g-factor for a thermal plus epithermal beam such as at PGAA facility in Korea. Beam parameters from Choi. • Compute g-factors for Maxwellian shapes at 30°K and 100°K using RNAL library	**Trkov (cont.)**	Completed Nov. 2002 (different approach)
15 December 2001	To develop two Slow Neutron Capture Gamma (SNCG) databases: Working Database (ENSDF format) (Firestone, first draft by 15 Dec. 2001). User Oriented Data Base (Firestone, first draft by 15 Dec. 2001). • Search & Retrievable (Firestone, first draft by 15 Dec. 2001). • Lone-style Formatted Table (Firestone, first draft by 15 Dec. 2001)	**Firestone**	Completed Aug. 2002 Completed Aug. 2002 Completed Aug. 2002 (feedback received only from: Heedong, Dick, Rick)
15 December 2001	V. Zerkin / R. Firestone to develop a platform independent retrieval and display program for the PGAA database (by 15 Dec. 2001)	**Zerkin Firestone**	Completed Aug. 2002
15 December 2001 (participants) 15 January 2002 (Lindstrom)	Benchmark of measurements of $k_{o,H}$ of C in thermal and cold beams to determine σ_o and to quantify target dependent background. Participants: NIST(USA), Budapest, Korea, India and Japan. Coordinator: R. Lindstrom (NIST). (Mat. distributed by Lindstrom by 1 July 2001; first measurement by participants will be sent to Lindstrom by 15 Dec. 2001, summary by Lindstrom by Jan. 2002)	Participants **Budapest Korea India Japan+ Lindstrom**	Lindstrom distributed samples before end of Dec. 2001 Korea reported results
15 December 2001 (participants) 15 January 2002 (Lindstrom)	Characteristics and benchmark result of reference materials for PGAA applications (Lead, R. Lindstrom, participants to return results of measurements to R. Lindstrom by 1 Dec. 2001; benchmark summary and material specification by R. Lindstrom by 15 Jan. 2002)	Experimental Participants **Budapest Korea India Vietnam Japan + Lindstrom**	Korea reported results

15 January 2002 (?)	All participants to report their measured k_x and σ_x values normalized to 2200 m/s value by correcting with g-factors appropriate to their facilities	All participants (experimental, as above)	Korea reported results

TECDOC

1 March 2002	**Foreword, summary, abstract**: (lead R. Paviotti-Corcuera, draft by March 2002	**Paviotti**	Completed March 2002
	Introduction: (Lead by R. Lindstrom). An overdue of development and PGAA applications (draft by 1 March 2002)	Lindstrom	Completed Sept. 2002
1 March 2002	**Nomenclature, Neutron Spectral shape dependent Formulism**: (A. Lone and A. Trkov). Describe formulism for reaction rates applicable to various facilities and give a brief description of parameters and nomenclature (draft by 1 March 2002)	**Lone Trkov**	As of September 2002 no news received. Task assumed by Heedong and Trkov

Completed Nov. 2002 |
1 March 2002	**Characteristics of PGAA Facilities**: Up to 3-page length descriptions of each existing facility, (coordinator H. Choi, draft by 1 March 2002)	**Choi**	Completed April 2002
1 March 2002	**Benchmark results and Characterization of Reference Materials:** (Lead R. Lindstrom and G. Molnar). Description of benchmarks and reference materials used for development of the PGAA database (draft by 1 March 2002)	**Lindstrom** + **Molnar**	Chapter written (out 2002) but no results shown in TECDOC chapter ??
1 March 2002	**ENSDF Evaluated Data Base**: (Z. Chunmei, D. Firestone and S. Frankle). Describe methodology of collation and evaluation data (draft by 1 Jan. 2002, write-up draft by 1 March 2002)	**Chunmei, Firestone** and **Frankle**	Completed Aug. 2002
1 March 2002	**New Prompt Gamma Ray Data**: (G. Molnar) Describe new k_o data measured under the CRP at Budapest and other facilities (draft by 1 March 2002)	**Molnar**	

1 March 2002	**Adopted Data Base and User Tables**: (R. Firestone) describe methodology and criterion of data selection (draft by 1 March 2002)	**Firestone**	Completed Aug. 2002
1 March 2002	**User information on structure and retrieval of PGAA data base with Appendix of a Lone style table**: (D. Firestone, V. Zerkin and R. Paviotti-Corcuera) Describe structure and retrieval software developed for the PGAA database (draft by 1 March 2002)	**Firestone, Zerkin Paviotti**	Completed Aug. 2002
1 March 2002	**Data Base:** (CD-ROM, WEB, etc. R. Firestone, V. Zerkin, R. Paviotti-Corcuera) (draft by 1 March 2002).	**Firestone Zerkin Pronyaev Paviotti**	Completed Aug. 2002
1 March 2002	**Data Base:** (CD-ROM, WEB, etc. R. Firestone, V. Zerkin, R. Paviotti-Corcuera) (draft by 1 March 2002).	**Firestone , Zerkin Pronyaev Paviotti**	Completed Aug. 2002
15 March 2002	The new σ_o values measured in the CRP co-ordinate work to be considered by S. Mughabghab for update of the σ_o recommended database. 15 March 2002 (?)	**S. Mughabghab**	15 March 2002

STATUS OF TECDOC

International Atomic Energy Agency

"Development of a Database for Prompt Gamma-ray Neutron Activation Analysis"

Third Research Coordination Meeting

IAEA Headquarters, Vienna, Austria
24 - 26 March 2003
Scientific Secretary R. Paviotti-Corcuera

IAEA-Technical Document (June 2001)

Title: "Data Base of Prompt γ-rays from slow neutron capture for elemental analysis"

Foreword, summary, abstract: (Lead R. Paviotti-Corcuera, dra*ft by 2002 March*).

Chapters:

Introduction: (Lead R. Lindstrom) An overview of development and PGAA applications *(draft by 2002 March)*

Nomenclature, Neutron Spectral shape dependent Formulism: (A. Lone and A. Trkov). Describe formulism for reaction rates applicable to various facilities and give a brief description of parameters and nomenclature *(draft by 2002 Mar.1)*

Characteristics of PGAA Facilities: Up to 3-page length descriptions of each existing facility, *(coordinator H. Choi, draft by 2002 March 1)*.

Benchmark results and Characterization of Reference Materials: (Lead R. Lindstrom and G. Molnar). Description of benchmarks and reference materials used for development of the PGAA database *(draft by 2002 March 1)*.

Isotopic Data: σ_o, resonance integrals, g-factors, **abundances:** (S. Mughabghab,*draft by 2002 Mar.1)*

ENSDF Evaluated Data Base: (Z. Chunmei, D. Firestone and S. Frankle). Describe methodology of collation and evaluation data *(draft by 2002 Jan 1, write-up draft by 2002 March 1)*.

New Prompt Gamma Ray Data: (G. Molnar) Describe new k_o data measured under the CRP at Budapest and other facilities *(draft by 2002 Mar.1)*.

Adopted Data Base and User Tables: (R. Firestone) Describe methodology and criterion of data selection *(draft by 2002 March 1)*.

User information on structure and retrieval of PGAA data base with Appendix of a Lone style table: (D. Firestone, V. Zerkin and R. Paviotti-Corcuera) Describe structure and retrieval software developed for the PGAA database *(draft by 2002 March 1)*.

The structure of the TECDOC as proposed during the second RCM is displayed above. By September 2002, some contributions were missing; a new structure was adopted for the TECDOC and responsibilities were reassigned. The new structure and responsibilities are shown below. By February 2003, IAEA-NDS had received some of the contributions, and parts were inserted in the chapters already written. At the present and last RCM, drafts of the chapters will be discussed and corrections introduced when necessary.

Data Base: (CD-ROM, WEB, etc. R. Firestone, V. Zerkin, V. Pronyaev and R. Paviotti-Corcuera) (*draft by 2002 March 1*).

International Atomic Energy Agency

TECDOC by September 2002

FOREWORD (Raquel)

1. INTRODUCTION: AN OVERVIEW OF DEVELOPMENT AND PGAA APPLICATIONS (R.M. Lindstrom).

2. NOMENCLATURES, WESTCOTT G-FACTORS, AND NEUTRON SPECTRAL SHAPE DEPENDENT FORMULISM. (H. D. Choi, and A. Trkov).

International Atomic Energy Agency

---

3. CHARACTERISTICS OF PGAA FACILITIES (H. D. Choi).

4. BENCHMARKS AND REFERENCE MATERIALS (R.M. Lindstrom).

5. ISOTOPIC DATA: THERMAL NEUTRON CROSS SECTIONS, AND ATOMIC MASSES (R. B. Firestone).

International Atomic Energy Agency

---

6. EVALUATION METHODOLOGY (R. B. Firestone).

7. ADOPTED DATABASE AND USER TABLES (R. B. Firestone).

8. RETRIEVAL SYSTEM (V. Zerkin, R. B. Firestone and R. Paviotti-Corcuera).

International Atomic Energy Agency

Appendix 4: Papers and some Final Reports

Determination of the prompt K_0-factors for B, N, Si, P and S, *H.-D. Choi, G.M. Sun and C.S. Park*

Final Summary Report (Korea) Development of a Database for Prompt γ-ray Neutron Activation Analysis, *H.-D. Choi, S.H. Byun, G.M. Sun, C.S. Park and C.S. Kang*

Prompt Gamma-ray Data Evaluation of Thermal Neutron Capture for A = 1 – 44, *Zhou Chunmei and Wu Zhendong*

Analysis of Alloys by Prompt Gamma-ray Neutron Activation, *A.G.C. Nair, K. Sudarshan, N. Raje, A.V.R. Reddy, S.B. Manohar and A. Goswami*

Progress Report (India) Evaluation and measurement of Prompt k_0-factors to use in prompt gamma-ray neutron activation analysis, *A.V.R. Reddy, A.G.C. Nair, A. Goswami, K. Sudarshan, Y.M. Scindia, R. Acharya and S.B. Manohar*

New Prompt Gamma-ray Data, *G.L. Molnár*

Determination of the prompt k_0-factors for B, N, Si, P and S

H.D. Choi, G.M. Sun and C.S. Park

Department of Nuclear Engineering, Seoul National University, Seoul 151-742, Korea

Abstract

The prompt k_0-factors were measured for the light elements like B, N, Si, P and S relative to 1951.14 keV line from the ^{35}Cl(n,γ) reaction or 2223.25 keV from the H(n,γ) reactions. The measurement was performed at the SNU-KAERI Prompt Gamma Activation Analysis facility upgraded recently. The measured data were tabulated for the hydrogen comparator and compared with other reported data. The comparison for each element showed reasonable agreement within acceptable discrepancy.

1. Introduction

Prompt Gamma Activation Analysis (PGAA) is a complementary method to the conventional neutron activation analysis and is characterized by its applicability for the light elements like H, B, N, Si, P and S which can hardly be analyzed by NAA. The excellent PGAA facilities developed recently using guided slow neutron beam greatly improved analytical performance and therefore application field is being expanded. In the standardization of analysis, the prompt k_0-method has been actively adopted by several groups to establish a unified standardization and the inter-comparison between facilities and between measurement and definition was performed accordingly.

Prompt k_0-factor is defined as[1],

$$k_0 = \frac{\Gamma_x(E_x^\gamma)}{\Gamma_c(E_c^\gamma)} \cdot \frac{\sigma_{0,x}}{\sigma_{0,c}} \cdot \frac{\theta_x / M_x}{\theta_c / M_c} \tag{1}$$

where x and c indicate the analyte and the comparator, respectively. Γ is the γ-emission intensity, σ_0 the 2200 m/s capture cross section, θ the isotopic abundance, and M the atomic mass. The prompt k_0-factor can be defined relative to a convenient comparator such as H, Cl and Ti etc. The definition can be related to a generalized experimental form by

$$k_0 = \frac{A_{sp,x} / \varepsilon(E_x^\gamma)}{A_{sp,c} / \varepsilon(E_c^\gamma)} \cdot \frac{\hat{g}_c}{\hat{g}_x} \cdot \frac{\left(\frac{R_{Cd}}{R_{Cd}-1}\right)_c}{\left(\frac{R_{Cd}}{R_{Cd}-1}\right)_x} = k_0(measured) \cdot \frac{\hat{g}_c}{\hat{g}_x} \cdot \frac{\left(\frac{R_{Cd}}{R_{Cd}-1}\right)_c}{\left(\frac{R_{Cd}}{R_{Cd}-1}\right)_x} \tag{2}$$

where A_{sp} is the specific count rate and ε is the full energy peak efficiency. The effective g-factor($\hat{g}$) and cadmium ratio(R_{Cd}) are correction factors to the measured value k_0(measured), which are required for standardizing the factor in facility-independent way. The use of the nearly pure thermal or cold neutrons at most facilities makes negligible the correction of the cadmium ratio. However, effective g-factor should be carefully corrected since it is dependent both on the (n,γ) cross section and on the neutron spectrum. The detailed description on the formalism and the effective g-factor is given elsewhere [2]. The importance of the effective g-factor correction has been already identified in the previous measurement for the strong non-1/v absorbers like Cd, Sm, Gd, Eu etc.[2]. Since the light elements like H, B, Si, P and S

targeted in this study are all 1/v absorbers in the thermal energy region, the correction of the effective g-factor can be neglected. Hence the k_0(measured) can be usually looked upon as k_0, which makes simple and possible the direct inter-comparison of the measured k_0 values between facilities without the above corrections. In this study, the prompt k_0-factor is determined relative to the 1951.14 keV from the ^{35}Cl(n,γ) reaction or 2223.25 keV from the H(n,γ) reaction.

2. Experimental

2.1. Apparatus

The SNU-KAERI PGAA facility is characterized by the unique polychromatic neutron beam obtained using the pyrolytic graphite crystals. The facility was constructed at HANARO research reactor in the Korea Atomic Energy Research Institute, which is operational at the thermal power of 24 MW. The effective neutron temperature is approximately 276 K. The facility has been utilized for the estimation of the analytical performance, the boron concentration analysis and the measurement of the prompt k_0-factors for the strong non-1/v absorbers since May 2001[2-5]. The neutron flux at the sample position was measured by activating the Au wire in the neutron beam. The true integrated flux and the conventional thermal equivalent flux are 7.9×10^7 n/cm^{2}s, 8.2×10^7 n/cm^{2}s, respectively. The cadmium ratio is 266, which is a medium level between the direct beam and the guided beam. The γ-ray spectrometer was comprised of a single bare HPGe detector before upgrade, and has been upgraded early this year to the triple modes which simultaneously operate in the single, Compton suppression and pair modes by adding the BGO/NaI(Tl) guard detector and the associated electronics. A layout of the arrangement of the detectors and surrounding shields is shown in Fig. 1. The guard detector is a symmetry-type BGO/NaI(Tl) scintillator divided into the front and side parts. The front part is a NaI(Tl) scintillator and the side part consists of the optically isolated 8-segment BGOs. The detector array is shielded by the lead with a thickness of 10 cm at least and the 4 mm thick borated plastic sheets. The lead step collimator is located in front of the opening of the guard detector. The 4 mm thick ^{6}LiF tiles are placed at the entrance of the collimator to prevent the neutrons directly incident on the detector. The detector is located at 25 cm distance from the sample and placed at 90° with respect to the
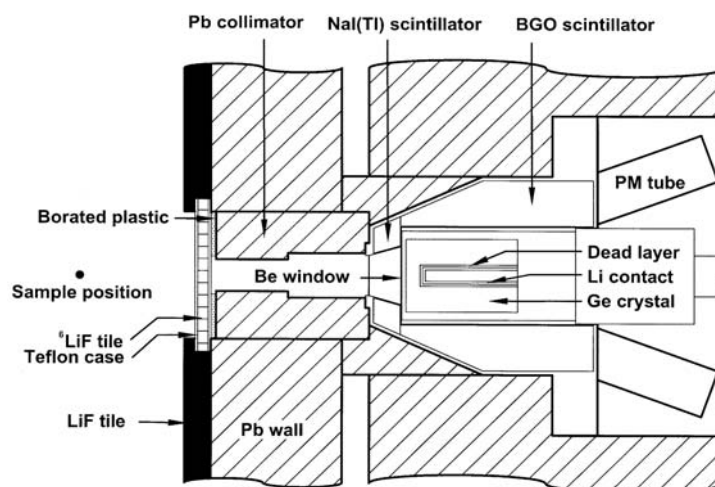
FIG. 1.   *A layout of the arrangement of the detectors and surrounding shields around the sample position.*

neutron beam direction. A block diagram of the spectrometer electronics is shown in Fig. *2*. The three 16 k multichannel buffers are controlled by a personal computer through the Ethernet. The energy resolution of the 43% n-type HPGe detector is 2.2 keV for the 1332.50 keV ^{60}Co γ-ray in the Compton suppression mode. After upgrade, the total background count rate was reduced to about 250 cps, a tenth of that in the single bare mode. The Compton continuum was effectively suppressed to a level of about 23 % when the guard detector was used in anticoincidence gating. The Compton mode suppressed the escape peaks as well as the Compton continuum, while the triangular peaks still remain induced by the inelastic scattering of the fast neutrons incident on the germanium crystal.

2.2. Sample preparation and measurement

The analytic samples for the 5 elements were prepared from high-grade stoichiometric materials which contain H or Cl as comparator element. For B and N which form compounds with H or Cl, the compound type samples were used. The used H compound samples are melamine and boric acid. The used Cl compound sample is ammonium chloride. For the rest elements Si, P and S which hardly form a stable chloride or hydride compound or whose analytical sensitivities deviate largely from Cl or H, the samples were prepared by mixing the appropriate elemental contents with NaCl. The samples were cold-pressed into disks with a diameter of 10 mm and mounted at the sample holder. After the data collection, the HYPERMET code was used for the spectrum analysis.

3. Results and discussion

3.1. Spectrometer calibration

The full energy peak efficiency curve of the spectrometer was calibrated both by the conventional method using the standard radioactive sources and by measuring the prompt γ-rays from the neutron capture reactions. In the low energy region of 60 keV ~ 1408 keV, ^{133}Ba, ^{134}Cs, ^{137}Cs, ^{152}Eu and ^{241}Am were used to generate the absolute full energy peak efficiency curve. The sample for the measurement of the prompt γ-rays was prepared from the mixture of the melamine and ammonium chloride powder. The sample was irradiated in the neutron beam for 80,000 s. The relative efficiency curve determined using the prompt γ-rays from the ^{14}N(n,γ) and ^{35}Cl(n,γ) reactions was normalized to the absolute efficiencies of the
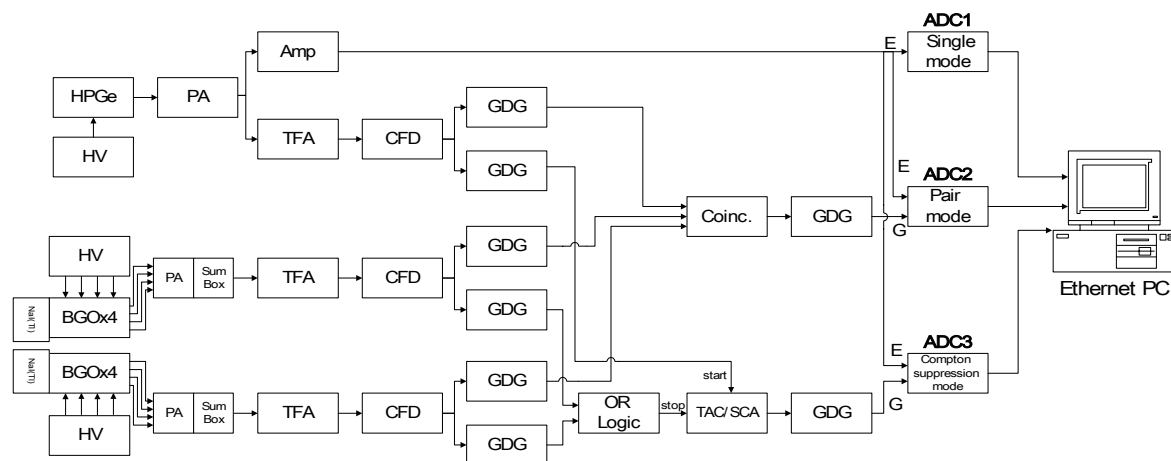
FIG. 2.   *Block diagram of the SNU-KAERI PGAA γ-ray spectrometer. E energy signal, G. gate signal to ADCs.*

low energy range to extend the curve up to 11 MeV. The γ-emission probabilities for the standard radioactive sources were taken from the IAEA-TECDOC[6] and the prompt γ-emission intensities were taken from the Lawrence Berkely National Laboratory (LBNL)'s adopted data[7]. All the data were fitted with 8th polynomials and the overall uncertainty of the efficiency curve was assigned from the 95% confidence limit curve (1.6σ). The absolute full energy peak efficiency curve is shown in Fig. 3. The relative 1σ-uncertainty is less than 2% in the energy range of 0.06 ~ 0.3 MeV, less than 1% in the energy range of 0.3 ~ 6 MeV, and 2% in the energy range of 6 ~ 11 MeV. Besides, the non-linearity calibration was performed to determine the measured prompt γ-ray energy.

3.2. Analytical sensitivity and prompt k_0-factor

3.2.1. Analytical sensitivity
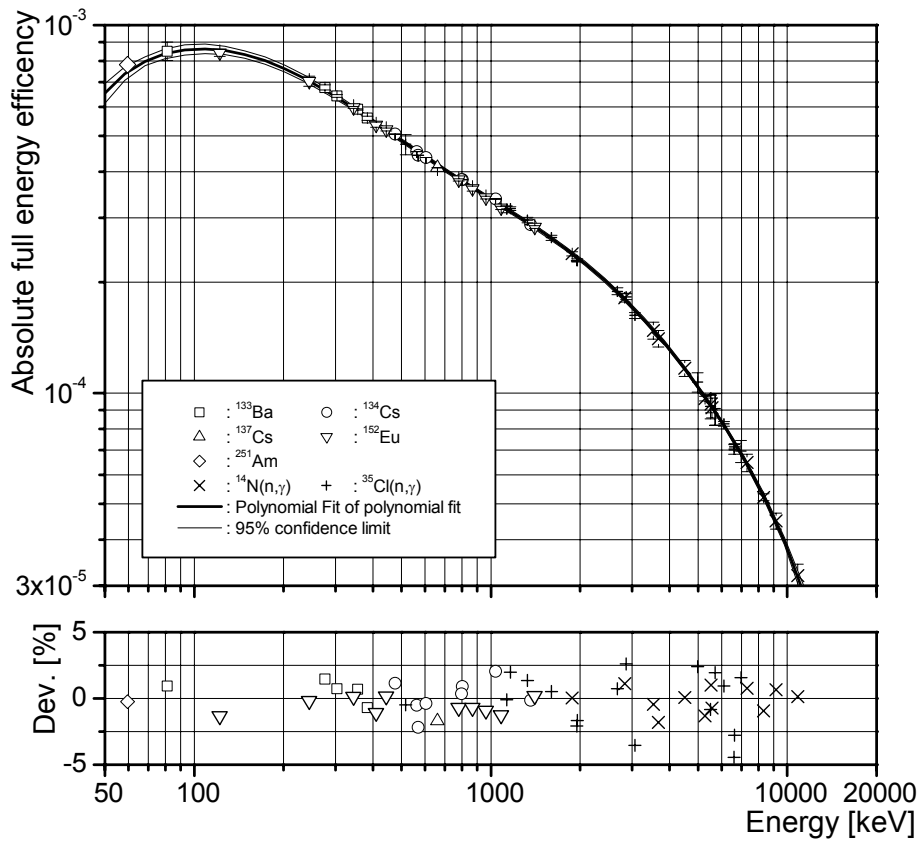
FIG. 3.   Efficiency curve for the Compton suppression mode of the γ-ray spectrometer of the SNU-KAERI PGAA facility.

The analytical sensitivity for each element was calibrated by so-called addition method and the resultant plots are shown in Fig. 4. The used prompt γ-lines from B, N, Si, P and S are 477.60 keV, 1884.82 keV, 3539.04 keV, 636.54 keV and 841.10 keV, respectively. Compound samples or mixed samples of analyte and comparator were measured to avoid the matrix effect on the determination of the prompt k_0-factor by using these analytical sensitivity data. Fig. 4a shows the increase of the count rate in proportion to the elemental mass of B. The B contents are 0.7, 1.7, 2.9 and 8.3 mg, respectively. The analytical sensitivity for B was determined to be 1229.5±72.6 cps/mg by linear-fitting the data excluding the point of 8.3 mg B content, which deviates greatly from the linear relation between the mass and count rate. Fig. 4b is the result for nitrogen samples prepared from the melamine. The N contents are 155.0, 206.8, 244.8, 266.2 and 413.1 mg, respectively. Fig. 4c shows the result for silicon samples prepared from the silicon oxide. The Si contents are 44.0, 122.1, 190.0 and 526.5 mg, respectively. Fig. 4d is the plot for phosphorous samples prepared from the phosphorous powder. The P contents are 29.1, 43.9, 111.1, 143.8 and 295.7 mg, respectively. Fig. 4e is the plot for sulphur samples prepared from the sulphur powder. The S contents are 105.1, 257.3, 347.1 and 623.9 mg, respectively. The analytical sensitivities for N, Si, P and S are
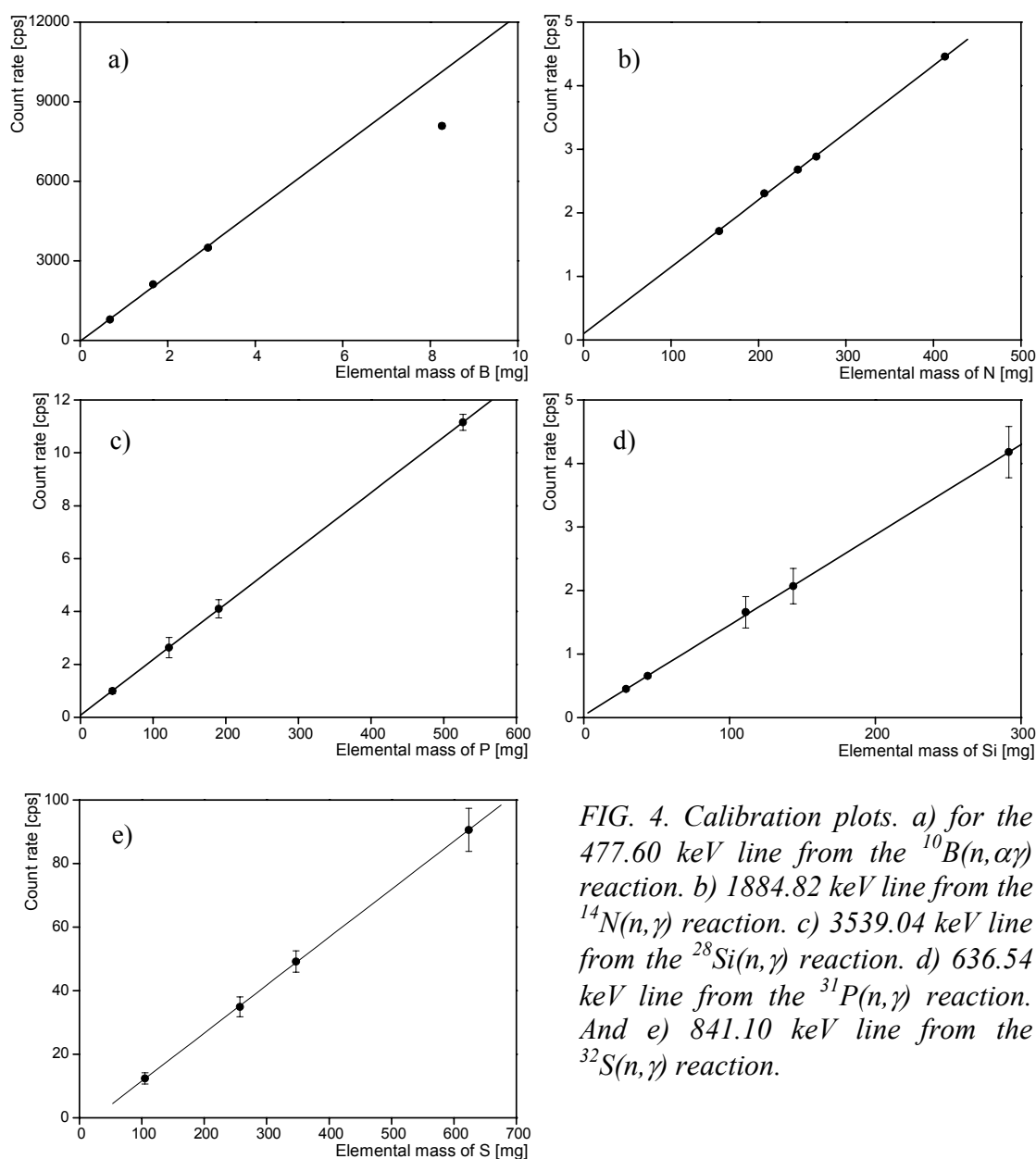
FIG. 4. Calibration plots. a) for the 477.60 keV line from the ^{10}B(n,αγ) reaction. b) 1884.82 keV line from the ^{14}N(n,γ) reaction. c) 3539.04 keV line from the ^{28}Si(n,γ) reaction. d) 636.54 keV line from the ^{31}P(n,γ) reaction. And e) 841.10 keV line from the ^{32}S(n,γ) reaction.

determined to be 0.0106±0.0001 cps/mg, 0.0210±0.0005 cps/mg, 0.0142±0.0002 cps/mg, and 0.151±0.001 cps/mg, respectively.

3.2.2. Prompt k_0-factors and partial cross sections

The k_0(H)(measured) values for light elements are listed in energy order in the Tables 1 - 5. The k_0(Cl)(measured) values were converted to the k_0(H)(measured) values by using the k_0(H)(measured) value for Cl 1951.14 keV determined from ammonium chloride sample, which is given as 1.81±0.034. In Table 1, the 477.60 keV line from the ^{10}B(n,αγ) reaction is listed. For the other elements, the most intense twenty lines are listed. The tables also contain the partial cross section for each line (σ_x)[11] given as

$$\sigma_x = k_0(H)(measured) \cdot \sigma_H \cdot (M_x / M_H) \tag{3}$$

where the partial cross section for H 2223.25 keV line (σ_H) is 0.3326±0.0007 b from Lawrence Berkeley National Laboratory (LBNL)'s adopted data[7] and M_x or M_H are the atomic masses.

Table 1. Prompt k_0-factors and partial cross section for B.

A	E_γ [keV]	unc.	k_0(H)(meas.)	unc.	σ_x [b]	unc.
10	477.60	0.03	2.03E+02	1.21E+01	7.25E+02	4.28E+01

Table 2. Prompt k_0-factors and partial cross section for N.

A	E_γ [keV]	unc.	k_0(H)(meas.)	unc.	σ_x [b]	unc.
14	1678.36	0.04	1.38E-03	3.76E-05	6.38E-03	1.74E-04
14	1681.73	0.20	2.75E-04	1.07E-05	1.27E-03	4.95E-05
14	1853.87	0.08	1.14E-04	5.47E-06	5.27E-04	2.53E-05
14	1884.82	0.01	3.29E-03	5.15E-05	1.52E-02	2.40E-04
14	1999.94	0.05	6.25E-04	2.51E-05	2.89E-03	1.16E-04
14	2520.76	0.01	9.46E-04	2.15E-05	4.37E-03	9.98E-05
14	2831.21	0.03	3.03E-04	6.33E-06	1.40E-03	2.94E-05
14	3532.30	0.02	1.58E-03	2.60E-05	7.30E-03	1.21E-04
14	3678.02	0.01	2.53E-03	3.93E-05	1.17E-02	1.83E-04
14	3855.38	0.06	1.57E-04	4.11E-06	7.26E-04	1.91E-05
14	4508.76	0.02	2.97E-03	4.97E-05	1.37E-02	2.32E-04
14	5269.13	0.02	5.23E-03	8.77E-05	2.42E-02	4.09E-04
14	5297.63	0.05	3.63E-03	9.04E-05	1.68E-02	4.19E-04
14	5533.30	0.02	3.51E-03	5.77E-05	1.62E-02	2.69E-04
14	5562.03	0.02	1.86E-03	3.20E-05	8.60E-03	1.49E-04
14	6322.42	0.03	3.33E-03	5.81E-05	1.54E-02	2.70E-04
14	7299.03	0.06	1.68E-03	9.15E-05	7.76E-03	4.23E-04
14	8310.16	0.06	7.33E-04	1.42E-05	3.39E-03	6.60E-05
14	9149.20	0.10	2.91E-04	7.04E-06	1.34E-03	3.27E-05
14	10829.48	0.04	2.54E-03	4.31E-05	1.17E-02	2.01E-04

Table 3. Prompt k_0-factors and partial cross section for Si.

A	E_γ [keV]	unc.	k_0(H)(meas.)	unc.	σ_x [b]	unc.
28	752.48	0.02	3.19E-04	6.70E-06	2.96E-03	6.24E-05
28	1273.35	0.01	3.34E-03	5.16E-05	3.10E-02	4.83E-04
28	1446.03	0.03	1.36E-04	4.12E-06	1.26E-03	3.83E-05
28	1867.46	0.03	1.30E-04	3.12E-06	1.20E-03	2.90E-05
28	2093.12	0.004	3.81E-03	5.83E-05	3.53E-02	5.45E-04
29	2235.48	0.03	3.06E-04	7.00E-06	2.84E-03	6.51E-05
28	2426.04	0.02	5.28E-04	1.10E-05	4.89E-03	1.02E-04
30	2780.74	0.01	2.54E-04	4.66E-06	2.35E-03	4.35E-05
30	3054.50	0.02	2.76E-04	5.10E-06	2.56E-03	4.76E-05
29	3101.37	0.07	1.54E-04	8.01E-06	1.43E-03	7.43E-05
28	3539.04	0.01	1.30E-02	2.04E-04	1.20E-01	1.91E-03
28	3660.87	0.01	7.89E-04	1.29E-05	7.31E-03	1.21E-04
29	3864.89	0.02	2.03E-04	3.63E-06	1.88E-03	3.39E-05
28	3954.37	0.02	4.85E-04	8.47E-06	4.49E-03	7.91E-05
28	4933.68	0.12	1.25E-02	4.86E-04	1.16E-01	4.51E-03
28	5106.60	0.03	7.18E-04	1.34E-05	6.65E-03	1.25E-04
28	6379.80	0.02	2.31E-03	3.63E-05	2.14E-02	3.39E-04
29	6743.11	0.07	2.05E-04	6.00E-06	1.90E-03	5.57E-05
28	7199.23	0.05	1.37E-03	5.32E-05	1.27E-02	4.94E-04
28	8472.44	0.04	4.36E-04	9.36E-06	4.04E-03	8.72E-05

Table 4. Prompt k_0-factors and partial cross section for P.

A	E_γ [keV]	unc.	k_0(H)(meas.)	unc.	σ_x [b]	unc.
31	78.12	0.002	5.82E-03	1.80E-04	5.95E-02	1.84E-03
31	512.57	0.01	7.67E-03	2.43E-04	7.84E-02	2.49E-03
31	636.54	0.01	3.06E-03	1.03E-04	3.13E-02	1.05E-03
31	1070.97	0.01	2.45E-03	7.59E-05	2.50E-02	7.78E-04
31	1322.41	0.02	5.08E-04	1.61E-05	5.19E-03	1.65E-04
31	2114.00	0.03	1.17E-03	3.69E-05	1.20E-02	3.78E-04
31	2151.05	0.02	9.54E-04	3.08E-05	9.75E-03	3.15E-04
31	2156.43	0.03	1.19E-03	3.82E-05	1.22E-02	3.91E-04
31	2585.47	0.03	9.00E-04	2.90E-05	9.20E-03	2.97E-04
31	2885.44	0.06	6.11E-04	2.03E-05	6.24E-03	2.08E-04
31	3057.60	0.05	1.04E-03	3.52E-05	1.06E-02	3.60E-04
31	3273.40	0.07	7.91E-04	2.74E-05	8.08E-03	2.81E-04
31	3522.01	0.06	2.16E-03	7.46E-05	2.21E-02	7.64E-04

31	3899.31	0.05	2.93E-03	9.87E-05	2.99E-02	1.01E-03
31	4199.30	0.30	5.46E-04	1.97E-05	5.58E-03	2.02E-04
31	4363.73	0.14	7.15E-04	2.63E-05	7.31E-03	2.69E-04
31	4660.52	0.12	5.81E-04	2.04E-05	5.94E-03	2.09E-04
31	4670.83	0.08	1.97E-03	6.70E-05	2.01E-02	6.86E-04
31	5265.02	0.52	5.99E-04	2.75E-05	6.12E-03	2.81E-04
31	6785.28	0.15	2.65E-03	9.02E-05	2.71E-02	9.24E-04

Table 5. Prompt k_0-factors and partial cross section for S.

A	E_γ [keV]	unc.	$k_0(H)$(meas.)	unc.	σ_x [b]	unc.
32	841.10	0.004	3.25E-02	6.78E-04	3.44E-01	7.21E-03
32	1471.50	0.01	8.22E-04	1.69E-05	8.70E-03	1.80E-04
32	1696.46	0.01	1.21E-03	2.62E-05	1.28E-02	2.79E-04
32	1964.38	0.02	6.30E-04	1.39E-05	6.67E-03	1.48E-04
32	2216.60	0.02	1.19E-03	2.79E-05	1.26E-02	2.96E-04
32	2379.70	0.01	1.99E-02	4.01E-04	2.11E-01	4.27E-03
32	2490.40	0.01	1.20E-03	2.59E-05	1.27E-02	2.75E-04
32	2753.22	0.01	2.59E-03	5.38E-05	2.74E-02	5.72E-04
32	2930.76	0.01	7.86E-03	1.59E-04	8.32E-02	1.69E-03
32	3220.55	0.01	1.15E-02	2.43E-04	1.22E-01	2.58E-03
32	3369.71	0.01	2.57E-03	5.23E-05	2.72E-02	5.56E-04
32	3723.61	0.03	1.25E-03	3.28E-05	1.32E-02	3.48E-04
32	4430.73	0.01	2.23E-03	5.33E-05	2.36E-02	5.66E-04
34	4638.02	0.01	6.62E-04	1.43E-05	7.00E-03	1.52E-04
32	4869.80	0.01	5.82E-03	1.21E-04	6.16E-02	1.29E-03
32	5047.21	0.01	1.48E-03	3.13E-05	1.57E-02	3.33E-04
32	5420.50	0.01	2.76E-02	5.60E-04	2.92E-01	5.96E-03
32	5583.32	0.02	7.38E-04	1.65E-05	7.81E-03	1.75E-04
32	7800.01	0.02	1.44E-03	3.03E-05	1.52E-02	3.22E-04
32	8640.78	0.02	1.04E-03	2.31E-05	1.10E-02	2.46E-04

3.3. Comparison with other reported data

The measured prompt k_0-factors were compared with those obtained at other facilities and the result is shown in Table 6. The IKI(thermal) values were measured at the thermal guide beam line at BRR, Hungary by Zs. Révay et al.[8]. The JAERI(cold) and JAERI(thermal) values were measured at the cold and thermal guide beam lines at JRR-3M, Japan by H. Matsue et al.

Table 6. Comparison of the k_0(measured) in the present work with those from other facilities.

Element	E_γ [keV]	Révay et al.(2000) IKI(thermal)	Matsue et al. JAERI(cold)[a]	Matsue et al. JAERI(thermal)[b]	Acharya et al. BARC(thermal)	Present work
B	477.60	200±0.6	204±16	206±19	168±10[c]	203±12
N	1884.82	3.14E-03±8.48E-05	3.75E-03±1.20E-04	3.18E-03±1.55E-04		3.29E-03±5.15E-05
Si	3539.04	1.28E-02±2.18E-04	1.13E-02±3.67E-04	1.21E-02±4.14E-04		1.30E-02±2.04E-04[d]
P	636.54	3.03E-03±1.52E-04	2.56E-03±7.23E-05	2.61E-03±9.83E-05		3.06E-03±1.03E-04[d]
S	841.10	3.37E-02±5.73E-04	3.08E-02±7.78E-04	3.08E-02±1.24E-03		3.25E-02±6.78E-04[d]

[a] values were converted from k_0(Cl) factors. Multiply by 1.86±0.061 to obtain k_0(Cl).
[b] values were converted from k_0(Cl) factors. Multiply by 1.80±0.061 to obtain k_0(Cl).
[c] values were converted from k_0(Cl) factors. Multiply by 1.86±0.07 to obtain k_0(Cl).
[d] values were converted from k_0(Cl) factors. Multiply by 1.81±0.034 to obtain k_0(Cl).

[9] and the BARC(thermal) value was measured at the thermal guide beam line at Dhruva research reactor, India by R.N. Acharya et al.[10]. This comparison between facilities was performed to evaluate the accuracy of the measured k_0-factors and the validity of the assumption that the measured prompt k_0-factors for the 1/v elements are facility-independent. The k_0(H) value for B 477.60 keV line is consistent with the IKI(thermal) value, the JAERI(cold) and JAERI(thermal) values within 1.5% while differed from the BARC(thermal) value by 17.4%. The k_0(H) value for N 1884.82 keV line differed from the JAERI(cold) by 14.1%. The k_0(H) value of Si 3539.04 keV line differed from the JAERI(cold) and JAERI(thermal) values by 12.7% and 6.8%, respectively. The k_0(H) value for P 636.54 keV line show the discrepancy of 16.2% from the JAERI(cold) value and the discrepancy of 14.7% from the JAERI(thermal) value, respectively. For other cases, they show the good consistency between the facilities within about 5%.

4. Conclusions

A successful upgrade of the facility has been done by addition of a Compton suppressor detector and modification of the surroundings. Background count is reduced by an order of magnitude. Improvement in the uncertainties of absolute efficiency is achieved at little cost of reduced efficiencies. The prompt k_0-factors were measured for the light elements B, N, Si, P and S. The measured k_0-factors are listed by k_0(H)'s and partial cross sections. These prompt k_0-factors are compared with the reported data and show a general agreement. The assumption that the prompt k_0-factors for 1/v absorbers show the facility-independent feature is validated for most of the light elements in this study. A detailed look of the discrepancies indicates a need for further study and inter-laboratory measurement.

REFERENCES

[1] MOLNÁR, G.L., RÉVAY, Z.S., PAUL, R.L., LINDSTROM, R.M., J. Radioanal. Nucl. Chem. 34 (1998) 21.
[2] SUN, G.M., BYUN, S.H., CHOI, H.D., submitted to J. Radioanal. Nucl. Chem.
[3] BYUN, S.H., SUN, G.M., CHOI, H.D., J. Radioanal. Nucl. Chem. 244 (2000) 413.
[4] BYUN, S.H., SUN, G.M., CHOI, H.D., Nucl. Instr. and Meth. A487 (2002) 521.
[5] BYUN, S.H., SUN, G.M., CHOI, H.D., Nucl. Instr. and Meth. A490 (2002) 538.
[6] IAEA-TECDOC-619, X-ray and Gamma-ray Standards for Detector Calibration, International Atomic Energy Agency, 1991.
[7] FIRESTONE, R.B., Lawrence Berkeley National Laboratory, USA, private communication.
[8] RÉVAY, Z.S., MOLNÁR, G.L., BELGYA, T., KASZTOVSZKY, Z.S, FIRESTONE, R.B., J. Radioanal. Nucl. Chem. 244 (2000) 383.
[9] MATSUE, H., YONEZAWA, C., J. Radioanal. Nucl. Chem. 249 (2001) 11.
[10] ACHARYA, R.N., SUDARSHAN, K., NAIR, A.G.C., SCINDIA, Y.M., GOSWAMI, A., REDDY, A.V.R., MANOHAR, S.B., J. Radioanal. Nucl. Chem. 250 (2001) 303.
[11] PRESTWICH, W.V., ISLAM, M.A., KENNETT, T.J., Nucl. Sci. Eng. 78 (1981) 182.

FINAL SUMMARY REPORT

Development of a Database for Prompt γ-ray Neutron Activation Analysis

H. D. Choi, S. H. Byun, G. M. Sun, C. S. Park, C. S. Kang

Department of Nuclear Engineering, Seoul National University

Seoul 151-742, Korea

1.   DEVELOPMENT OF SNU-KAERI PGAA FACILITY

Development of a PGAA facility in HANARO, Korea Atomic Energy Research Institute (KAERI) has been initiated by the program of developing the Boron Neutron Capture Therapy(BNCT). The plan was in time with the start of the IAEA CRP, "Development of a database for prompt γ-ray neutron activation analysis." Due to the existing plan and limited space in HANARO, the first difficulty was on the way of neutron beam extraction from an existing beam line(ST1) which was already dedicated to another device. A new method of using polychromatic neutrons was devised by collecting and focusing all the high ordered diffracted neutrons obtained from pyrolytic graphite(PG) crystals set at the Bragg angle 45° [1]. A vertical diffracted beam line was installed and consisted of collimators, shields for background neutrons and γ-rays, and beam catcher. The thermal equivalent neutron flux and the beam area is 8.2×10^7 n/cm²s and 2×2 cm² at the sample position, respectively. The corresponding Cd ratio for gold is 266. A beam uniformity of 12% was measured in the central beam area of 1×1 cm². The detection system initially comprised of a single HPGe (43%), signal electronics and a fast 16k ADC. The sample-to-detector distance is 25 cm. The details of the facility and performance are given in Ref. [2]. In the last year of the CRP, the detection system was upgraded by installing a NaI(Tl)-BGO guard detector and the associated electronics. Three modes of detection including single, Compton-suppressed and pair modes have been possible since. With several modifications including a reduction of the collimator aperture in front of the detector, the total background count rate has been reduced by a factor of 10 at the expense of about a quarter reduction in the full energy peak efficiencies [3].

2.   BEAM CHARACTERIZATION

Since less was known about the details of the polychromatic neutrons obtained from Bragg diffraction by PG crystal, several experimental and theoretical studies were undertaken to access the beam characteristics [4]. A neutron time-of-flight(TOF) measurement was done by using a 3 m TOF spectrometer. Neutrons of diffraction orders 1 – 6 were resolved and the relative intensities were determined after corrections for detection efficiency, attenuation on the flight path and beam chopper transmission. Absolute neutron intensity was measured from gold wire activation. About 90% of the diffracted beam flux comprised of the neutrons from diffraction orders 2 – 4. Resolving the higher diffraction orders above 6 were never achieved in the TOF measurement due to its low intensity and the spectrometer's finite resolution. Instead, theoretical approaches were taken to get the intensity predictions for higher diffraction orders. In the description of higher order diffraction, the most crucial parts were the Debye-Waller factor and the thermal diffuse scattering which describe the radical decrease of reflectivity for increasing diffraction order. The Debye-Waller factor for PG crystal was

available from x-ray studies even though their consistencies were not good. The parameter for the thermal diffuse scattering from PG crystal was little known and hence was determined from a fit to the observed neutron TOF intensities of diffraction orders 1 – 6. Hence the model could describe closely the observed intensities of orders 3 – 6 and predict even higher orders above 6.

Validation of the determined neutron spectrum has been done by comparing calculated beam quantities and measured ones for such as effective capture cross section and Cd ratio. The calculation has been done for the effective $^{10}B(n,\alpha)$ cross section and Cd ratios by using the spectral information of the beam and the datasets from evaluated data library. Measurement of the effective quantities by using a thin and "black" 1/v absorber samples was performed based on the principle provided in the 2nd CRP meeting [5]. The measured effective $^{10}B(n,\alpha)$ cross section is 3987±40 b. Accordingly, the derived effective quantities of the beam are: effective temperature 269±5 °K, effective velocity 2120±20 m/s. To access the epithermal component in the diffracted neutron beam, Cd ratios were measured for ^{35}Cl, ^{113}Cd, $^{149,150,152,154}Sm$, ^{157}Gd and ^{179}Au. The Cd ratio for gold was performed in the typical way of activating a wire (0.1 mmϕ) while those for the rest nuclides were performed by observing count rates of the prompt capture gamma's under irradiating a normal diffracted beam and a Cd-filtered diffracted beam on the target. The Cd-filtered beam was prepared by placing a Cd plate of thickness 0.5 mm at the position of beam collimator, which is sufficiently far upstream the target. The observed Cd ratios were in the range 370 – 400 except that of Au(266). The measured Cd ratios indicate an almost negligible portion of epithermal neutrons in the diffracted beam. The main origin of epithermal neutrons in the diffracted beam was traced to the background neutrons scattered from the structural materials of the PG mount and goniometer which were inevitably immersed in the strong white beam. By including the background neutrons (less than 0.5% of the total neutrons) for which the spectral shape of the Maxwellian + 1/E tail is assumed and whose magnitude is fitted to explain the observed Cd ratios, the final comparison between the calculated effective temperature and the measured one shows consistency within ~3 % [4].

3.   BENCHMARK MEASUREMENT

The normal position of the detector was chosen as 25 cm distant from the target. After assembling the whole detector system, the gain of the amplifier was adjusted to cover the range of gamma-ray energy up to about 13 MeV. A commercial data acquisition software was used for displaying and on-line analyses of the accumulating spectrum on the connected desktop PC. Detailed analysis of the peaks was done off-line by a DOS version of HYPERMET. The observed total background rate is about 3 kcps. Typical resolution for the 1333 keV ^{60}Co gamma-ray is 2.2 keV. Efficiency calibration of the detector has been performed by using a set of radioisotope sources and (n,γ) reactions. The standard radioisotopes ^{137}Cs, ^{241}Am, ^{134}Cs, ^{152}Eu, ^{133}Ba and ^{226}Ra were used to generate the absolute efficiency curve in the low energy range of 60 – 2204 keV by fixing the scale. The gamma emission probabilities were taken from IAEA-TECDOC-619 [6]. For the absolute efficiency curve in the higher energy range, the prompt gamma-rays from the (n,γ) reactions of ^{35}Cl and ^{14}N were measured to extend the energy range to 10829 keV. The KCl sample and the melamine sample were prepared and irradiated for a period to reduce the statistical uncertainty of the weakest peak below 1% for each spectrum. The absolute gamma intensities for (n,γ) reactions of Cl and N were taken from the Budapest-LBNL dataset [7]. The measured datasets were combined with normalization determined through a fitting process by use of the 8th order polynomial form [8] in the whole energy range of 60 – 10829 keV. The relative 1σ uncertainty is less than 3% for the lower energy range and less than 5% for the whole energy range. For an accurate determination of energy, non-linearity of the

spectrometer system was studied. The twenty γ-rays emitted from [134]Cs and [152]Eu were used in the energy range 120 keV - 1800 keV, while the prompt γ-rays detected in high intensity from the [35]Cl(n,γ) and the [14]N(n,γ) reactions were used in the higher energy region. The magnitude of non-linearity was within ±1.5 channel in the whole 16k channels. The observed non-linearities were fitted with a 5th-order polynomial. The detailed procedure was taken from the prescribed method given in Ref. [9]. The overall energy uncertainty is about 0.1 − 0.3 keV.

For a simple description of the sensitivity of the spectrometer, use of Ti 1381.5 keV line was agreed upon in the first CRP meeting. Titanium metal foils of 0.25 mm thickness were distributed. Three samples of different shapes or sizes were irradiated. The measured sensitivities(cps/mg) are : 2.02±0.01 for 6 mmφ disk, 1.952±0.003 for 13 mmφ disk, 1.327±0.003 for 2.5 cm square foil. The decreasing sensitivity for larger area sample indicates that the flux degradation at the outer beam edge influences the average count rate. Very good statistics of monitor counts, however, can be obtained within several minutes even with the smallest disk of 6 mmφ. Test measurement of elemental analysis was performed for the distributed sample of unknown composition. The 145 mg sample of a mixture of complex aluminosilicate and graphite was irradiated for 30000 sec. Hence the weight concentrations are obtained by using the count rate and sensitivity for each detected element. The sensitivity for boron is used from measurement while those for other elements are deduced from boron sensitivity, detection efficiency and nuclear data. The oxygen concentration was difficult to extract from the measured spectrum and hence obtained by assuming the amount equal to the full sample weight subtracted by the total amounts of all the other detected elements. The relative yields for the strong lines of Ti and the concentration of elements in the unknown sample are given in the separate report [10].

4.   PROMPT GAMMA MEASUREMENTS

4.1.   Non-1/v absorbers : [113]Cd, [149]Sm, [151]Eu, [155,157]Gd

Generalized k_0 factors applicable to non-1/v absorbers had been discussed by many studies in the instrumental neutron activation analysis(INAA). In PGAA, experimental determination of k_0 factors for non-1/v absorbers has the difficulty that no detailed information is typically available about the neutron spectrum even though the capture rate for these nuclides is influenced by the facility-dependent neutron spectrum. No remedy to determine the prompt k_0 factors experimentally had existed for non-1/v absorbers to give the k_0 factors as composite constants. Hence a general formalism was derived [11] in the similar manner as the k_0 standardization was done in INAA. For the k_0 factor of non-1/v absorber element relative to good 1/v comparator element such as ^{1}H or [35]Cl, the experimental ratio of the specific activities of the two elements needs to be corrected by g-factors and Cd-ratios. Each correction compensates the capture effect due to the non-1/v behavior in thermal and epithermal energy region, respectively. Due to the great difficulty to determine the g-factors accurately and experimentally, however, the only feasible way to get the g-factor correction is at the moment using the calculated g-factors based on the neutron spectral information and evaluated dataset of pointwise capture cross sections for the nuclides. Since the SNU-KAERI PGAA beam has a simple and well-defined neutron spectrum, the g-factor correction is straightforward. Actual g-factors were obtained from simple calculations by using the discrete nature of beam spectrum and pointwise capture cross sections taken from JEF-2.2 library [12].

Experimental measurement of non-1/v absorbers were taken for the selected nuclides, [113]Cd, [149]Sm, [151]Eu, [155,157]Gd. Comparator γ-line was taken for 1951.14 keV from [35]Cl(n,γ) reaction. Due to the huge difference in capture cross sections between the non-1/v absorber nuclides

and chlorine comparator, compound-type samples had the difficulty of Cl peak buried in the high counting rate of Compton background continuum produced by the γ-rays from the strongly absorbing non-1/v nuclide. Hence mixtures of elemental compounds with proper amounts of NaCl were prepared and irradiated. In addition to a normal beam irradiation, the sample was also irradiated with Cd-filtered beam to measure the Cd-ratio for the non-1/v nuclide under study. Preparing the Cd-filtered beam was described in the section 2, beam characterization. Most intense 20 γ-lines were identified and analyzed in each spectrum. The prompt k_0 factors relative to Cl were produced after g-factor correction. All the measured Cd-ratios for the non-1/v nuclides indicated negligible captures by epithermal neutrons in the beam and hence the correction on the measured k_0 factor by Cd-ratios was trivial. The relative intensities for the γ-lines were also produced.

The validation of the obtained k_0 factors was performed by several ways. A direct comparison with the values reported from other laboratories only confirmed the existing inconsistency since those reported values lacked in g-factor correction. A second approach was deriving 2200 m/s cross section from the determined k_0 factor of each non-1/v nuclide's strongest γ-line by use of the well-known data for mass and abundance. Here the three existing datasets for absolute γ-intensities – ENSDF, Lone Table [13], Budapest-LBNL dataset [7] - were used to derive the corresponding set of 2200 m/s capture cross section of the non-1/v nuclide. The derived datasets were compared with those of Mughabghab [14]. The best consistency was judged for the dataset derived by the recent Budapest-LBNL dataset [7]. For the rest of the most intense 20 γ-lines, the measured k_0 factors were also converted to 2200 m/s cross sections by use of the absolute γ-intensities in the Budapest-LBNL dataset. They were consistent each other. Details of formalism, experimental procedures and numerical results are being published elsewhere [11].

4.2. Light elements: B, C, N, Si, P, S

Even though a successful formalism and measurement of prompt k_0 factors were achieved for the strong non-1/v absorbers, the most of measured data lacked the required accuracy for k_0-standardization, which is less than 1%. To improve this drawback, upgrade of the facility had been taken by installing a Compton-suppressed spectrometer and reduced spectral background by other actions including the change of Pb collimator with smaller aperture and an addition of neutron shields around the detector. As a result, the total background count rate from the HPGe detector was reduced to about 250 cps. New efficiency and non-linearity calibrations were followed in the same procedure and methods taken for the bare detector before the system upgrade. Even though the absolute efficiencies were halved, roughly, from those of the previous system, the measured efficiencies were closer to a smooth fitting line and hence the uncertainty of the efficiency was reduced to within 2% in the whole range of 0.06 – 11 MeV. The upgraded spectrometer and improved calibration were applied to a measurement of prompt gamma's for light elements – B, C, N, Si, P, S.

The comparator was chosen as the 1951.14 keV line from $^{35}Cl(n,\gamma)$ reaction or the 2223.25 keV line from $^{1}H(n,\gamma)$ reaction. Whenever a suitable compound is available of both the analyte and the comparator elements, compound-type sample was used. Otherwise, samples of the element mixed with NaCl were prepared and used. Hence various masses of samples were prepared including those of melamine, urea, graphite, boric acid, ammonium chloride, and mixtures with NaCl. The samples were cold-pressed into disk of diameter 10 mm and irradiated after mounting at sample holder. The collected spectra were analyzed by HYPERMET. From analyses of spectra, the $k_0(H)$ values were obtained. In cases of Si, P and S, the $k_0(Cl)$ values were obtained and then converted to $k_0(H)$ values by using $k_0(H)$ of Cl

which was determined in measuring the ammonium chloride sample. The partial cross sections were also obtained from the measured $k_0(H)$ values and by using the cross section of H [7]. The details of procedure and results for the light elements are listed in a separate report [15]. The measured $k_0(H)$ values were compared with reported values from other facilities including IKI, Budapest, JAERI thermal and cold beam facility and Dhruva, India. They were consistent each other within about 5 %. Notable discrepancies among the reporting facilities, however, exist for the extreme $k_0(H)$ values far beyond the quoted uncertainties. The measurement of carbon samples had no sufficient beam time and no reliable data were obtained for the CRP.

5.   CONCLUSION

Through participating in the present CRP, the development and upgrade of the SNU-KAERI facility have been possible to go advanced in many aspects. It turned out that the novel technique is feasible for obtaining and using polychromatic neutrons with good quantity and clean quality by the Bragg diffraction from PG crystals. Spectrometer calibration and analysis have been achieved at the level of front-end quality. For the k_0-standardization to be valid for non-1/v absorbers in a facility-independent way, two correction factors are identified to apply for any facility and the formalism is given. These were verified in the actual measurement and validation of prompt k_0 factors for ^{113}Cd, ^{149}Sm, ^{151}Eu, ^{155,157}Gd. The $k_0(H)$'s and partial cross sections were also obtained for the good 1/v absorbers in the light elements, B, N, Si, P, S. They show a general consistency with the reported values even though the detailed magnitude of discrepancy needs more scrutiny and inter-comparison to confirm the facility-independent nature of k_0 factors.

REFERENCES

[1]   BYUN, S.H., CHOI, H.D., Design features of a prompt gamma neutron activation analysis system at HANARO, J. Radioanal. Nucl. Chem. **244** (2000) 413-416.

[2]   BYUN, S.H., SUN, G.M., CHOI, H.D., Development of a prompt gamma activation analysis facility using diffracted polychromatic neutron beam, Nucl. Instrum. Method **A 487** (2002) 521-529.

[3]   SUN, G.M., PARK, C.S., CHOI, H.D., "Improvement of the gamma-ray spectrometer of SNU-KAERI PGAA facility," 2002 KNS autumn meeting (Proc. Korean Nuclear Society, Yongpyong, 2002), The Korean Nuclear Society, Taejon (2002) (in Korean).

[4]   BYUN, S.H., SUN, G.M., CHOI, H.D., Characterization of a polychromatic neutron beam diffracted by pyrolytic graphite crystals, Nucl. Instrum. Method **A 490** (2002) 538-545.

[5]   LINDSTROM, R.M., "Development of a database for prompt γ-ray neutron activation analysis," Summary report of the second IAEA research coordination meeting, INDC(NDS)-424, Vienna (2001) 93-94.

[6]   INTERNATIONAL ATOMIC ENERGY AGENCY, X-ray and gamma-ray standards for detector calibration, IAEA-TECDOC-619, Vienna (1991).

[7]   FIRESTONE, R.B., Database of IAEA Coordinated Research Project for Prompt Gamma-Ray Neutron Activation Analysis (2002) private communication.

[8]   KIS, Z., et al., Comparison of efficiency functions for Ge gamma-ray detectors in a wide energy range, Nucl. Instrum. Method **A 418** (1998) 374.

[9]   FAZEKAS, B., et al., A new method for determination of gamma-ray spectrometer non-linearity, Nucl. Instrum. Method **A 422** (1999) 469.

[10] CHOI, H.D., SUN, G.M., BYUN, S.H., KANG, C.S., KIM, N.B., Benchmark measurements of the gamma spectroscopy performed by the SNU-KAERI PGAA facility, Progress report (2001) submitted to IAEA Nuclear Data Section on 26 August 2001.

[11] SUN, G.M., BYUN, S.H., CHOI, H.D., Prompt k_0-factors and relative γ-emission intensities for the strong non-1/v absorbers ^{113}Cd, ^{149}Sm, ^{151}Eu and ^{155,157}Gd, J. Radioanal. Nucl. Chem. (2002) in print.

[12] JEF-2.2 Nuclear Data Library, OECD Nuclear Energy Agency (2000).

[13] M.A. LONE, R.A. LEAVITT and D.A. HARRISON, Atomic Nucl. Data Tables **26** (1981) 511.

[14] S.F. MUGHABGHAB, Neutron Cross Sections, Vol. 1: Neutron Resonance Parameters and Thermal Cross Sections (Academic Press, New York, 1981).

[15] CHOI, H.D., SUN, G.M., PARK, C.S., Determination of prompt k_0-factors for B, N, Si, P and S, Progress report (2002) submitted to IAEA Nuclear Data Section on 19 December 2002.

Prompt γ-Ray Data Evaluation of Thermal-Neutron Capture for A=1-44

ZHOU Chunmei and WU Zhendong

China Nuclear Data Center
China Institute of Atomic Energy
P.O. Box 275(41)
Beijing 102413, P.R. China

Abstract: The method of prompt γ-ray data evaluation for thermal-neutron capture and how to calculate the prompt gamma-ray emission probability (absolute intensity) of thermal-neutron capture have been briefly presented. The prompt capture γ-ray data of some stable nuclei for A=1-44 have been evaluated. The ENSDF format has been adopted. The checks of physics and format have been made. The examples are given to illustrate its application.

1. Introduction

The energies and intensities, and their decay schemes of thermal-neutron capture γ-ray are one of the basic data of nuclear physics research, nuclear technology application and nuclear engineering design. Today, the technique of neutron-induced Prompt γ Activation Analysis (PGAA) is widely applied in material science, chemistry, geology, mining, archaeology, food analysis, environment, medicine, and so on. The availability of high-quality guided (or filtered) thermal and cold neutron beams at high and medium flux research reactors has greatly facilitated the advancement of the PGAA method during the 1990s.

PGAA is a non-destructive radioanalytical method, capable of rapid and simultaneous multielement analysis involving the entire Periodic Table, from hydrogen to uranium. The inaccuracy and incompleteness of the data available for use in PGAA are significant handicap in the qualitative and quantitative analysis of complicated γ spectra. Accurate and complete neutron capture γ-ray energy and intensity data are important for PGAA. The international database for PGAA is developing under the organization of Nuclear Data Section, IAEA.

The method of neutron-capture prompt γ-ray data evaluation and how to calculate the prompt gamma-ray emission probability (absolute intensity) of thermal-neutron capture are presented, and the data evaluation of ^{26}Mg(n,γ), ^{28}Si(n,γ) and ^{13}C(n,γ) is taken as an examples

how to evaluate the prompt γ-ray data, and how to calculate the prompt gamma-ray emission probability (absolute intensity) of thermal-neutron capture and how to give decay schemes in the text.

2   Main Evaluation Program

Main codes of thermal-neutron capture prompt γ-ray data evaluation and their functions are listed in Table 1. These codes are mainly from International Network[1] of Nuclear Structure and Decay Data Evaluation, the ENSDF data format is adopted in data evaluation.

Table 1   Main codes and their functions of prompt γ-ray

data evaluation for thermal-neutron capture

Code name	Main functions
GTOL	Level energy calculation by fitting to γ-energies
	Intensities balance calculation & checking
LWA	Limit-weighted and unweighted average of measured data
HSICC	Internal conversion coefficients calculation
RADLST	Energy balance calculation & checking
FMTCHK	ENSDF data format checking
PANDOR	ENSDF physics checking
ENSDAT	Drawing decay schemes & listing data tables

3.   Flow Chart of Prompt Neutron Capture γ Data Evaluation

The main flow chart of thermal-neutron capture γ-ray data evaluation is given in Fig.1. The basic characters are as follows:

a. Measured data collection

Evaluator retrieves related references from Nuclear Science References File, NSRF. On the basis of the retrieval, all measured data are collected from journals, reports, and private communications.

b. Measured data evaluation and recommendation of the best measured data

Gathered all related-data are analyzed and compared, treated by mathematical method (for example, limit-weighted or unweighted average of measured data). And then, the best-measured data and decay scheme can been recommended on the basis of the measured data evaluation.

c. Establishment of temporary data file

After recommendation of the best-measured data, the evaluated data are put into computer by hand, the temporary data file can be set up in ENSDF data format.

d. Theoretical calculation

Format checking must be done for temporary data file, and correction to old one should be done if necessary. Then, physics analysis and theoretical calculation are done and calculation results will be put into the gapes with no measured data so that recommended data become a self-consistent and complete data set.

e. Recommendation of complete data set

A complete data set of thermal-neutron capture prompt γ-ray data and its decay scheme is recommended as evaluated data set.

Start

```
┌─────────────────────────────────────────────┐
│   Nuclear Science References File, NSRF      │
└─────────────────────────────────────────────┘

┌─────────────────────────────────────────────┐
│        Retrieve required all References      │
└─────────────────────────────────────────────┘

┌─────────────────────────────────────────────┐
│     Collect measured data & related imformation     │
└─────────────────────────────────────────────┘

┌─────────────────────────────────────────────┐
│      Evaluate measued data & decay scheme     │
└─────────────────────────────────────────────┘

┌─────────────────────────────────────────────┐
│       Set up temporary data file in ENSDF     │
└─────────────────────────────────────────────┘

┌─────────────────────────────────────────────┐
│    Physics analysis & theoretical calculation │
│       fill all gapes with no measured data    │
└─────────────────────────────────────────────┘

┌─────────────────────────────────────────────┐
│          Recommende complete data sets        │
│      (complete data set and decay scheme)     │
└─────────────────────────────────────────────┘

┌─────────────────────────────────────────────┐
│          Physics & format checking            │
└─────────────────────────────────────────────┘

┌─────────────────────────────────────────────┐
│           Review & correct data file          │
└─────────────────────────────────────────────┘

┌─────────────────────────────────────────────┐
│        Put evaluated data files into ENSDF    │
└─────────────────────────────────────────────┘
```

Fig. 1 Flow chart of prompt γ-ray data evaluation for thermal-neutron capture

4.   Gamma-ray Absolute Intensity Calculation

In the experimental measurements, relative prompt gamma-ray intensities are measured. In the practical applications, prompt gamma-ray absolute intensities (emission probabilities) should be known. In general, the prompt gamma-ray emission probabilities per 100 neutron captures must be given for PGAA application.

Main and general methods of thermal-neutron capture prompt gamma-ray intensity calculation are summarized as follows:

4.1   Calculation from Gamma-ray Decaying to Ground State

When a nuclide captures a thermal-neutron, the gamma-rays decay in to its ground state, as shown in Fig. 2. If there are m gamma-rays decaying to ground state, I_k is the relative intensity for the k-th gamma-ray, α_k is its total internal conversion coefficient, the equation can be written as follows,

$$N\sum_{k=1}^{m} I_k(1+\alpha_k) = 100 \tag{1}$$

were N is normalization factor for gamma-ray emission probability per 100 neutron captures,

$$N = 100/\sum_{k=1}^{m} I_k(1+\alpha_k) \tag{2}$$

For light nuclides, the total internal conversion coefficient α_k is quite small and can be neglected, so

$$N = 100/\sum_{k=1}^{m} I_k \tag{3}$$

From Eq. (2) or (3), normalization factor N, and then, absolute gamma-ray emission probabilities for thermal-neutron capture can be calculated.

The relative gamma-ray data[2] for ^{26}Mg(n,γ) E_n=thermal are given in Ttable 2 and its decay scheme is shown in Fig. 3. In Table 2, the gamma-ray energies, their relative intensities and levels are given, from which, using Eq. (3) formula, N(=2.584) was calculated, and the absolute gamma-ray decay intensities also can be calculated , as shown in Fig. 3.
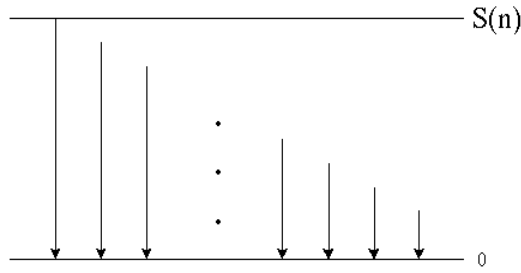
Fig. 2 Skeleton scheme of gamma-ray decaying to ground state from high excitation state
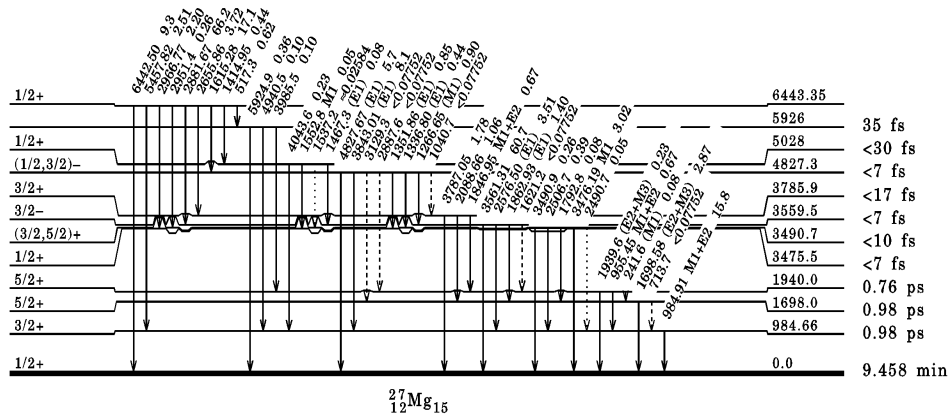
Fig. 3 Decay scheme and gamma-ray intensity from ^{26}Mg(n,γ) thermal neutron reaction

Table 2   Prompt gamma-ray data from ^{26}Mg(n,γ) thermal neutron reaction

E_γ/keV		E(level)/keV		I_γ *	Mult.**	δ**
241.6	4	1940.0	1	0.03 1	(M1)	
517.3	3	6443.35	4	0.24 3		
713.7		1698.0	1	<0.03		
955.45	8	1940.0	1	0.26 3	M1+E2	−0.08 6
984.91	3	984.66	8	6.1 3	M1+E2	+0.02 2
1040.7		4827.3	4	<0.03		
1266.65	18	4827.3	4	0.35 3	(M1)	
1336.80	20	4827.3	4	0.17 2	(E1)	
1351.86	8	4827.3	4	0.33 3	(E1)	
1414.95	18	6443.35	4	0.17 2		
1467.3	5	5028	1	0.03 1	(E1)	
(1537.2)		5028	1	≈0.01		
1552.8	7	5028	1	0.02 1	M1	
1615.28	5	6443.35	4	6.6 3		
1621.2		3559.5	1	<0.03		
1698.58	5	1698.0	1	1.11 7	(E2+M3)	≈0.0
1792.8 3		3490.7	7	0.03 1		
1846.95	18	3785.9	4	0.26 3	M1+E2	−0.0 3
1862.93	10	3559.5	1	0.54 4	(E1)	
1939.6 4		1940.0	1	0.09 2	(E2+M3)	≈0.0
2088.66	11	3785.9	4	0.41 3		
(2490.7)		3475.5	2	0.02 1		

E_γ/keV		E(level)/keV		$I_\gamma{}^*$	Mult.**	δ^{**}
2506.7	23	3490.7	7	0.15 2		
2576.50	6	3559.5	1	1.36 8	(E1)	
2655.86	6	6443.35	4	1.44 7		
2881.67	4	6443.35	4	25.6 8		
2887.6		4827.3	4	<0.03		
2951.4	4	6443.35	4	0.10 2		
2966.77	22	6443.35	4	0.85 6		
3129.3		4827.3	4	<0.03		
3476.19	9	3475.5	2	1.17 6	M1	
3490.9	6	3490.7	7	0.10 2		
3561.31	4	3559.5	1	23.5 7		
3787.05	15	3785.9	4	0.69 6		
3843.01	8	4827.3	4	3.14 16	(E1)	
3985.5	6	5926 2		0.04 1		
4043.6	3	5028 1		0.09 2		
4827.67	6	4827.3	4	2.20 13	(E1)	
4940.5	3	5926 2		0.04 1		
5457.82	15	6443.35	4	0.97 7		
5924.9	4	5926 2		0.14 2		
6442.50	6	6443.35	4	3.59 17		

   *   Relative intensity.

  ** Multipolarity and its mixture ratio for gamma-ray.

4.2 Calculation from Primary Gamma-ray Decaying from Capture State

When a nuclide captures a thermal-neutron, the nuclide is deexcited from its capture state by mean of decaying primary gamma-rays, as shown in Fig. 4. Suppose that there is n primary gamma-rays, j_i is the relative intensity of i-th primary gamma-ray and α_i is its total internal conversion coefficient of i-th primary gamma-ray, then,

$$N\sum_{i=1}^{m} j_i(1+\alpha_i) = 100 \tag{4}$$

$$N = 100 / \sum_{i=1}^{m} j_i(1+\alpha_i) \tag{5}$$

And for light nuclide, Eq. (5) becomes

$$N = 100 / \sum_{i=1}^{m} j_i \tag{6}$$

The primary gamma-ray data[3,4] for ^{28}Si(n,γ) E_n=thermal are listed in Table 3, and their decay scheme is given in the Fig. 5. From table 3, the normalization factor N(0.5917) and the gamma-ray absolute decay intensities for each gamma-ray can be calculated, as shown in Fig. 5.
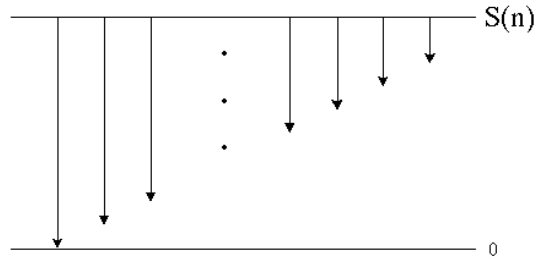
Fig. 4   Skeleton scheme of primary gamma-rays from captured state
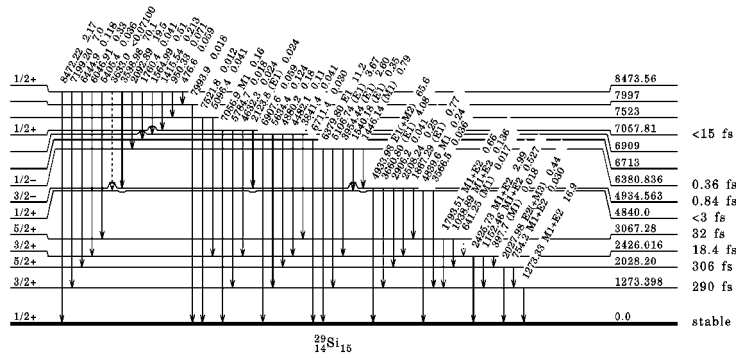
Fig. 5   Decay scheme and gamma-ray intensity from ^{28}Si(n,γ) thermal neutron reaction

Table 3   Prompt gamma-ray data from ^{28}Si(n,γ) thermal neutron reaction

E_γ/keV		E(level)/keV		I_γ*		Mult.**	δ**	
397.7	4	2426.016	15	0.03	1	(M1)		
476.6	3	8473.56	3	0.10	2			
(641.25)		3067.28	8	0.029	15	(M1)		
754.2	4	2028.20	6	0.05	2	M1+E2	−0.03	3
950.33	13	8473.56	3	0.12	2			
1038.89	10	3067.28	8	0.23	3	M1+E2	+0.04	2
ˣ1071.0	5			0.08	2			
1152.46	6	2426.016	15	0.89	4	M1+E2	+0.09	8
1273.33	3	1273.398	11	28.5	14	M1+E2	+0.197	9
1415.54	9	8473.56	3	0.36	4			
1446.14	4	6380.836	13	1.34	5	(M1)		
1540.18	6	6380.836	13	0.59	5	(E1)		
1564.99	5	8473.56	3	0.87	6			
1760.4	5	8473.56	3	0.07	2			
1793.51	4	3067.28	8	1.12	6	M1+E2	+0.26	2
1867.29	5	4934.563	13	1.30	6	(E1)		
2027.98	9	2028.20	6	0.74	7	E2(+M3)	0.0	
2092.89	3	8473.56	3	33.0	12			
2123.8	6	7057.81	17	0.04	1	(E1)		
2425.73	4	2426.016	15	5.06	20	M1+E2	−0.32	7
2508.24	13	4934.563	13	0.42	5			

E_γ/keV		E(level)/keV		I_γ *		Mult.**	δ**	
2906.2	5	4934.563	13	0.07	2			
3538.98	4	8473.56	3	118.5	36			
3566.5	5	4840.0	4	0.06	2			
3633.0		8473.56	3	<0.12				
3660.80	6	4934.563	13	6.9	3	(E1)		
3841.4	6	6909		0.07	2			
3954.44	5	6380.836	13	4.4	3	(E1)		
4482.1	4	6909		0.18	5			
4632.3	7	7057.81	17	0.04	2			
4839.6	4	4840.0	4	0.40	5	M1		
4880.2	5	6909		0.30	5			
4933.98	3	4934.563	13	110.8	34	E1(+M2)	–0.05	10
5096.4	7	7523		0.07	2			
5106.74	6	6380.836	13	6.2	3	(E1)		
5405.4	9	8473.56	3	0.06	2			
5634.4	4	6909		0.21	3			
5784.7	7	7057.81	17	0.03	1			
6046.91	16	8473.56	3	0.55	6			
6379.80	4	6380.836	13	19.0	10	E1		
6444.9	5	8473.56	3	0.20	4			
6711.4	9	6713		0.05	2			
6907.6	7	6909		0.10	3			
7056.9	4	7057.81	17	0.27	5	M1		
7199.20	5	8473.56	3	11.9	5			
7521.8	9	7523		0.02	1			
7993.9	9	7997		0.03	1			
8472.22	7	8473.56	3	3.66	20			

* Relative intensity.   ** Multipolarity and its mixture ratio for gamma-ray.

x Unplaced in level scheme

5 Physical Consistent Check

The most important is the physical consistent check of intensity balance check for each levels.

For decay gamma-ray to ground state, the Eq. (1) becomes

$$\sum_{k=1}^{m} I_k(1+\alpha_k) = 100/N \tag{7}$$

For primary gamma-ray from captured state, the Eq. (4) becomes as follows,

$$\sum_{i=1}^{n} J_i(1+\alpha_i) = 100/N \tag{8}$$

from Eq. (7) and (8), Eq.(9) can be got as,

$$\sum_{i=1}^{n} J_i(1+\alpha_i) \approx \sum_{k=1}^{m} I_k(1+\alpha_k) \tag{9}$$

The Eq. (9) is correct within their uncertainty range. For other levels, in addition to

captured state and ground state, the intensities coming into and going out the level j are the same within thier uncertainty range, as shown in Fig. 6.

$$\sum_{k=1}^{m} I_{jik}(1+\alpha_{jik}) - \sum_{i=1}^{n} I_{joi}(1+\alpha_{joi}) \approx 0 \qquad (10)$$

In formula (10), I_{jik}, α_{jik}, I_{joi}, and α_{joi} are gamma-ray relative intensities and their internal conversion coefficients for coming into and going out level J respectively.

In Table 4, the calculation and checking results of intensity balance for each levels from ^{28}Si(n,γ) reaction are given. From Table 4 it can be seen that the intensities are consistent within their uncertainties.
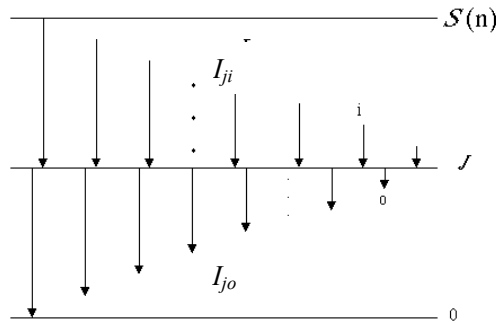
Fig. 6   Skeleton scheme of intensity balance calculation for excitation level

Table 4 Calculation and checking results of intensity balance from ^{28}si(n,γ) reaction at E_n=thermal

LEVEL	RI[@] (OUT)		RI[@] (IN)		RI[@] (NET)		TI[#] (OUT)		TI[#] (IN)		TI[#] (NET)		NET FEEDING[*] (CALC)	
0	0.000		169	4	−169	4	0.000		169	4	−169	4	0.2	23
1273.398 11	28.5	14	27.4	7	1.1	16	28.5	14	27.4	7	1.1	16	0.7	10
2028.20 6	0.79	8	0.83	8	−0.04	11	0.79	8	0.83	8	−0.04	11	−0.02	7
2426.016 15	5.98	21	5.7	4	0.3	4	5.98	21	5.7	4	0.3	4	0.17	23
3067.28 8	1.38	7	1.43	7	−0.05	10	1.38	7	1.43	7	−0.05	10	−0.03	6
4840.0 4	0.46	6	0.59	5	−0.13	8	0.46	6	0.59	5	−0.13	8	−0.08	5
4934.563 13	119	4	120	4	0	5	119	4	120	4	0	5	0	3
6380.836 13	31.5	11	33.0	12	−1.5	17	31.5	11	33.0	12	−1.5	17	−0.9	10
6713	0.050	20	0.070	20	−0.02	3	0.050	20	0.070	20	−0.02	3	−0.012	17
6909	0.86	9	0.87	6	−0.01	11	0.86	9	0.87	6	−0.01	11	−0.01	7
7057.81 17	0.38	6	0.36	4	0.02	7	0.38	6	0.36	4	0.02	7	0.01	4
7523	0.090	23	0.120	20	−0.03	3	0.090	23	0.120	20	−0.03	3	−0.018	18
7997	0.030	10	0.100	20	−0.070	23	0.030	10	0.100	20	−0.070	23	−0.041	14
8473.56 3	169	4	0.000		169	4	169	4	0.000		169	4	100.3	23

[@] relative intensity.   [#] relative intensity including internal conversion.   [*] absolute intensity balance.

6 Application

The prompt γ-ray data and their decay schemes of thermal-neutron capture for stable nuclei[8-10] [1]H, ^{2}H, [6]Li, [7]Li, [9]Be, ^{12}C, ^{13}C, ^{14}N, ^{16}O, [17]O, ^{19}F, [20]Ne, [21]Ne, [22]Ne, [23]Na, [24]Mg, [25]Mg, [26]Mg, [27]Al, [28]Si, [29]Si, [30]Si, ^{31}P, [32]S, [33]S, [34]S, [35]Cl, [36]Ar, [36]S, [37]Cl, [39]K, [40]Ar, [40]Ca, [40]K, [41]K, [42]Ca, [43]Ca, [44]Ca and others[11] have been evaluated by using these programs.

The data evaluation of [13]C(n,γ) reaction at E=thermal[5] is taken as an example to show its application. The evaluated data of ENSDF format for [13]C(n,γ) reaction at E=thermal are given in Table 5. The evaluated level data and γ-radiation data are listed in Table 6 and 7, respectively. The decay scheme of [13]C(n,γ) reaction at E=thermal is given in Fig. 7. The γ-ray intensities balance is given in Table 8. From these tables and scheme it can be seen that the evaluated data are self-consistent in physics and intensity balance.

Table 5 ENSDF format listing of evaluated data for [13]C(n,γ) reaction at E=thermal

```
14C        13C(N,G) E=THERMAL                1982MU14
14C    C   TARGET JPI=1/2-.
14C    C   1982MU14: MEASURED EG AND IG, DEDUCED SN.
14C    C   EVALUATED SN=8176.44 KEV 1 (1995AU04).
14C    CL E          FROM EG USING LEAST-SQUARES FIT TO DATA.
14C    CL J,T        FROM 1996FIZY, except as noted.
14C    CG E          FROM 1996FIZY, EXCEPT AS NOTED.
14C    CG E(A)       FROM LEVEL ENERGY DIFFERENCES.
14C    CG RI         INTENSITIES PER 100 NEUTRON CAPTURES FROM 1982MU14.
14C      N 1
14C      PN
14C    L 0.0         0+                5730 Y     40
14C 3  L %B-=100$
14C    L      6093.82201-             7 FS       LT
14C    G 6092.4     2 16.3      8
14C 3 G FL=0.0
14C    L      6589.5 30+             3.0 FS     4
14C    G 495.4      3 8.0       3
14C 3 G FL=6093.82
14C    L      6902.7 30-             25 FS      3
14C    G 808.9      2 3.6       3
14C 3 G FL=6093.82
14C    L   8176.44 1 0-,1-                          S
14C    CL J          FROM S-WAVE NEUTRON CAPTURE
14C    G 1273.81     174.9      10
14C 3 G FL=6902.7$ FLAG=A
14C    CG            EG=1273.9 2 (1982MU14)
14C    G 1586.92     188.5      5
14C 3 G FL=6589.5$ FLAG=A
14C    CG            EG=1586.8 2 (1982MU14)
14C    G 2082.53     182.5      5
14C 3 G FL=6093.82$ FLAG=A
```

```
14C   CG          EG=2082.6 3 (1982MU14)
14C   G 8174.0    3 84.0    23
14C 3 G FL=0.0$ FLAG=A
14C   CG          EG=8173.92 (1982MU14)
```

Table 6   Level listing of evaluated data for ^{13}C(n,γ) reaction E=thermal

^{14}C Levels

E(level)+		Jπ*	T$_{1/2}$*			Comments
0.0		0+	5730	y	40	%β$^-$=100
6093.82	20	1-	<7	fs		
6589.5	3	0+	3.0	fs	4	
6902.7	3	0-	25	fs	3	
(8176.44	1)	0-,1-				Jπ : from s-wave neutron capture

+   From Eγ using least-squares fit to data.
*   From 1996FIZY, except as noted.

Table 7   γ-ray listing of evaluated data for ^{13}C(n,γ) reaction E=thermal

γ (^{14}C)

Eγ+		E(level)	Iγ$^{\#@}$		Comments
495.4	3	6589.5	8.0	3	
808.9	2	6902.7	3.6	3	
1273.81 *	17	(8176.44)	4.9	10	Eγ=1273.9 2 (1982Mu14)
1586.92 *	18	(8176.44)	8.5	5	Eγ=1586.8 2 (1982Mu14)
2082.53 *	18	(8176.44)	2.5	5	Eγ=2082.6 3 (1982Mu14)
6092.4	2	6093.82	16.3	8	
8174.0 *	3	(8176.44)	84.0	23	Eγ=8173.9 2 (1982Mu14)

+   From 1996FIZY, except as noted.
*   From level energy differences.
#   Intensities per 100 neutron captures from 1982MU14.
@   For intensity per 100 neutron captures, multiply by 1.
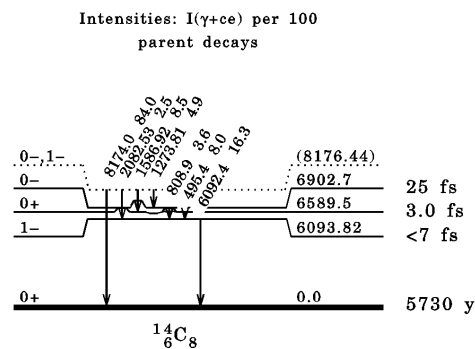
Fig. 7   Decay scheme of evaluated data for ^{13}C(n,γ) reaction E=thermal

Table 8   Intensities balance listing of evaluated data for ^{13}C(n,γ) reaction *E*=thermal

LEVEL		RI (OUT)		RI (IN)		RI (NET)		TI (OUT)		TI (IN)		TI (NET)		NETFEEDING (CALC)	
0.0		0.0		100.3	25	-100.3	25	0.0		100.3	25	-100.3	25	-0.3	25
6093.82	20	16.3	8	14.1	7	2.2	11	16.3	8	14.1	7	2.2	11	2.2	11
6589.5	3	8.0	3	8.5	5	-0.5	6	8.0	3	8.5	5	-0.5	6	-0.5	6
6902.7	3	3.6	3	4.9	10	-1.3	11	3.6	3	4.9	10	-1.3	11	-1.3	11
8176.44	1	100.	3	0.0		100.	3	100.	3	0.0		100.	3	100.	3

7   Discussion

In general, neutron binding energy is high, and captured state is a high excitation state and its decay scheme is quite complex. A lot of weak-intensity gamma-ray are unable to be measured experimentally. Besides, measured uncertainties from background deducting and gamma-spectra analysis lead to gamma-ray intensity uncertainties. Strictly speaking, intensities of coming into and going out a level are unable to be exactly same, only can be consistent within their uncertainties. The normalization factors from primary gamma-rays from captured state and decay gamma-rays to ground state are different since above reasons. In the data evaluation, normalization factor in thermal-neutron capture reaction is usually calculated from the gamma-rays of decay to ground state.

References

[1]   T.W. Burrows. ENSDF Physics Analysis Codes. Private Communication (1998)

[2]   S.Raman, et al., Phys.Rev. C46, 972 (1992)

[3]   N.A.Islam, et al., Phys.Rev. C41, 1272 (1990)

[4]   T.A.Walkiewiez, et al., Phys.Rev. C45, 1597 (1992)

[5]   S.F.Mughabghab, et al., Phys. Rev. C26, 2810 (1982)

[6]   G.Audi,et al., Nucl. Phys. A 595, 409(1995)

[7]   R.B.Firestone, et al., Table of Isotopes (8th Edition) Vol.1 (1996)

[8]   Zhou Chunmei,   INDC(CPR)-051. Thermal-neutron capture data for A=1-25 (2000)

[9]   Zhou Chunmei, et al., INDC(CPR)-054. Thermal-neutron capture data for A=26-35 (2001)

[10] Zhou Chunmei, et al., INDC(CPR)-057. Thermal-neutron capture data for A=36-44 (2003)

[11] Zhou Chunmei, INDC(CPR)-055. Thermal-neuton capture data update and revision for some nuclides with A>190 (2001)

Analysis of Alloys by Prompt Gamma ray Neutron Activation

A. G. C. Nair[a], K. Sudarshan[a], N. Raje[b], A.V. R. Reddy[a], S.B. Manohar[a] and,

A. Goswami[a*]

[a]Radiochemistry Division, [b]Analytical Chemistry Division

Bhabha Atomic Research Centre

Trombay, Mumbai - 400 085

INDIA

Abstract

A Prompt Gamma ray Neutron Activation Analysis method based on efficiency calibration using the prompt gamma rays emitted from the constituent elements of the sample has been used to determine the composition in some alloys non-destructively. This method is independent of sample geometry and size. The results are in good agreement with the reported composition.

Introduction

The Prompt Gamma ray Neutron Activation Analysis (PGNAA) is emerging as an attractive tool for the determination of elemental concentration in various types of samples (1-3). The method is based on the measurement of prompt gamma rays emitted following neutrons capture by the elements present in the sample. The energies of the gamma ray are characteristic of the isotopes of the elements and their intensities are proportional to their concentration. Therefore, the prompt gamma ray spectrum from a sample carries qualitative as well as quantitative information of the elements present in the sample. The PGNAA method is ideally suited for determination of most of the elements including low Z elements like H, B, Si, P, S, and Ti. These low Z elements are difficult to detect or have low sensitivities in off line neutron activation analysis (NAA). However, the technique is also applicable to heavier elements. One of the main problems associated with PGNAA is the low sensitivity due to the low intensity of the neutron beams (usually $\sim 10^6$-10^8n/cm^2/s). Small sample amounts are used for analysis in order to avoid the cumbersome procedures required to correct for the effect of absorption and scattering of neutrons and absorption of gamma rays by the sample. The large sample analysis has been taken up by limited groups of analysts using the neutron beam irradiation facility from research reactors with guided beams (4-7). Analysis of large sample under different/varying geometrical conditions would greatly enhance the applicability of the PGNAA technique for varieties of samples like alloys, precious archeological samples and geological samples. The large sample analysis also attains its utmost importance when the normal strategy of sub sampling to mg level becomes some times questionable in terms of representativeness and homogeneity (8,9).

---

[*] Corresponding Author (E-mail: agoswami@apsara.barc.ernet.in, FAX: 91-22-25505151)

The general methodologies adopted in PGNAA are broadly based on four approaches: namely, absolute method, comparative method, monostandard method or k_0- method and the internal monostandard method (4-6). Several Prompt k_0- factors are compiled / updated to pave the way for increased accuracy of PGNAA measurements which allow to perform multielement analysis without standards. The k_0-values are determined in advance for a neutron beam facility. The principle and the details of the calculations of this method are discussed elsewhere (1-3).

An internal mono-standard method, similar to that of the k_0-method of conventional NAA, especially suited for bulk samples was originally proposed by Sueki et.al (6). Instead of an external comparator, an element present in the sample itself was taken as a standard/comparator and the concentration of the constituents were obtained relative to this. The element that can be easily determined or that is present in major proportion in the sample is taken as the comparator element. The method being relative takes care of the problems like neutron self-shielding, scattering and fluence rate variations. The ratio of measured full energy peak areas (A_x/A_c) of the gamma rays from an isotope of the element x to that of the element c is related to weight ratio (W_x/W_c) of the elements by the expression

$$\frac{W_x}{W_c} = \frac{A_x.(\sigma\varepsilon\theta a)_c.M_x}{A_c.(\sigma\varepsilon\theta a)_x.M_c} = \frac{A_x.M_x}{A_c.M_c} \cdot \frac{1}{k_0} \cdot \frac{\varepsilon_c}{\varepsilon_x} \tag{1}$$

where $(\sigma\theta\varepsilon a)$ is the product of neutron absorption cross section, isotopic abundance, full energy peak detection efficiency and, gamma ray abundance. M_x and M_c, are the atomic weights of the element of interest and the comparator. The relative efficiency value $\varepsilon_c/\varepsilon_x$ either can be predetermined or generated using the prompt gamma rays of the comparator. Under favorable conditions, concentration ratios calculated using equ. (1) can be converted to percentage composition by material balance. Otherwise a known concentration of any element in the matrix can be used to obtain the absolute concentration values.

We report an internal mono-standard method to determine the relative elemental concentrations from single irradiation. This method incorporates a new methodology to calculate the relative efficiency from the prompt gamma rays of several nuclides present in the sample and is applicable to the samples of irregular size or shape. The method has been validated by analyzing some reference alloy standards like Ferrotitanium (BCS 243/4), Ferrosilicon alloy (BCS 305/1) and alloy-718 containing elements like Fe, Ti, Cr, Ni and Mo.

Experimental

The neutron beam facility at 100 MW Dhruva research reactor, Bhabha Atomic Research Centre, Mumbai, India was utilised in the present experiment. A mono-energetic (55meV) reflected neutron beam from graphite crystal was used in the present studies. The dimension of neutron beam was 2.5×10 cm. The thermal equivalent flux was measured by gold activation and found to be about 1.6×10^6 n-cm^{-2}-s^{-1}.

A 40% coaxial horizontal HPGe detector was used for measurement of prompt gamma rays. It was kept at a distance of about 30cm from sample position and at an angle of 90° with respect to the beam direction. The detector was surrounded by 30cm thick lead block, having a collimator of 4cm dia. A 1cm thick boron carbide sheet, having a central aperture of 4cm dia. was placed in front of the lead collimator to minimise the stray neutrons entering the detector. The detector was coupled to a PC based 8 k multi-channel analyser. The resolution of the detector was 2.0 keV at 1332 keV. The MCA was calibrated in the energy region of 0.1 to 8 MeV using the delayed gamma rays from ^{152}Eu and ^{60}Co, and prompt gamma rays from ^{36}Cl. The alloy-718 in the form of 1.5mm thick plates and the other samples in powder form, were wrapped in polytetraflouroethylene (PTFE) tape of 0.1mm thickness. They were suspended from a quartz rod kept above the beam path with a Teflon string. The weight of the samples ranged from 2-6 grams. The samples were irradiated for sufficiently long time to achieve good counting statistics. Photo peak areas under the individual gamma lines were determined by analyzing the gamma ray spectra using the software PHAST developed in Electronics Division, Bhabha Atomic Research Centre (10). The software has features for energy calibration and determination of peak shape parameters. A second order polynomial in energy was used to calibrate the width (FWHM) of the individual peaks. The measured FWHM and shape parameters as function of energy were used to deconvolute the multiplets.

Efficiency calibration

In conventional neutron activation analysis (relative method), the sample and standard are irradiated and counted under identical geometrical conditions. In absolute method, the full energy peak detection efficiency calibration is a prerequisite. When the sample is of non-standard geometry, determination of the γ-ray detection efficiency is extremely difficult. The efficiency is normally simulated with Monte Carlo calculations (8-9). The methods like Monte Carlo calculation for efficiency are cumbersome. However, when the sample is homogeneous, γ-rays from any radionuclide in the sample can be used to obtain the relative full-energy peak detection efficiency of the γ-rays. When gamma rays from more than one radionuclide are required to cover the requisite energy range, the commonly used expression for efficiency, the polynomial in logarithm of energy can be written as

$$\ln \varepsilon_E = k_j + \sum_{i=0}^{m} a_i (\ln E)^i \quad (2)$$

Where ε_E is the full energy peak detection efficiency of gamma ray of energy E, k_j is a constant characteristic of the jth nuclide and *m* is the order of the polynomial that can be chosen depending on the energy range of interest. The various functional forms that are used to represent the efficiency in different energy ranges is reviewed by Kis et al.(11). Once the relative efficiency calibration curve is constructed, the relative concentration are calculated using equ.(1).

The prompt gamma ray peak areas corresponding to Fe, Cr, Ti, and Ni were corrected for their gamma ray abundances and fed as input data for relative efficiency calculation. The relative efficiencies thus obtained as a function of gamma ray energy (E) were fitted to a fifth order polynomial using the equ. (2). A standard nonlinear least square program was used for efficiency fitting by imposing a condition that the peak areas of the gamma lines from a particular isotope are to be fitted with a particular constant k_j so that the relative efficiencies for all the gamma lines from different isotopes fall on a single curve. The details of the efficiency calibration are given in Ref.12.

RESULTS AND DISCUSSION

Figure 1. shows typical prompt gamma ray spectrum of the Fe-Ti alloy sample. The important gamma ray energies and the corresponding nuclides are also shown in the figure. The higher energy portion of the spectrum is complex because of the presence of first and second escape peaks. One of the important parameters in the equ.(1) for calculating the relative concentration is the relative efficiency ratio, which was obtained from equ.(2). A typical in-situ efficiency curve obtained for the alloy-718 sample is given in Fig.2. Here gamma rays from Fe, Ni, Co and Ti present in the sample were used in equ.(2) to obtain the efficiency curve. The errors shown include the errors arising from counting statistics, abundances of gamma rays and peak area fitting in deconvoluting multiplets. Though, Sukei et.al.[6] used the gamma rays from sample for relative efficiency calibration. They used a linear function in logarithm of energy and efficiency over a limited energy range. The method used here for efficiency calibration is more general for any form of equation and more realistic over a wide range of energy. The concentration ratios with respect to Fe were determined from the relative efficiency values using eqn.(1) for all the three samples. The corresponding thermal neutron cross-sections values were taken from Ref.13. The gamma ray abundance values were taken from the latest relevant Nuclear Data Sheets and Ref.14. The relevant nuclear data used in the calculation are given in Table.1. The relative concentration values were converted to % composition using the material balance with the assumption that the sum of the amount of all the constituent elements of the matrix is equal to the sample weight [15]. It is to be noted here that inability to identify or determine the concentration of one or more major constituents of the matrix results in systematically higher concentration of the remaining elements determined by this method. Results of analysis carried out for the major and minor elements in three types of alloys are given in Table.2. The values are the average from replicate measurements. The errors quoted are the standard deviations and range from 2-6%. For simple systems like that of Ferro-titanium or Ferro-Silicon the values are in good agreement with the reported concentration as seen from Table 2. The value of Al is higher as the contribution from the detector casing caused by activation from scattered neutrons couldn't be corrected for. For alloy-718 sample, it was not possible to determine Nb, which is present at 5% level, due to the interference from Mo, Ni and Co. Accordingly; the results correspond to 95% of the material present and are systematically higher. Though it is advisable to use system determined ratio $(\sigma\theta a)_x/(\sigma\theta a)_c$ or k_0 values, we found that the use of literature values of thermal neutron absorption cross section (σ), isotopic abundance(θ) and gamma ray abundance (a) does

not alter the results significantly for the elements determined in this work as they are 1/v nuclei.

Conclusions

In order to use the PGNAA as truly non-destructive technique, it is essential that it should be possible to determine the elemental concentrations in a sample independent of its size, shape and amount. We developed a method to determine the relative concentrations of the elements with respect to a major constituent element of the sample using an in-situ efficiency calibration methodology taking into account prompt gamma rays from the individual components of the sample. The method was validated by analysing some alloy standards. The relative concentration values were converted to % composition using material balance. This method is independent of geometry of the sample. The values given are average values obtained from multiple gamma rays of a given element as well as multiple measurements. The results are good within 10% of the reported values. The results demonstrate the potential of the PGNAA technique as a non-destructive tool for obtaining compositional characteristics of a matrix. Further, the present method of obtaining relative efficiency from gamma rays of the sample itself makes it a geometry independent method.

Acknowledgements

References

[1] C. Yonezawa, and H. Matsue; J. Radioanal. Nucl. Chem., 244 (2000) 373.

[2] R. L. Paul, and R. M. Lindstrom; J. Radioanal. Nucl. Chem., 243 (2000) 181.

[3] G. L. Molnar, Zs. Revay, R. L. Paul, and R. M. Lindstrom; J. Radioanal. Nucl. Chem., 234 (1998) 21.

[4] S. K. Latif, Y. Oura, M. Ebihara, G. W. Kallemcyn, H. Nakahara, C. Yonezawa, T. Matsue, and H. Sawahata; J. Radioanal. Nucl. Chem. 239 (1999) 577.

[5] ZS. Kasztovszky, ZS. Revay, T. Belgya, and G. L. Molnar; J. Radioanal. Nucl. Chem., 244 (2000) 379.

[6] K. Sueiki, K. Kobayashi, Sato, H. Nakahara, and T. Tomizawa; Anal. Chem., 68 (1996) 2203.

[7]   H. Nakahara, Y. Oura, K. Sueiki, M. Ebihara, W. Sato, S. K. Latif, T. Tomizawa, S. M. Enomoto, C. Yonezawa, and Y. Ito; J. Radioanal. Nucl. Chem., 244 (2000) 405.

[8] R. M. W. Overwater, P. Bode, J. J. M. De Goeij, and J. Eduard Hoogenboom; Anal. Chem., 68 (1996) 341.

[9] P. Bode, R. M. W. Overwater, and J. J. M. De Goeij; J. Radioanal. Nucl. Chem. 216(1) (1997) 5.

[10] P. K. Mukopadhyay, Proceedings of the symposium on Intelligent Nuclear Instrumentation, Mumbai, 2001, p.313.

[11] Z. Kis, J. Fazekas, J. Ostor, Zs. Revay, T. Belgya, G. L. Molnar, and L. Koltay; Nucl. Instr. and Meth. A418 (1998) 374.

[12] K. Sudarshan, A. G. C. Nair, and A. Goswami, J. Radiochem. Nucl. Chem., 2002 (in press).

[13] S. F. Mughabghab, M. Divadeenam and, N. E. Holden; Neutron Cross sections, Vol.1: Neutron Resonance Parameters and Thermal Cross Sections, Part A Z=1-60 (Academic Press, New York, 1981).

[14] Z. Chunmei, and R. B. Firestone; INDC (CPR)-054, IAEA Nuclear Data Section, Vienna, Austria.

[15] D. L. Perry, R. B. Firestone, G. L. Molnar, Zs. Reavy, Zs. Kasztovszky, R. C. Gatti, and P. Wilde; J. Anal. At. Spectrom. 17 (2002) 32.
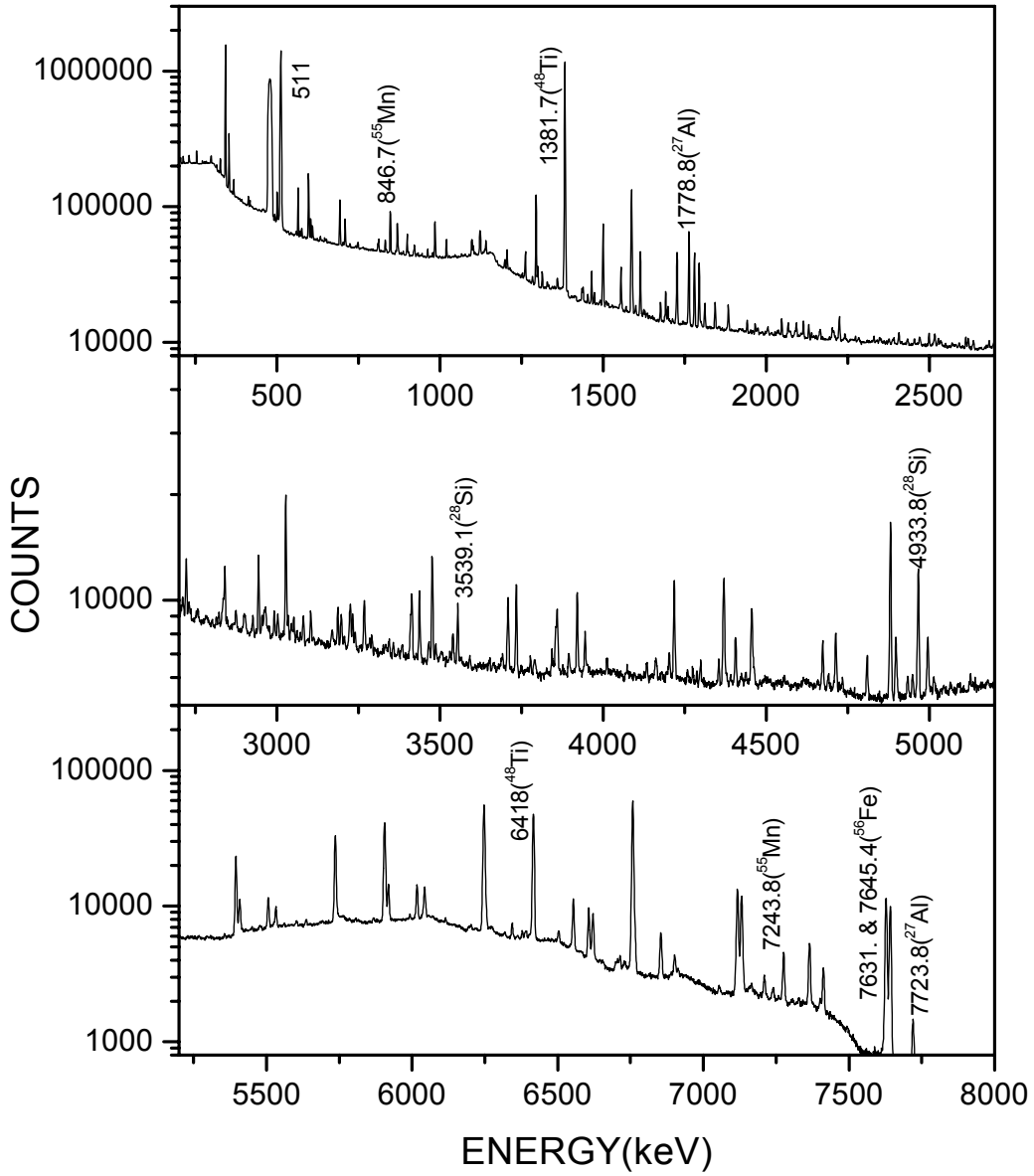
Fig.1. Prompt gamma ray spectrum of the ferro-titanium alloy BCS-243/4
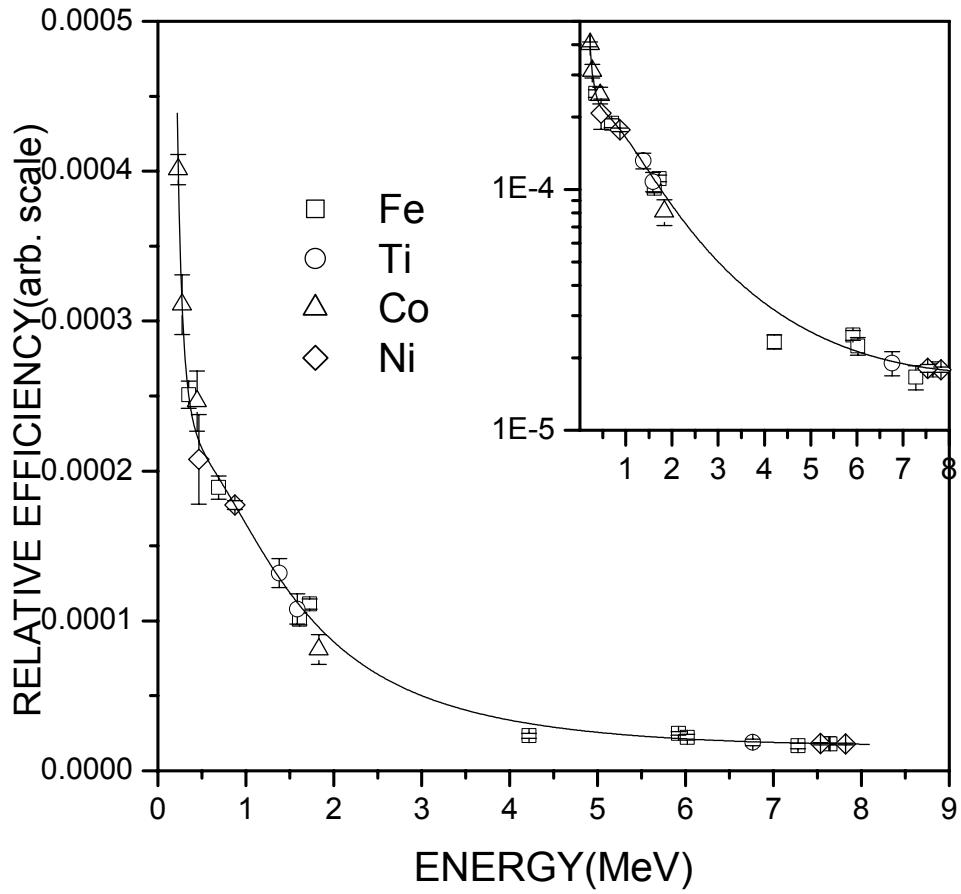
Fig.2. Relative in-situ efficiency calibaration from Alloy-718 sample.
(Inset shows in logarithm scale)

TABLE-1: NUCLEAR CONSTANTS USED IN THE ANALYSIS

Capturing Isotope	Isotopic Fraction	Cross Section (barn)	Energy (keV)	Gamma abundance (%)
^{27}Al	1.00	0.231	7723.8	26.8
^{27}Al	1.00	0.231	1778.8	100.00
^{59}Co	1.00	37.18	229.8	15.71
^{59}Co	1.00	37.18	277.4`	15.26
^{59}Co	1.00	37.18	555.9	13.86
^{50}Cr	0.04345	15.9	749.1	80.0
^{52}Cr	0.8379	0.76	7937.9	17.2
^{53}Cr	0.095	18.2	834.8	26.86
^{56}Fe	0.9175	2.59	7631.0	29.1
^{56}Fe	0.9175	2.59	692.1	4.75
^{55}Mn	1.00	13.36	846.8	98.9
^{55}Mn	1.00	13.36	7057.8	11.06
^{55}Mn	1.00	13.36	7243.8	12.13
^{95}Mo	0.1592	13.4	778.2	96.16
^{60}Ni	0.2623	2.9	7819.6	37.5
^{28}Si	0.9227	0.173	4933.8	65.7
^{48}Ti	0.737	7.88	1381.7	85.8
^{48}Ti	0.737	7.88	6418.3	30.5

Table.2. Results of analysis of alloy samples by PGNAA

(All concentrations are given as % weight)

Alloy sample	Alloy-718[a]	Fe-Ti BCS-243/4[c]	Fe-Si BCS-305/1[c]
Fe	19.3±0.5 (18)	44±2(46.7)	24±1(23.2)
Ti	0.69 ±0.07 (0.5)	37±4(38.2)	-
Ca	-	-	(0.33)
Co	0.43 ±0.04(0.03) [b]	-	-
Cu	-	(0.14)	-
Ni	58±1(52)	-	-
Cr	18.8±0.1(18)	-	-
Mo	2.2±0.2(3)	-	-
P	-	-	(0.03)
Si	-	3.6±0.2(3.8)	76±3(75)
Al	(0.5)	14±1(10.5) [b]	(1.38)
Mn	-	0.49±0.11(0.52)	-
Nb	(5)	-	-

1. [a] The nominal composition is given in parenthesis

2. [b] Interference from background materials

3. [c] Numbers in parenthesis are the certified values

List of legends

PROGRESS REPORT FOR THE PERIOD:
1 OCTOBER 2001 - 31 DECEMBER 2002

Radiochemistry Division
Bhabha Atomic ResearchCentre,
Mumbai, 400 085, India.

COORDINATED RESEARCH PROJECT:
Development of a Data Base for Prompt Gamma-Ray Neutron Activation Analysis

TITLE OF THE PROJECT:
Evaluation and measurement of prompt k_o-factors to use in prompt gamma-ray neutron activation analysis

IAEA Research Contract No. 10733/ Regular Budget Fund:

Chief Investigator:
Annareddy V.R. Reddy

Co-investigators:
A.G.C. Nair, A. Goswami, K. Sudarshan, Y.M. Scindia, R. Acharya and S.B. Manohar

Progress Report

In continuation of our development work on prompt gamma-ray neutron activation analysis (PGNAA), we report a brief summary of the experimental results. As mentioned in our previous report, we have used a PGNAA facility using a reflected neutron beam at Dhruva research reactor. A tangential beam of the neutrons from the reactor core was reflected by a graphite crystal and taken to the experimental site. The beam is mainly composed of 1st order reflection, having neutron energy 0.05eV. The neutron beam characteristics like dimension, homogeneity and thermal equivalent flux were evaluated. The absolute efficiency, in the energy range of 0.1-8.5 MeV, of the detection system consisting of 40% HPGe and PC based MCA, was determined using delayed gamma rays from ^{152}Eu and the prompt gamma rays from ^{36}Cl and ^{49}Ti. The prompt gamma-ray spectra of elements such as V, Zn, S, N, Sc, Mn, Se, Cu, Ca and Si have been acquired and their corresponding prompt k_0-factors were determined with respect to 1951 keV of ^{36}Cl. We have also developed a k_0-based internal mono standard PGNAA method, which utilizes in situ efficiency calibration using the prompt gamma rays of isotopes/elements in the sample. This method takes care of gamma-ray self attenuation and is independent of size and shape (geometry) of the sample. This internal mono standard based methodology of PGNAA has been applied to analyse the samples such as (i) aluminosilicate and graphite mixture as a part of the benchmark experiments, (ii) Lake sediment certified reference material, IAEA CRM SL-3 to check the validity of some of the determined k_0-factors, and (iii) alloy samples containing elements like Fe, Ti, Si, Mo and Nb. The results of the above mentioned work have been reported below, under following headings.

1. Measurement of prompt k_0-factors

2. Results on benchmark experiments

3. Checking of prompt k_0-factors: Analysis of IAEA CRM SL-3

4. Application of k_0-based PGAA for the composition analysis of alloys

1. Measurement of Prompt k_0-factors

Prompt gamma-ray spectra of the elements were acquired using the elemental standards either in the form of chloride salts or an intimate mixture of the same with NH_4Cl. In addition to the prompt k_0-factors in our last report, the determined values of prompt k_0 factors of other elements: N, Si, V, Zn, S, Sc, Mn, Cu, Se and Mo are given in Table 1. These values have been compared with the literature values, which were obtained from the k_0 (H) values of Revay et al#. In order to ascertain the accuracy of the values and reproducibility of the experimental conditions, the k_0-factor of ^{36}Cl for 786+788 keV with respect to 1951 keV was determined for each sample. An average value of 1.327±0.016 was obtained compared to the literature k_0 value of 1.33.

Table 1. Measured and literature prompt k_0 factors with respect to 1951 keV of ^{36}Cl

Element	Capturing Isotope	Gamma-ray used (keV)	$k_{0, Cl}$ Measured	Literature value #
N	^{14}N	1884	5.78E-3	5.65E-3
Si	^{28}Si	3538	0.0.0181	0.023
	^{28}Si	4934	0.0197	0.0219
V	^{51}V	1434	0.56	0.53
Zn	^{67}Zn	1077	0.032	0.030
	^{68}Zn	1007	4.13E-3	4.6E-3
S	^{32}S	841	5.95E-2	6.06E-2
	^{32}S	5420	5.10E-2	5.2E-2
Sc	^{45}Sc	584	0.22	0.22
Mn	^{55}Mn	846	1.32	1.28
Cu	^{63}Cu	278	0.068	0.083
Se	^{76}Se	6600	0.036	0.041
	^{77}Se	1308	0.020	0.025
Mo	^{95}Mo	778	0.113	0.115

values converted using $k_{0, H}$ values from the reference: ZS.Revay et.al. J. Radioanal. Nucl. Chem., 244 (2000) 383.

2. Benchmark experiments

We have determined the sensitivity for the two titanium foils at 1381 keV prompt gamma-ray of ^{49}Ti and results are given in Table 2. The elemental concentration of the IAEA supplied aluminosilicate and graphite mixture was determined using the k_0-based internal mono standard PGNAA method. Here we report relative elemental concentration using Fe as the comparator element and arrived at the absolute elemental concentration values using reported Fe concentration value of 8.48% from the reference of IAEA, INDC (NDS)-424, 2001 by Revay and Molnar. The relative concentration values were arrived at using the equation:

$$\frac{W_x}{W_c} = \frac{A_x.(\sigma\theta a)_c.M_x}{A_c.(\sigma\theta a)_x.M_c} = \frac{A_x.M_x}{A_c.M_c}.\frac{1}{k_0}.\frac{\varepsilon_c}{\varepsilon_x}$$

where $(\sigma\theta\varepsilon a)$ is the product of neutron absorption cross section, isotopic abundance, full energy peak detection efficiency and, gamma ray abundance. M_x and M_c, are the atomic weights of the element of interest and the comparator. The relative efficiency value $\varepsilon_c/\varepsilon_x$ can either be predetermined or generated using the prompt gamma rays of the comparator.

Table 2 Detection sensitivity for 1381 keV prompt gamma-ray of ^{49}Ti

Ti sample		Live time (s)	Net counts	Sensitivity
Shape and size	Mass (mg)			(cps/mg)
2.5 cm square	628	7528	81830 (1.1%)	0.017
6 mmϕ disk	36.2	4095	4610 (9%)	0.031

Table 3 Results of aluminosilicate and graphite mixture sample

The mass of the sample = 1.182 g.

Element	Element/Fe ratio	Concentration (Wt.%)
Fe	1	8.48
Si	2.42	20.52
Ca	0.15	1.27
K	0.27	2.29
Al	2.88	24.4
H	0.0146	0.123
B	2.44E-4	2.06E-3

3.   Checking of prompt k_0-factors: Analysis of IAEA CRM SL-3

As part of quality assurance program, we have also analysed the IAEA SL-3 CRM and arrived at the elemental concentration ratio with respect to Si for a few major constituent elements, the value of which showed good agreement with recommended ones (Table 4). The literature concentration value of Si (267.33 mg/g) (Ref: IAEA/RL/143, AQCS, 1986) was used for conversion to absolute concentration.

Table 4. Results of the IAEA SL-3 analysis(the relative concentration values with

respect to Si) (mass of the sample = 5.5 g)

Element	Element/Fe ratio	Concentration (mg/g)	Literature value (mg/g)
Si	1	267.3	267.3
Ca	0.527	140.86	111.1
K	0.369	9.86	8.74
Ti	0.0079	2.11	2.61

4. Application of k_0-based PGAA for the composition analysis of alloys

The present k_0-based internal mono standard PGNAA has been used to determine the composition in some alloys non-destructively. The method has been validated by analyzing some reference alloy standards like Ferrotitanium (BCS 243/4), Ferrosilicon alloy (BCS 305/1) and alloy-718 containing elements like Fe, Ti, Cr, Ni and Mo. The results of analysis of the alloy samples are given in Table 5. The detailed information of this work can be found in the enclosed manuscript submitted to NIM-A journal for publication (enclosed as an attached file).

Table 5. Results of analysis of alloy samples by PGNAA (All concentrations are in wt.%)

Alloy sample	Alloy-718[a]	Fe-Ti BCS-243/4[c]	Fe-Si BCS-305/1[c]
Fe	19.3±0.5 (18)	44±2(46.7)	24±1(23.2)
Ti	0.69 ±0.07 (0.5)	37±4(38.2)	-
Ca	-	-	(0.33)
Co	0.43 ±0.04(0.03) [b]	-	-
Cu	-	(0.14)	-
Ni	58±1(52)	-	-
Cr	18.8±0.1(18)	-	-
Mo	2.2±0.2(3)	-	-
P	-	-	(0.03)
Si	-	3.6±0.2(3.8)	76±3(75)
Al	(0.5)	14±1(10.5) [b]	(1.38)
Mn	-	0.49±0.11(0.52)	-
Nb	(5)	-	-

1. [a] The nominal composition is given in parenthesis

2. [b] Interference from background materials

[c]Numbers in parenthesis are the certified values

Summary and conclusion

The present PGNAA system has the following drawbacks: (i) The available neutron flux is relatively low which in turn yields lower sensitivity, (ii). Since gamma spectrum acquisition was carried out in singles mode, we have worked under high gamma ray background condition. This results in poor detection limit for almost all elements. For this reason we could not successfully carry out the experiment on neutron velocity measurement. The present system has been utilized for a limited sample analysis. We are in the process of getting a dedicated neutron beam facility for PGNAA at our institute and also in the process of installing a Compton suppressed gamma ray spectrometer system.

NEW PROMPT GAMMA-RAY DATA

G. L. Molnár

Institute of Isotope and Surface Chemistry
Chemical Research Centre, Budapest, Hungary

In view of the inadequacy of the available data for analytical applications, much emphasis has been put on new measurements. It was important to involve a variety of neutron beam facilities in order to crosscheck each others' results, and study some specific problems. The present contribution describes the main achievements and illustrates the quality of the new experimental data.

1. Experimental activities

The largest amount of new data came from Hungary, the Institute of Isotope and Surface Chemistry, Budapest. Neutron capture reactions on all naturally occurring elements except 4 noble gases (He, Ne, Ar, Kr), i.e. 79 elements from H to U, have been studied at the Budapest Research Reactor's guided thermal neutron beam PGAA facility. The ^{10}B(n,$\alpha\gamma$) reaction on natural boron was also measured. The results will be described and illustrated in the next sections.

In India, at the Bhabha Atomic Research Centre (BARC) a thermal guided beam was used for experiments. Activities were concentrated on the experimental determination of prompt k_0-factors with respect to the 1951 keV gamma line from the ^{35}Cl(n,γ)^{36}Cl reaction using a mixture of ammonium chloride and other stoichiometric compounds [1, 2]. Emission probabilities of capture gamma rays from ^{60}Co were also determined [2, 3].

In Korea, the Seoul National University – KAERI PGAA system was used to measure the prompt k_0-factors for major non-1/v nuclides and to determine the corresponding effective g-factors for their polychromatic diffracted neutron beam [4].

In Vietnam, at the Atomic Energy Commission, Dalat prompt k_0-factors with respect to the 1951 keV gamma line from chlorine were measured for a number of elements using a filtered thermal neutron beam [5]. All facilities tested the reliability of their k_0-factors in a number of applications.

2. Energies, partial cross sections and k_0-values

The largest amount of new experimental data comes from the Budapest experiments. Capture gamma-ray spectra were measured with natural targets, using a carefully calibrated Compton suppression spectrometer [6]. To achieve a consistent energy calibration, all elemental targets have also been measured together with a chlorine target. The precise energies of two surrounding peaks from the ^{35}Cl(n,γ) reaction [7] were used to determine the energies of two distinct peaks, which were then used for the energy calibration of elemental spectra after nonlinearity correction. The accurate new energy and relative intensity data were sufficient to identify over 13,000 gamma rays of 79 elements with the emitting nuclide using ENSDF evaluated data.

By means of internal k_0-standardisation [8], measurements with composite targets

(stoichiometric compounds, mixtures or solutions) yielded accurate normalising factors with respect to the H(n,γ) cross section. This way a very accurate determination of partial gamma-ray production cross sections and related k_0-factors has become possible. The whole data set was provided to the CRP for further evaluation, described elsewhere is this document. Energies and k_0-factors for the most important gamma lines of 79 elements were published in Ref. [9] (erratum in Ref. [10]), while the library was introduced in Refs. [11-13]. The partial cross sections and k_0-factors for the best used lines have recently been redetermined (in important cases with several targets) [14] and complemented with gamma lines from short-lived decay [15]. These data are summarised in Table 1.

Table 1. Partial γ-ray production cross sections for the elements as redetermined by internal standardisation at the Budapest thermal guide [14].

Z	El.	E_γ (keV)	σ_γ (b)		Z	El.	E_γ (keV)	σ_γ (b)	
1	H	2223	0.3326	± 0.0007	47	Ag	658	1.93	± 0.04
3	Li	2032	0.038	± 0.001	48	Cd	558	1866	± 21
4	Be	6809	0.0054	± 0.0005	49	In	5893	2.1	± 0.2
5	B	478	713	± 5	50	Sn	1293	0.134	± 0.002
6	C	1261	0.00120	± 0.00002	51	Sb	922	0.086	± 0.004
		4945	0.00262	± 0.00003	52	Te	603	2.4	± 0.2
7	N	1884	0.01450	± 0.00010	53	I	133	1.42	± 0.05
8	O	871	0.000175	± 0.000008	54	Xe	667	6.9	± 1
9	F	1633	0.0093	± 0.0003	55	Cs	5505	0.306	± 0.004
11	Na	472	0.497	± 0.005	56	Ba	1435	0.308	± 0.006
12	Mg	584	0.0327	± 0.0007	57	La	567	0.333	± 0.007
13	Al	1778	0.233	± 0.004	58	Ce	662	0.23	± 0.02
14	Si	3538	0.119	± 0.002	59	Pr	177	1.06	± 0.02
15	P	637	0.031	± 0.001	60	Nd	696	33.2	± 0.7
16	S	842	0.3570	± 0.0010	62	Sm	333	4900	± 60
17	Cl	1951	6.51	± 0.04	63	Eu	90	1450	± 20
19	K	770	0.91	± 0.02	64	Gd	182	7680	± 170
20	Ca	1942	0.34	± 0.01	65	Tb	75	0.35	± 0.04
21	Sc	584	1.83	± 0.03	66	Dy	184	146	± 3
22	Ti	1381	5.18	± 0.05	67	Ho	137	14.5	± 0.7
23	V	1434	5.2	± 0.1	68	Er	185	57	± 2
24	Cr	836	1.38	± 0.02	69	Tm	205	8.7	± 0.1
25	Mn	846	13.3	± 0.2	70	Yb	639	1.5	± 0.1
26	Fe	7631	0.68	± 0.01	71	Lu	150	13.7	± 0.4
27	Co	230	7.18	± 0.07	72	Hf	213+214	1.97	± 0.04
28	Ni	466	0.843	± 0.009	73	Ta	270	2.60	± 0.04
29	Cu	278	0.893	± 0.009	74	W	146	0.97	± 0.02
30	Zn	1077	0.358	± 0.004	75	Re	208	4.5	± 0.2
31	Ga	690	0.26	± 0.03	76	Os	187	2.08	± 0.04
32	Ge	595	1.59	± 0.04	77	Ir	351	2.42	± 0.08
33	As	166	1.00	± 0.01	78	Pt	356	6.17	± 0.05
34	Se	6601	0.57	± 0.03	79	Au	214	7.77	± 0.05
35	Br	1249	0.054	± 0.001	80	Hg	5967	53	± 2
37	Rb	555+556	0.132	± 0.002	81	Tl	873	0.168	± 0.006
38	Sr	1836	1.02	± 0.01	82	Pb	7367	0.137	± 0.003
39	Y	6080	0.85	± 0.02	83	Bi	319	0.017	± 0.002
40	Zr	213+214	0.125	± 0.006	90	Th	256	0.093	± 0.004
41	Nb	499	0.065	± 0.005	92	U	4060	0.186	± 0.003
42	Mo	778	2.04	± 0.05					
44	Ru	539	1.5	± 0.1					
45	Rh	470	2.5	± 0.07					
46	Pd	616	0.638	± 0.006					

As the other CRP participants (and other laboratories) have measured only k_0-factors with respect to the 1951 keV chlorine line, comparison with the adopted set and the new Budapest data is possible only for the inferred similar k_0-factors. In Table 2, the available data are compared with the adopted set from the CRP and the new Budapest data [14] in such a manner. To assess the possible dependence on neutron beam characteristics, data from the NIST-University of Maryland thermal beam facility, as well as recent data obtained in thermal and cold guided beams at the Japan Atomic Energy Research Institute (JAERI) are also included.

It is quite obvious from Table 2 that for $1/v$ nuclides the agreement is generally good at the quoted uncertainty level. It is especially gratifying that the very precise JAERI data corroborate the adopted values and so do the new Budapest data. Moreover, the cold neutron data from JAERI agree well with similar data from NIST and with the thermal data, supporting the $1/v$ nature of the cross section. The only exceptions are the well-known cases, i.e. ^{113}Cd, ^{149}Sm and ^{155,157}Gd for which the g-factor strongly deviates from unity.

3. Capture gamma-ray spectra

For many applications it is important to know the full capture gamma–ray spectrum. To assess the quality and completeness of the new adopted data library comprising over 33,000 gamma lines, the ^{59}Co(n,γ)^{60}Co reaction has been selected as an illustrative example. Cobalt is a monoisotopic element, and this reaction is one of the cross section standards for neutron dosimetry. Hence accurate gamma-ray emission probabilities per capture can be inferred by dividing the partial cross sections for individual gamma rays with the total capture cross section. Moreover, for this case a new measurement from the BARC participants has come about, and several fairly complete evaluated data sets are available as well.

In Table 3, the gamma-ray energies, elemental partial cross sections and intensities per 100 captures for the ^{59}Co(n,γ)^{60}Co reaction from the adopted set are compared with similar data from the Budapest and BARC measurements and from the ENSDF and LANL evaluations described in this document, as well as the compilation by Lone *et al.* [16]. As can be seen, the Budapest data as as complete as the ENSDF set, help improve the energy precision, and serve as the dominant source of accurate partial cross sections and intensities per capture.

At the bottom of Table 3 the total number of gamma rays, the sum of all intensities and the percentage of the Q-sum (calculated as the energy-weighted sum of all transition intensities, divided by the neutron binding energy, S_n) are shown for each set. It is obvious that the ENSDF intensities have been normalised to the Q-sum (but not the LANL set), and the value of 87 % for the adopted set is a more realistic estimate for the discrete transitions. The Q-sum of 79 % for the Lone data is not very far from this number, but this may be fortuitous as many lines are missing and many individual intensities strongly deviate from the accurate new values. This is most notable for the three strongest lines, the 230 keV, 277 keV and 556 keV transition.

Table 2. Comparison of the library $k_{0,Cl}$-factors with other measurements for the most prominent γ rays of selected elements

Z	Target Isotope	E(dE)	Adopted	Dalat th. beam [5]	BARC th. guide [1]	SNU diffr. beam [4]	NIST- th. beam [17]	JAERI th. guide [18, 19]	NIST cold guide [17]	JAERI cold guide [18, 19]	Budapest th. guide [14]
1	1-H	2223.25	1.848(11)		1.800(16)		2.00(10)	1.80(6)	2.05(11)	1.86(6)	1.803(10)
3	7-Li	2032.30(4)	0.0307(8)	0.0230(5)*							
5	10-B	477.595(3)	369.5(23)		312(22)			371(31)		380(32)	360(3)
6	12-C	1261.765(9)	0.000579(15)	0.00041(1)*				0.000573(5)		0.000551(6)	0.000546(9)
	12-C	4945.301(3)	0.001218(25)					0.00124(3)		0.001160(17)	0.001192(13)
7	14-N	1884.821(16)	0.00588(8)	0.00567(11)				0.005800(13)		0.005890(18)	0.00569(4)
11	23-Na	472.202(9)	0.1165(11)				0.105(4)	0.11600(41)	0.105(4)	0.1160(25)	0.1181(13)
12	25-Mg	585.00(3)	0.0072(3)				0.0065(2)		0.0064(3)		
13	27-Al	1778.92(3)	0.0482(10)				0.0467(18)	0.0440(4)	0.0463(21)	0.0433(14)	0.0472(9)
14	28-Si	2092.902(18)	0.00660(13)	0.00603(11)							
	28-Si	3538.966(22)	0.0237(4)				0.0214(7)	0.02180(10)	0.0216(9)	0.02110(11)	0.0231(5)
15	31-P	636.663(21)	0.0056(3)					0.00572(9)		0.00570(9)	0.0055(3)
16	32-S	840.993(13)	0.0606(11)	0.0603(15)			0.0558(18)	0.0554(10)	0.0562(23)	0.0570(12)	0.0608(13)
17	35-Cl	786.3020(10)	0.540(3)		1.30(3)&		1.28(6)&	1.330(45)&	1.26(7)&	1.350(44)&	
	35-Cl	788.4280(10)	0.856(9)		1.30(3)&		1.28(6)&	1.330(45)&	1.26(7)&	1.350(44)&	
	35-Cl	1951.1400(20)	1	1	1	1		1		1	1
19	39-K	770.3050(20)	0.1294(18)		0.116(4)		0.126(4)	0.127(4)	0.122(5)	0.128(4)	0.127(3)
20	40-Ca	1942.67(3)	0.0492(10)		0.045(2)		0.0461(16)	0.047(2)	0.0459(19)	0.0464(16)	0.0463(14)
22	48-Ti	341.706(5)	0.215(3)		0.187(6)*			0.211(3)		0.2250(16)	
	48-Ti	1381.745(5)	0.606(15)	0.433(10)*	0.604(13)		0.582@	0.582(6)	0.591@	0.591(6)	0.591(7)
	48-Ti	1585.941(5)	0.0730(10)		0.056(3)*						
24	50-Cr	749.09(3)	0.0614(10)		0.065(8)			0.0562(20)		0.0601(25)	
	50-Cr	834.849(22)	0.149(3)		0.138(8)			0.141(5)		0.142(5)	0.145(2)
	50-Cr	7938.46(23)	0.0457(11)		0.048(3)						
25	55-Mn	314.398(20)	0.1488(22)					0.152(5)		0.149(8)	0.150(3)
26	56-Fe	352.347(12)	0.0274(3)				0.0253(9)	0.0273(10)	0.0248(10)	0.0269(11)	
	56-Fe	7631.136(14)	0.0654(13)					0.0568(24)*		0.0537(27)*	0.0676(14)

Table 2. Comparison of the library $k_{0,Cl}$-factors …

Z	Target Isotope	E(dE)	Adopted	Dalat th. beam [5]	BARC th. guide [1]	SNU diffr. beam [4]	NIST- th. beam [17]	JAERI th. guide [18, 19]	NIST cold guide [17]	JAERI cold guide [18, 19]	Budapest th. guide [14]
27	59-Co	229.879(17)	0.682(8)		0.58(4)			0.67(2)		0.664(22)	0.702(8)
	59-Co	277.161(17)	0.643(8)		0.55(4)*			0.619(21)		0.615(21)	
	59-Co	555.972(13)	0.547(6)		0.46(3)*			0.516(18)	0.460(12)*	0.509(20)	
	59-Co	1515.720(25)	0.165(3)		0.186(6)*						
	59-Co	1830.800(25)	0.1616(24)		0.19(1)*						
	59-Co	6485.99(3)	0.220(6)		0.185(15)*						
	59-Co	7214.42(3)	0.131(3)		0.156(6)*						
28	58-Ni	464.978(12)	0.0804(10)				0.075(3)	0.081(3)	0.074(3)	0.0811(28)	0.0781(9)
29	63-Cu	278.250(14)	0.0787(14)		0.068(4)			0.077(3)		0.0762(25)	0.0831(9)
	63-Cu	384.45(5)	0.00617(13)		0.019(1)&			0.0174(7)&		0.0166(6)&	
	65-Cu	385.77(3)	0.01155(18)		0.019(1)&			0.0174(7)&		0.0166(6)&	
	63-Cu	7306.93(4)	0.0283(15)		0.0261(14)						
37	85-Rb	556.82(3)	0.00599(17)	0.00210(5)*							
38	87-Sr	898.055(11)	0.0449(8)					0.042(2)		0.0425(14)	0.0434(6)
	87-Sr	1836.067(21)	0.0658(12)								0.0634(7)
49	113-Cd#	558.32(3)	92.6(16)		41(2)*	90(6)	132(7)*	81(2)	66(4)*	61.5(1.5)*	90.7(11)
55	133-Cs	116.3740(20)	0.059(6)					0.172(6)&		0.172(6)&	
	133-Cs	116.612(4)	0.061(6)					0.172(6)&		0.172(6)&	
	133-Cs	307.015(4)	0.0612(13)					0.0692(25)*		0.0711(26)*	0.0546(7)*
56	138-Ba	627.29(5)	0.01200(25)		0.0106(3)			0.0111(4)		0.0108(4)	
	135-Ba	818.514(12)	0.00865(17)		0.012(2)*						
	137-Ba	1435.77(4)	0.0126(3)		0.011(1)			0.0118(4)		0.0118(4)	
62	149-Sm#	333.97(4)	178.4(24)	188(4)		172(14)	339(18)*	131(9)*	111(7)*	116(1)*	178(2)
63	151-Eu#	89.847(6)	52.7(11)			46(3)					
64	157-Gd#	181.931(4)	257(11)			277(15)	222(12)	255(3)	236(13)	214(1)*	267(6)
	155-Gd#	199.2130(10)	71.9(23)			68(5)					
	157-Gd#	944.174(10)	110.0(25)	162(3)							

Table 2. Comparison of the library $k_{0,Cl}$-factors …

Z	Target Isotope	E(dE)	Adopted	Dalat th. beam [5]	BARC th. guide [1]	SNU diffr. beam [4]	NIST- th. beam [17]	JAERI th. guide [18, 19]	NIST cold guide [17]	JAERI cold guide [18, 19]	Budapest th. guide [14]
	155-Gd[#]	1187.120(21)	12(4)		111(4)[&*]	105(6)[&*]					
	157-Gd[#]	1187.122(9)	51(3)		111(4)[&*]	105(6)[&*]					
73	181-Ta	402.623(3)	3.29(8)	0.156(3)[*]							
80	199-Hg	367.947(9)	7.00(15)		5.8(3)			7.11(26)		7.01(14)	6.82(12)
	199-Hg	1693.296(11)	1.57(5)		1.37(8)			1.41(5)		1.40(5)	
	199-Hg	5967.02(4)	1.74(4)								1.43(6)[*]
82	207-Pb	7367.78(7)	0.00370(8)					0.00338(6)		0.00329(3)	0.00361(8)

[*] Value deviating significantly from Adopted Value.
[&] Doublet line.
[#] Non 1/v nuclide.
[@] Normalizing transition. Set equal to corresponding JAERI value.

Table 3. Comparison of new experimental γ-ray data from Budapest and BARC with evaluated data and the Lone compilation for cobalt

Energy (keV)					Elemental cross section		Intensity per 100 captures					
Adopted	ENSDF	LANL	Budapest	Lone	Adopted	Budapest	Adopted	ENSDF	LANL	Budapest	BARC	Lone
58.483(21)	58.90(22)	58.9	58.90(22)		0.411(4)	0.392(4)	1.105(11)	1.03(3)	48	1.054(11)		
158.517(17)	158.46(5)	158.46	158.519(12)		1.204(15)	1.204(15)	3.24(4)	2.682(16)	2.43	3.24(4)		2.21(16)
171.175(21)	171.3(3)	171.3			0.059(16)		0.16(4)	0.135(23)	0.12			
171.98(7)	172.1(4)	172.1			0.035(20)		0.09(5)	0.079(23)	0.07			
174.91(7)	174.91(5)	174.91	175.41(8)		0.0116(13)	0.0116(13)	0.031(4)	0.543(8)	0.49	0.031(4)		
195.90(3)	195.84(5)	195.84	195.891(17)		0.190(4)	0.190(4)	0.511(11)	0.461(7)	0.42	0.511(11)		
217.833(24)	217.88(20)	217.88	218.03(25)		0.013(5)	0.013(5)	0.035(13)	0.041(3)	0.04	0.035(13)		
220.043(21)	220.00(11)	220	219.96(10)		0.032(6)	0.032(6)	0.086(16)	0.090(3)	0.08	0.086(16)		
224.12(7)	224.1(3)	224.1			0.106(23)		0.29(6)	0.24(3)	0.22			
229.879(17)	229.72(4)	229.72	229.811(12)	230.2(20)	7.18(8)	7.18(8)	19.31(22)	16.70(10)	15.18	19.31(22)	15.99(70)	26
233.90(10)	233.89(11)	233.89	233.86(8)		0.050(5)	0.050(5)	0.134(13)	0.075(3)	0.07	0.134(13)		
254.379(17)	254.23(5)	254.23	254.371(12)	254.5(20)	1.294(16)	1.294(16)	3.48(4)	3.03(6)	2.75	3.48(4)	2.89(26)	4.38
277.161(17)	277.08(3)	277.08	277.199(11)	277.4(20)	6.77(8)	6.77(8)	18.21(22)	15.36(8)	13.96	18.21(22)	15.52(74)	19.9
297.99(5)	297.55(8)	297.55	298.004(25)		0.0463(14)	0.0463(14)	0.125(4)	0.254(8)	0.23	0.125(4)		
337.296(18)	337.32(7)	337.32	337.314(15)		0.226(4)	0.226(4)	0.608(11)	0.484(12)	0.44	0.608(11)		
349.954(24)	349.87(8)	349.87	349.885(24)		0.124(4)	0.124(4)	0.334(11)	0.254(8)	0.23	0.334(11)		
370.02(9)	370.09(10)	370.09	369.94(6)		0.0432(25)	0.0432(25)	0.116(7)	0.105(4)	0.09	0.116(7)		
391.218(15)	391.222(21)	391.22	391.221(12)	391.8(20)	1.079(14)	1.079(14)	2.90(4)	2.519(16)	2.29	2.90(4)	2.66(19)	2.59
393.952(21)	393.18(19)	393.18	393.04(5)		0.021(5)	0.122(3)	0.056(13)	0.223(12)	0.2	0.328(8)		
435.677(17)	435.71(5)	435.71	435.671(12)	435.4(20)	0.789(10)	0.789(10)	2.12(3)	1.72(3)	1.56	2.12(3)	1.69(10)	1.22
447.711(19)	447.68(9)	447.68	447.717(11)	447.3(20)	3.41(4)	3.41(4)	9.17(11)	7.70(10)	7	9.17(11)	7.79(33)	6.81
461.061(18)	461.04(3)	461.04	461.064(15)	460.6(20)	0.519(9)	0.519(9)	1.396(24)	1.180(9)	1.07	1.396(24)	0.832(62)	0.61
484.257(16)	484.21(3)	484.21	484.284(11)	483.8(20)	0.804(11)	0.804(11)	2.16(3)	1.859(20)	1.69	2.16(3)		2.06
497.269(16)	497.277(18)	497.28	497.264(13)	497.2(20)	2.16(4)	2.16(4)	5.81(11)	4.91(3)	4.46	5.81(11)	4.82(40)	4.43
532.17(7)	532.11(4)	532.11	532.29(4)		0.0655(24)	0.0655(24)	0.176(7)	0.160(8)	0.14	0.176(7)		
555.972(13)	555.972(12)	555.97	555.941(10)	556.4(20)	5.76(6)	5.76(6)	15.49(16)	13.17(11)	11.97	15.49(16)	14.10(63)	13.1

Energy (keV)					Elemental cross section		Intensity per 100 captures					
Adopted	ENSDF	LANL	Budapest	Lone	Adopted	Budapest	Adopted	ENSDF	LANL	Budapest	BARC	Lone
589.17(14)	589.35(11)	589.35	589.06(11)		0.031(4)	0.031(4)	0.083(11)	0.067(8)	0.06	0.083(11)		
602.71(4)	602.714(25)	602.71	602.59(11)		0.132(7)	0.132(7)	0.355(19)	0.330(9)	0.3	0.355(19)		
617.15(5)	617.15(5)	617.15	617.15(3)		0.0570(22)	0.0570(22)	0.153(6)	0.140(7)	0.13	0.153(6)		
665.48(3)	665.52(4)	665.52	665.39(3)		0.0769(24)	0.0769(24)	0.207(7)	0.174(7)	0.16	0.207(7)		
680.15(3)	680.214(13)	680.21	680.078(24)		0.273(5)	0.273(5)	0.734(13)	0.652(10)	0.59	0.734(13)		
710.650(14)	710.653(10)	710.65	710.493(16)	710.5(20)	0.015(4)	0.660(12)	0.040(11)	1.579(20)	1.43	1.78(3)	1.60(12)	0.84
715.438(21)	715.38(8)	715.38	715.28(10)		0.051(5)	0.051(5)	0.137(13)	0.108(9)	0.1	0.137(13)		
717.310(18)	717.420(10)	717.42	717.302(14)	717.7(20)	0.845(14)	0.845(14)	2.27(4)	1.971(24)	1.79	2.27(4)	2.19(13)	0.86
726.640(21)	726.714(13)	726.71	726.616(21)		0.448(10)	0.448(10)	1.20(3)	1.081(15)	0.98	1.20(3)		
728.76(3)	728.758(23)	728.76	728.58(6)		0.024(6)	0.183(8)	0.065(16)	0.438(11)	0.4	0.492(22)		
744.25(7)	744.27(6)	744.27	744.17(7)		0.067(4)	0.067(4)	0.180(11)	0.145(8)	0.13	0.180(11)		
779.96(8)	779.99(7)	779.98	779.87(8)		0.066(6)	0.066(6)	0.178(16)	0.174(11)	0.16	0.178(16)		
781.79(4)	781.81(3)	781.8	781.74(4)		0.146(6)	0.146(6)	0.393(16)	0.440(13)	0.4	0.393(16)		
785.628(21)	785.730(10)	785.72	785.614(17)	785.7(20)	2.41(7)	2.41(7)	6.48(19)	5.86(8)	5.33	6.48(19)	6.17(25)	5.19
798.97(7)	799.04(3)	799.03	798.97(9)		0.120(10)	0.120(10)	0.32(3)	0.283(8)	0.26	0.32(3)		
824.82(11)	824.89(10)	824.88	824.83(11)		0.035(4)	0.035(4)	0.094(11)	0.085(8)	0.08	0.094(11)		
827.02(9)	827.04(7)	827.03	826.92(10)		0.049(4)	0.049(4)	0.132(11)	0.127(8)	0.12	0.132(11)		
829.38(9)	829.46(8)	829.45	829.27(7)		0.056(4)	0.056(4)	0.151(11)	0.122(9)	0.11	0.151(11)		
837.63(12)	837.63(14)	837.62	837.78(16)		0.022(3)	0.022(3)	0.059(8)	0.052(7)	0.05	0.059(8)		
854.06(4)	854.154(22)	854.14	854.04(3)		0.187(6)	0.187(6)	0.503(16)	0.429(10)	0.39	0.503(16)		
862.30(6)	862.31(4)	862.3	862.17(12)		0.079(8)	0.079(8)	0.212(22)	0.189(8)	0.17	0.212(22)		
883.11(4)	883.21(5)	883.2	883.08(6)		0.075(5)	0.075(5)	0.202(13)	0.184(9)	0.17	0.202(13)		
884.98(4)	883.21(5)	883.2	885.01(4)		0.156(6)	0.156(6)	0.420(16)	0.184(9)	0.17	0.420(16)		
901.28(3)	901.289(15)	901.28	901.148(18)		0.418(9)	0.418(9)	1.124(24)	1.043(18)	0.95	1.124(24)	0.97(13)	
908.37(3)	908.38(3)	908.37	908.15(4)		0.100(4)	0.100(4)	0.269(11)	0.245(8)	0.22	0.269(11)		
928.48(3)	928.43(3)	928.42	928.30(6)	928.2(20)	0.145(9)	0.145(9)	0.390(24)	0.375(10)	0.34	0.390(24)	1.24(12)	1.01
930.612(23)	930.622(17)	930.61	930.47(5)		0.408(22)	0.408(22)	1.10(6)	0.997(18)	0.91	1.10(6)		
944.07(6)	944.06(5)	944.05			0.18(7)		0.48(19)	0.421(25)	0.38			
945.314(17)	945.329(17)	945.32		944(2)	0.98(4)		2.64(11)	2.24(4)	2.04			2.21

Energy (keV)					Elemental cross section		Intensity per 100 captures					
Adopted	ENSDF	LANL	Budapest	Lone	Adopted	Budapest	Adopted	ENSDF	LANL	Budapest	BARC	Lone
947.41(6)	947.42(4)	947.41	947.19(7)		0.121(7)	0.121(7)	0.325(19)	0.252(9)	0.23	0.325(19)	2.96(12)	
963.58(3)	963.58(3)	963.57	963.34(5)		0.191(11)	0.191(11)	0.51(3)	0.436(13)	0.4	0.51(3)		
968.57(18)	968.75(22)	968.74	968.34(13)		0.022(3)	0.022(3)	0.059(8)	0.048(10)	0.04	0.059(8)		
972.82(16)	972.51(15)	972.5	971.16(24)		0.082(8)	0.030(7)	0.221(22)	0.235(11)	0.21	0.081(19)		
1001.80(12)	1002.10(8)	1002.09	1001.73(7)		0.069(5)	0.069(5)	0.186(13)	0.150(10)	0.14	0.186(13)		
1005.668(22)	1005.70(4)	1005.69	1005.52(4)		0.127(6)	0.127(6)	0.342(16)	0.310(11)	0.28	0.342(16)		
1023.64(3)	1023.645(24)	1023.64	1023.42(12)		0.22(3)	0.22(3)	0.59(8)	0.506(12)	0.46	0.59(8)		
1059.42(12)	1059.51(10)	1059.5	1059.43(14)		0.043(4)	0.043(4)	0.116(11)	0.099(9)	0.09	0.116(11)		
1069.90(7)	1069.93(11)	1069.92	1069.98(14)		0.058(6)	0.058(6)	0.156(16)	0.102(10)	0.09	0.156(16)		
1075.66(10)	1075.68(7)	1075.67	1075.35(12)		0.099(7)	0.099(7)	0.266(19)	0.187(11)	0.17	0.266(19)		
1092.36(3)	1092.358(22)	1092.35	1092.15(6)		0.035(13)	0.348(22)	0.09(4)	0.945(22)	0.86	0.94(6)	1.05(13)	
1103.73(6)	1103.77(3)	1103.76	1103.59(5)		0.277(12)	0.277(12)	0.75(3)	0.680(20)	0.62	0.75(3)	0.67(22)	
1117.76(8)	1117.93(5)	1117.92	1117.68(6)		0.106(5)	0.106(5)	0.285(13)	0.287(12)	0.26	0.285(13)		
1134.89(10)	1134.76(13)	1134.75	1134.24(12)		0.032(4)	0.032(4)	0.086(11)	0.088(10)	0.08	0.086(11)		
1146.31(20)	1146.1(3)	1146.09	1146.45(15)		0.035(4)	0.035(4)	0.094(11)	0.051(11)	0.05	0.094(11)		
1158.95(14)	1158.86(15)	1158.85	1158.92(14)		0.032(4)	0.032(4)	0.086(11)	0.060(8)	0.05	0.086(11)		
1176.71(23)	1176.9(3)	1176.89			0.015(6)		0.040(16)	0.034(8)	0.03			
1195.37(10)	1195.70(8)	1195.69	1195.33(6)		0.059(4)	0.059(4)	0.159(11)	0.141(9)	0.13	0.159(11)		
1206.47(3)	1206.67(12)	1206.66	1206.14(14)		0.072(11)	0.072(11)	0.19(3)	0.28(3)	0.25	0.19(3)		
1207.77(3)	1207.97(7)	1207.96	1207.71(5)		0.202(12)	0.202(12)	0.54(3)	0.40(3)	0.36	0.54(3)		
1215.96(3)	1215.80(14)	1215.79	1215.965(20)		0.520(9)	0.520(9)	1.399(24)	0.8(3)	0.7	1.399(24)	1.38(10)	
1216.44(18)	1216.45(18)	1216.44		1215.6(20)	0.24(22)		0.6(6)	0.6(3)	0.5		1.38(10)	0.78
1226.78(5)	1226.80(4)	1226.79	1226.72(5)		0.100(4)	0.100(4)	0.269(11)	0.268(10)	0.24	0.269(11)		
1238.566(24)	1238.575(22)	1238.56	1238.436(24)		0.290(7)	0.290(7)	0.780(19)	0.733(18)	0.67	0.780(19)		
1246.70(9)	1246.75(8)	1246.74	1246.65(8)		0.061(4)	0.061(4)	0.164(11)	0.143(9)	0.13	0.164(11)		
1262.62(5)	1262.56(10)	1262.55	1262.25(8)		0.037(3)	0.037(3)	0.100(8)	0.110(9)	0.1	0.100(8)		
1271.71(8)	1271.92(10)	1271.91	1271.61(9)		0.059(4)	0.059(4)	0.159(11)	0.133(11)	0.12	0.159(11)		
1274.32(4)	1274.28(3)	1274.27	1274.05(4)		0.205(6)	0.205(6)	0.551(16)	0.503(15)	0.47	0.551(16)		
1277.46(3)	1277.50(3)	1277.49	1277.29(3)		0.175(6)	0.175(6)	0.471(16)	0.459(14)	0.42	0.471(16)		

Energy (keV)					Elemental cross section		Intensity per 100 captures					
Adopted	ENSDF	LANL	Budapest	Lone	Adopted	Budapest	Adopted	ENSDF	LANL	Budapest	BARC	Lone
1283.22(7)	1283.28(3)	1283.27	1283.01(3)		0.194(6)	0.194(6)	0.522(16)	0.524(15)	0.48	0.522(16)		
1334.74(6)	1334.74(5)	1334.72	1332.89(13)		0.155(9)	0.068(8)	0.417(24)	0.402(16)	0.37	0.183(22)		
1341.70(7)	1341.2(3)	1341.18	1341.0(3)		0.013(3)	0.013(3)	0.035(8)	0.035(10)	0.03	0.035(8)		
1362.53(4)	1362.51(6)	1362.49	1362.35(6)		0.092(6)	0.092(6)	0.247(16)	0.187(10)	0.17	0.247(16)		
1379.74(6)												
1382.44(9)	1382.43(7)	1382.41	1382.53(18)		0.062(6)	0.062(6)	0.167(16)	0.185(10)	0.17	0.167(16)		
1419.30(8)	1419.37(7)	1419.35	1419.22(8)		0.077(6)	0.077(6)	0.207(16)	0.252(14)	0.23	0.207(16)		
1429.17(13)	1429.33(14)	1429.31	1429.08(9)		0.055(5)	0.055(5)	0.148(13)	0.155(15)	0.14	0.148(13)		
1472.04(3)	1472.03(3)	1472.01	1471.91(9)		0.195(8)	0.195(8)	0.524(22)	0.751(24)	0.68	0.524(22)		
1505.14(17)	1505.01(18)	1504.99			0.062(16)		0.17(4)	0.143(18)	0.13			
1507.33(3)	1507.368(23)	1507.35	1507.28(3)		0.463(9)	0.463(9)	1.245(24)	1.63(4)	1.48	1.245(24)	1.433(80)	
1515.720(25)	1515.769(14)	1515.75	1515.695(25)	1516.1(20)	1.738(25)	1.738(25)	4.67(7)	6.11(17)	5.55	4.67(7)	5.26(23)	2.93
1539.20(12)	1539.18(17)	1539.16	1539.07(12)		0.035(4)	0.035(4)	0.094(11)	0.097(12)	0.09	0.094(11)		
1542.14(12)	1542.53(25)	1542.51	1542.33(15)		0.032(4)	0.032(4)	0.086(11)	0.083(14)	0.08	0.086(11)		
1544.85(12)	1545.01(12)	1544.99	1544.73(9)		0.054(4)	0.054(4)	0.145(11)	0.195(15)	0.18	0.145(11)		
1553.65(3)	1553.70(6)	1553.68	1553.72(6)		0.120(6)	0.120(6)	0.323(16)	0.428(20)	0.39	0.323(16)		
1556.08(9)	1556.11(8)	1556.09	1556.00(7)		0.099(6)	0.099(6)	0.266(16)	0.307(18)	0.28	0.266(16)		
1611.11(18)	1612.3(3)	1612.28	1612.33(25)		0.028(5)	0.028(5)	0.075(13)	0.059(12)	0.05	0.075(13)		
1639.29(17)	1639.37(14)	1639.35	1638.66(24)		0.038(5)	0.038(5)	0.102(13)	0.123(13)	0.11	0.102(13)		
1646.95(22)	1647.08(21)	1647.06	1646.89(18)		0.034(4)	0.034(4)	0.091(11)	0.081(12)	0.07	0.091(11)		
1651.04(13)	1651.07(13)	1651.05	1650.96(11)		0.065(4)	0.065(4)	0.175(11)	0.142(13)	0.13	0.175(11)		
1678.14(12)	1677.92(20)	1677.89	1678.05(15)		0.045(6)	0.045(6)	0.121(16)	0.097(13)	0.09	0.121(16)		
1690.72(3)	1690.77(4)	1690.74	1690.76(9)	1690.6(20)	0.215(14)	0.215(14)	0.58(4)	0.80(3)	0.73	0.58(4)		0.81
1692.83(5)	1692.81(4)	1692.78	1692.92(9)		0.214(14)	0.214(14)	0.58(4)	0.76(3)	0.69	0.58(4)		
1703.91(10)	1704.24(7)	1704.21	1703.85(6)		0.074(5)	0.074(5)	0.199(13)	0.284(15)	0.26	0.199(13)		
1774.65(4)	1774.65(3)	1774.62	1774.63(9)		0.30(8)	0.30(8)	0.81(22)	1.02(3)	0.93	0.81(22)	0.891(28)	
1786.01(17)	1785.97(18)	1785.94	1786.18(16)		0.157(9)	0.157(9)	0.422(24)	0.35(7)	0.32	0.422(24)		
1787.45(4)	1787.4(3)	1787.37			0.08(5)		0.22(13)	0.19(7)	0.17			
1799.92(4)	1799.91(3)	1799.88	1799.92(4)	1802.1(20)	0.269(7)	0.269(7)	0.724(19)	0.99(3)	0.9	0.724(19)		1.98

Energy (keV)					Elemental cross section		Intensity per 100 captures					
Adopted	ENSDF	LANL	Budapest	Lone	Adopted	Budapest	Adopted	ENSDF	LANL	Budapest	BARC	Lone
1808.82(7)	1808.40(18)	1808.37	1808.81(4)		0.211(7)	0.211(7)	0.568(19)	0.44(11)	0.4	0.568(19)		
1808.98(10)	1809.56(24)	1809.53			0.15(8)		0.40(22)	0.34(11)	0.31			
1818.58(5)	1818.57(5)	1818.54	1818.62(4)	1818.7(20)	0.179(7)	0.179(7)	0.481(19)	0.64(3)	0.58	0.481(19)		0.84
1830.800(25)	1830.793(21)	1830.76	1830.77(3)	1831(2)	1.704(23)	1.704(23)	4.58(6)	6.05(21)	5.5	4.58(6)	4.95(26)	6.21
1839.76(11)	1839.69(11)	1839.66	1839.81(9)		0.065(4)	0.065(4)	0.175(11)	0.208(16)	0.19	0.175(11)		
1844.96(8)	1845.01(9)	1844.98	1844.67(7)		0.092(5)	0.092(5)	0.247(13)	0.327(23)	0.3	0.247(13)		
1852.70(3)	1852.709(25)	1852.68	1852.70(3)	1853.3(20)	0.456(10)	0.456(10)	1.23(3)	1.55(6)	1.41	1.23(3)	1.171(83)	1.31
1888.77(4)	1889.07(8)	1889.04	1889.00(8)	1890(2)	0.089(6)	0.089(6)	0.239(16)	0.251(16)	0.23	0.239(16)		1.16
1909.52(8)	1910.4(4)	1910.37			0.024(11)		0.06(3)	0.055(14)	0.05			
1924.59(12)	1924.62(12)	1924.59	1924.51(16)		0.041(4)	0.041(4)	0.110(11)	0.183(15)	0.17	0.110(11)		
1933.82(8)	1933.75(8)	1933.72	1933.77(15)		0.094(6)	0.094(6)	0.253(16)	0.287(18)	0.26	0.253(16)		
1982.35(8)	1982.37(17)	1982.33	1982.22(22)		0.046(5)	0.046(5)	0.124(13)	0.158(18)	0.14	0.124(13)		
1986.31(19)	1986.27(16)	1986.23	1986.38(20)		0.045(5)	0.045(5)	0.121(13)	0.171(18)	0.16	0.121(13)		
1998.42(13)	1998.52(14)	1998.48	1998.47(11)		0.069(7)	0.069(7)	0.186(19)	0.196(19)	0.18	0.186(19)		
2022.51(16)	2022.19(11)	2022.15	2021.77(10)		0.082(6)	0.082(6)	0.221(16)	0.246(19)	0.22	0.221(16)		
2032.83(7)	2032.95(4)	2032.91	2032.74(4)	2033.6(20)	0.393(11)	0.393(11)	1.06(3)	1.31(6)	1.19	1.06(3)	1.026(51)	1.09
2063.75(9)	2063.86(11)	2063.82	2063.18(22)		0.023(7)	0.061(8)	0.062(19)	0.226(18)	0.2	0.164(22)		
2074.83(8)	2074.88(9)	2074.84	2074.98(20)		0.102(9)	0.102(9)	0.274(24)	0.47(3)	0.47	0.274(24)		
2099.19(7)	2099.25(7)	2099.21	2099.02(22)		0.089(8)	0.089(8)	0.239(22)	0.371(21)	0.34	0.239(22)		
2121.54(8)	2121.3(3)	2121.26	2121.23(25)		0.023(5)	0.023(5)	0.062(13)	0.078(15)	0.07	0.062(13)		
2128.88(16)	2128.75(14)	2128.71	2128.48(10)		0.058(6)	0.058(6)	0.156(16)	0.173(16)	0.16	0.156(16)		
2158.11(18)	2158.16(17)	2158.12	2157.99(16)		0.057(6)	0.057(6)	0.153(16)	0.169(18)	0.15	0.153(16)		
2172.07(20)	2171.69(11)	2171.65	2171.61(16)		0.043(5)	0.043(5)	0.116(13)	0.279(21)	0.25	0.116(13)		
2200.50(10)												
2203.65(17)	2203.77(19)	2203.73	2203.47(14)	2204.7(20)	0.038(4)	0.038(4)	0.102(11)	0.142(16)	0.13	0.102(11)		0.59
2211.37(8)	2210.8(7)	2210.76	2211.07(15)		0.040(4)	0.040(4)	0.108(11)	0.046(19)	0.04	0.108(11)		
2221.61(4)	2221.53(10)	2221.49	2221.62(5)		0.261(8)	0.261(8)	0.702(22)	0.81(8)	0.74	0.702(22)		
2240.31(5)	2240.5(8)	2240.46	2240.5(3)	2241.4(20)	0.026(5)	0.026(5)	0.070(13)	0.050(19)	0.05	0.070(13)		0.5
2249.87(24)	2249.75(22)	2249.7	2249.05(18)		0.026(5)	0.043(5)	0.070(13)	0.123(16)	0.11	0.116(13)		

Energy (keV)					Elemental cross section		Intensity per 100 captures					
Adopted	ENSDF	LANL	Budapest	Lone	Adopted	Budapest	Adopted	ENSDF	LANL	Budapest	BARC	Lone
2262.12(21)	2262.4(4)	2262.35			0.041(16)		0.11(4)	0.094(18)	0.09			
2265.8(3)	2265.7(4)	2265.65	2265.94(19)		0.030(4)	0.030(4)	0.081(11)	0.090(18)	0.08	0.081(11)		
2279.78(6)	2279.94(20)	2279.89	2279.77(3)		0.079(11)	0.079(11)	0.21(3)	0.33(6)	0.3	0.21(3)		
2281.57(9)	2281.80(15)	2281.75	2281.63(12)	2279.8(20)	0.123(11)	0.123(11)	0.33(3)	0.46(6)	0.42	0.33(3)		0.57
2309.66(10)	2309.68(11)	2309.63	2309.62(11)	2308.1(20)	0.087(6)	0.087(6)	0.234(16)	0.329(23)	0.3	0.234(16)		0.38
2319.46(10)	2319.41(10)	2319.36	2319.46(9)		0.122(7)	0.122(7)	0.328(19)	0.342(24)	0.31	0.328(19)		
2338.78(15)	2338.6(3)	2338.55	2338.03(16)		0.051(6)	0.051(6)	0.137(16)	0.135(22)	0.12	0.137(16)		
2346.57(23)	2346.4(6)	2346.35	2346.30(21)		0.040(6)	0.040(6)	0.108(16)	0.050(16)	0.05	0.108(16)		
2357.56(10)	2357.56(8)	2357.51	2356.74(20)		0.038(5)	0.038(5)	0.102(13)	0.57(3)	0.52	0.102(13)		
2361.32(16)	2361.43(22)	2361.38	2362.02(16)		0.040(5)	0.040(5)	0.108(13)	0.142(18)	0.13	0.108(13)		
2363.92(9)												
2400.11(20)	2399.6(3)	2399.55	2399.22(13)		0.043(4)	0.043(4)	0.116(11)	0.146(19)	0.13	0.116(11)		
2431.29(9)	2430.90(24)	2430.85			0.063(14)		0.17(4)	0.144(19)	0.13			
2434.18(16)	2434.5(3)	2434.45	2433.7(4)		0.015(4)	0.015(4)	0.040(11)	0.119(19)	0.11	0.040(11)		
2434.58(22)	2434.5(3)	2434.45			0.052(15)		0.14(4)	0.119(19)	0.11			
2453.82(20)	2454.0(3)	2453.95	2453.77(12)		0.072(5)	0.072(5)	0.194(13)	0.139(21)	0.13	0.194(13)		
2469.64(12)	2469.6(3)		2469.1(3)		0.019(4)	0.019(4)	0.051(11)	0.136(25)		0.051(11)		
2472.36(17)	2472.4(5)		2472.46(19)		0.035(4)	0.035(4)	0.094(11)	0.099(24)		0.094(11)		
2482.4(3)	2482.41(23)	2482.35			0.064(16)		0.17(4)	0.146(20)	0.13			
2488.52(8)	2488.64(21)	2488.58			0.07(3)		0.19(8)	0.165(20)	0.15			
2501.63(18)	2501.4(3)	2501.34	2501.57(21)		0.067(7)	0.067(7)	0.180(19)	0.135(20)	0.12	0.180(19)		
2527.12(7)	2527.10(11)	2527.04	2526.87(20)	2526.5(20)	0.146(8)	0.146(8)	0.393(22)	0.51(3)	0.46	0.393(22)		0.27
2546(3)												
2557.46(21)	2557.55(18)	2557.49	2557.40(18)		0.086(6)	0.086(6)	0.231(16)	0.219(22)	0.2	0.231(16)		
2569.92(9)	2569.74(11)	2569.68	2569.55(16)	2569.1(20)	0.154(7)	0.154(7)	0.414(19)	0.58(3)	0.53	0.414(19)		0.41
2607.47(10)	2607.58(13)	2607.52	2607.42(7)	2606.5(20)	0.165(8)	0.165(8)	0.444(22)	0.57(3)	0.52	0.444(22)		0.34
2616.66(21)	2616.59(18)	2616.53	2616.70(19)		0.040(5)	0.040(5)	0.108(13)	0.223(22)	0.2	0.108(13)		
2629.8(4)	2628.8(5)	2628.74			0.061(22)		0.16(6)	0.141(24)	0.13			
2631.5(3)	2632.2(4)	2632.14	2631.51(22)		0.034(5)	0.034(5)	0.091(13)	0.107(22)	0.1	0.091(13)		

Energy (keV)					Elemental cross section		Intensity per 100 captures					
Adopted	ENSDF	LANL	Budapest	Lone	Adopted	Budapest	Adopted	ENSDF	LANL	Budapest	BARC	Lone
2641.3(3)	2641.35(24)	2641.29	2639.7(6)		0.023(5)	0.023(5)	0.062(13)	0.187(22)	0.17	0.062(13)		
2655.77(16)												
2661.05(17)	2661.2(4)	2661.14	2660.96(22)		0.037(6)	0.037(6)	0.100(16)	0.101(20)	0.09	0.100(16)		
2680.64(24)	2680.66(18)	2680.6			0.11(3)		0.30(8)	0.262(23)	0.24			
2692.02(15)	2692.25(20)	2692.19	2692.03(14)		0.076(7)	0.076(7)	0.204(19)	0.227(22)	0.21	0.204(19)		
2718.99(7)			2720.1(4)			0.038(6)				0.102(16)		
2721.8(3)	2720.2(9)	2720.13			0.038(6)		0.102(16)	0.044(22)	0.04			
2727.19(13)	2727.18(15)	2727.11	2727.2(3)	2726.8(20)	0.100(7)	0.100(7)	0.269(19)	1.68(10)	1.53	0.269(19)		0.29
2733.8(6)												
2740.06(18)	2739.58(20)	2739.51	2739.4(3)	2740.4(20)	0.103(7)	0.103(7)	0.277(19)	0.34(3)	0.31	0.277(19)		0.33
2744.93(10)	2745.8(9)	2745.73	2746.5(3)		0.033(6)	0.033(6)	0.089(16)	0.094(23)	0.09	0.089(16)		
2758.97(24)	2759.1(6)	2759.03	2759.02(18)		0.039(6)	0.039(6)	0.105(16)	0.114(21)	0.1	0.105(16)		
2768.29(20)	2768.5(5)	2768.43	2768.60(17)		0.034(6)	0.034(6)	0.091(16)	0.130(22)	0.12	0.091(16)		
2777.61(13)	2777.6(3)	2777.53	2777.5(4)		0.020(6)	0.020(6)	0.054(16)	0.224(24)	0.2	0.054(16)		
2790.22(20)	2789.5(4)	2789.43			0.080(19)		0.22(5)	0.184(23)	0.17			
2801.43(18)	2801.8(4)	2801.73	2801.66(17)	2802.7(20)	0.063(8)	0.063(8)	0.169(22)	0.169(23)	0.15	0.169(22)		0.15
2809.84(18)												
2832.98(19)	2831.8(13)	2831.73	2831.6(3)		0.031(5)	0.031(5)	0.083(13)	0.08(3)	0.07	0.083(13)		
2837.35(19)	2836.9(6)	2836.83	2836.98(17)		0.061(6)	0.061(6)	0.164(16)	0.18(3)	0.16	0.164(16)		
2861.4(3)	2861.3(7)	2861.23	2860.3(4)		0.040(8)	0.040(8)	0.108(22)	0.14(3)	0.13	0.108(22)		
2866.77(20)	2866.5(7)	2866.43	2865.2(6)	2867(2)	0.041(7)	0.041(7)	0.110(19)	0.13(3)	0.12	0.110(19)		0.45
2884.78(7)	2884.50(24)	2884.43	2884.65(14)	2883.1(20)	0.070(7)	0.070(7)	0.188(19)	0.32(3)	0.29	0.188(19)		0.35
2891.01(19)	2892.4(5)	2892.32			0.063(18)		0.17(5)	0.144(22)	0.13			
2900.50(24)	2899.9(4)	2899.82			0.076(20)		0.20(5)	0.174(22)	0.16			
2926.19(18)	2926.39(17)	2926.31	2926.60(13)	2926.6(20)	0.116(8)	0.116(8)	0.312(22)	0.42(3)	0.38	0.312(22)		0.49
2953.9(4)	2954.0(3)	2953.92	2955.3(4)	2953.5(20)	0.045(7)	0.045(7)	0.121(19)	0.226(23)	0.2	0.121(19)		0.38
2978.11(17)	2978.03(22)	2977.95	2976.72(16)	2978.5(20)	0.075(7)	0.075(7)	0.202(19)	0.293(23)	0.27	0.202(19)		0.36
2995.43(13)	2995.38(22)	2995.3	2995.01(12)	2995(2)	0.097(7)	0.097(7)	0.261(19)	0.293(23)	0.27	0.261(19)		0.31
3007.0(4)	3006.3(3)	3006.22	3007.56(20)		0.058(6)	0.058(6)	0.156(16)	0.202(21)	0.18	0.156(16)		

Energy (keV)					Elemental cross section		Intensity per 100 captures					
Adopted	ENSDF	LANL	Budapest	Lone	Adopted	Budapest	Adopted	ENSDF	LANL	Budapest	BARC	Lone
3009.80(23)												
3047.81(24)	3048.6(3)	3048.52	3047.6(4)	3049.6(20)	0.036(9)	0.037(9)	0.097(24)	0.205(20)	0.19	0.100(24)		0.25
3084.58(20)	3084.9(6)	3084.81	3084.66(25)		0.035(6)	0.035(6)	0.094(16)	0.096(16)	0.09	0.094(16)		
3096.63(20)	3097.01(20)	3096.92	3096.43(16)	3097.7(20)	0.061(7)	0.061(7)	0.164(19)	0.314(22)	0.28	0.164(19)		0.26
3121.33(19)	3121.5(4)	3121.41	3121.27(19)		0.051(8)	0.051(8)	0.137(22)	0.174(21)	0.16	0.137(22)		
3127.0(4)	3128.0(4)	3127.91	3126.88(23)	3125.8(20)	0.050(7)	0.050(7)	0.134(19)	0.189(21)	0.17	0.134(19)		0.24
3155.11(20)	3154.2(10)	3154.11	3153.4(5)		0.020(5)	0.020(5)	0.054(13)	0.071(20)	0.06	0.054(13)		
3193.65(16)	3193.63(21)	3193.54	3193.63(12)	3194.4(20)	0.089(6)	0.089(6)	0.239(16)	0.360(24)	0.33	0.239(16)		0.52
3200.33(13)	3200.1(5)	3200.01	3201.7(5)		0.020(5)	0.020(5)	0.054(13)	0.142(20)	0.13	0.054(13)		
3216.43(19)	3216.24(18)	3216.15	3216.77(22)	3217(2)	0.105(13)	0.105(13)	0.28(4)	0.53(3)	0.48	0.28(4)		0.53
3222.0(3)	3222.1(11)	3222.01			0.033(17)		0.09(5)	0.076(23)	0.07			
3238.16(19)	3238.4(3)	3238.31	3238.29(19)		0.089(8)	0.089(8)	0.239(22)	0.211(21)	0.19	0.239(22)		
3238.5(3)												
3248.02(19)	3248.1(3)	3248.01	3248.20(17)		0.069(7)	0.069(7)	0.186(19)	0.210(20)	0.19	0.186(19)		
3279.2(4)	3279.6(7)	3279.5	3279.0(3)		0.058(7)	0.058(7)	0.156(19)	0.17(4)	0.15	0.156(19)		
3283.78(13)	3284.1(5)	3284	3283.74(15)	3282.8(20)	0.101(8)	0.101(8)	0.272(22)	0.31(4)	0.28	0.272(22)		0.4
3291.56(18)	3290.4(13)	3290.3	3291.9(3)		0.035(6)	0.035(6)	0.094(16)	0.080(22)	0.07	0.094(16)		
3298.2(4)	3296.9(10)	3296.8	3299.2(3)		0.045(7)	0.045(7)	0.121(19)	0.100(21)	0.09	0.121(19)		
3303.2(3)	3303.0(5)	3302.9	3304.5(4)		0.036(6)	0.036(6)	0.097(16)	0.149(22)	0.14	0.097(16)		
3321.50(21)	3320.7(4)	3320.6	3319.8(3)		0.027(6)	0.027(6)	0.073(16)	0.145(18)	0.13	0.073(16)		
3329.4(3)	3328.3(6)	3328.2	3329.3(5)		0.024(5)	0.024(5)	0.065(13)	0.121(18)	0.11	0.065(13)		
3335.29(14)	3335.35(18)	3335.25	3335.29(11)	3334(2)	0.104(7)	0.104(7)	0.280(19)	0.413(24)	0.38	0.280(19)		0.35
3348.74(15)	3349.3(6)	3349.2	3348.7(3)		0.025(5)	0.025(5)	0.067(13)	0.087(15)	0.08	0.067(13)		
3380.22(14)	3380.28(10)	3380.18	3379.86(25)	3379.4(20)	0.210(10)	0.210(10)	0.56(3)	0.77(3)	0.7	0.56(3)		0.8
3391.11(19)	3391.5(4)	3391.4	3392.3(4)		0.026(5)	0.026(5)	0.070(13)	0.142(16)	0.13	0.070(13)		
3401.28(18)	3401.8(3)	3401.7	3400.0(4)		0.028(6)	0.023(6)	0.075(16)	0.201(20)	0.18	0.062(16)		
3410.1(3)					0.032(14)		0.09(4)					
3454.24(7)	3454.1(3)	3453.99	3452.8(3)		0.049(7)	0.049(7)	0.132(19)	0.240(20)	0.22	0.132(19)		
3479.93(16)	3480.1(4)	3479.99	3479.4(3)		0.050(5)	0.050(5)	0.134(13)	0.174(19)	0.16	0.134(13)		

Energy (keV)					Elemental section	cross	Intensity	per 100	captures			
Adopted	ENSDF	LANL	Budapest	Lone	Adopted	Budapest	Adopted	ENSDF	LANL	Budapest	BARC	Lone
3494.31(22)	3493.2(9)	3493.09	3492.1(4)		0.036(5)	0.036(5)	0.097(13)	0.12(3)	0.11	0.097(13)		
3496.88(24)												
3503.47(12)	3503.8(4)	3503.69	3503.5(4)		0.035(5)	0.035(5)	0.094(13)	0.129(16)	0.12	0.094(13)		
3514.88(24)	3513.7(7)	3513.59	3512.5(8)		0.023(5)	0.023(5)	0.062(13)	0.075(16)	0.07	0.062(13)		
3562.3(3)	3562.2(3)	3562.09	3562.23(19)	3561.2(20)	0.064(7)	0.064(7)	0.172(19)	0.175(15)	0.16	0.172(19)		0.19
3575.6(3)	3576.1(3)	3575.99	3575.24(22)		0.049(6)	0.049(6)	0.132(16)	0.173(15)	0.16	0.132(16)		
3619.7(3)	3619.7(3)	3619.58	3619.4(3)		0.059(8)	0.059(8)	0.159(22)	0.212(18)	0.19	0.159(22)		
3639.1(3)	3639.7(17)	3639.58	3639.4(6)		0.021(6)	0.021(6)	0.056(16)	0.029(13)	0.03	0.056(16)		
3650.9(4)	3651.2(5)	3651.08	3650.7(3)		0.028(6)	0.028(6)	0.075(16)	0.100(15)	0.09	0.075(16)		
3664.13(21)	3664.2(3)	3664.08	3664.61(25)	3663.7(20)	0.080(9)	0.080(9)	0.215(24)	0.248(21)	0.22	0.215(24)		0.16
3669.9(4)	3670.0(7)	3669.88			0.047(16)		0.13(4)	0.108(18)	0.1			
3677.05(13)	3677.50(25)	3677.38	3676.95(14)		0.109(8)	0.109(8)	0.293(22)	0.364(23)	0.33	0.293(22)		
3694.07(18)	3693.28(24)	3693.16	3692.0(3)		0.039(11)	0.058(12)	0.10(3)	0.221(15)	0.2	0.16(3)		
3749.21(7)	3749.23(9)	3749.1	3748.76(7)	3749(2)	0.415(13)	0.415(13)	1.12(4)	1.53(6)	1.39	1.12(4)	1.33(73)	1.34
3757.9(4)	3758.2(5)	3758.07			0.060(19)		0.16(5)	0.138(19)	0.13			
3795.05(22)	3795.2(3)	3795.07	3795.0(3)		0.029(6)	0.029(6)	0.078(16)	0.130(13)	0.12	0.078(16)		
3815.20(19)	3815.19(17)	3815.06	3814.69(17)	3814.9(20)	0.081(7)	0.081(7)	0.218(19)	0.307(16)	0.28	0.218(19)		0.34
3823.54(19)	3823.67(23)	3823.54	3823.64(18)		0.073(7)	0.073(7)	0.196(19)	0.229(14)	0.21	0.196(19)		
3840.83(15)	3841.44(13)	3841.31	3840.75(9)	3842.9(20)	0.129(8)	0.129(8)	0.347(22)	0.413(18)	0.38	0.347(22)		0.21
3897.02(17)	3897.2(3)	3897.06	3897.21(22)	3899.5(20)	0.092(7)	0.092(7)	0.247(19)	0.271(23)	0.25	0.247(19)		0.59
3902.90(12)	3902.5(4)	3902.36	3903.2(6)		0.046(6)	0.046(6)	0.124(16)	0.207(22)	0.19	0.124(16)		
3929.84(12)	3929.84(9)	3929.7	3929.14(14)	3929.4(20)	0.272(11)	0.272(11)	0.73(3)	0.99(3)	0.9	0.73(3)	0.999(24)	0.8
3966.15(18)	3966.74(11)	3966.6	3965.99(13)	3966.3(20)	0.239(11)	0.239(11)	0.64(3)	0.77(3)	0.7	0.64(3)		0.75
3976.92(24)	3976.9(3)	3976.76	3976.22(21)	3975.7(20)	0.057(6)	0.057(6)	0.153(16)	0.234(18)	0.21	0.153(16)		0.24
3994.92(24)	3994.98(24)	3994.84			0.095(17)		0.26(5)	0.218(15)	0.2			
3995.2(4)			3996.7(4)		0.033(6)	0.033(6)	0.089(16)			0.089(16)		
4026.26(12)	4026.73(12)	4026.58	4026.14(8)	4028.4(20)	0.272(10)	0.272(10)	0.73(3)	0.91(3)	0.83	0.73(3)		1.66
4032.03(18)	4032.77(13)	4032.62	4032.06(10)		0.208(9)	0.208(9)	0.559(24)	0.74(3)	0.67	0.559(24)		
4042.20(19)	4043.7(8)	4043.55	4043.7(6)		0.013(5)	0.013(5)	0.035(13)	0.059(13)	0.05	0.035(13)		

Energy (keV)					Elemental cross section		Intensity per 100 captures					
Adopted	ENSDF	LANL	Budapest	Lone	Adopted	Budapest	Adopted	ENSDF	LANL	Budapest	BARC	Lone
4076.11(16)	4075.94(24)	4075.79	4075.6(3)		0.048(7)	0.048(7)	0.129(19)	0.194(14)	0.18	0.129(19)		
4111.57(14)	4112.4(4)	4112.25	4111.7(10)		0.038(6)	0.038(6)	0.102(16)	0.121(12)	0.11	0.102(16)		
4148.74(21)	4150.2(4)	4150.05	4150.8(7)		0.086(21)	0.086(21)	0.23(6)	0.220(23)	0.2	0.23(6)		
4155.64(24) 4156.50(14)	4155.62(18)	4155.47	4155.5(9)		0.128(8)	0.128(8)	0.344(22)	0.48(3)	0.44	0.344(22)		
4208.01(12)	4207.99(12)	4207.83	4207.33(12)	4207.9(20)	0.255(13)	0.255(13)	0.69(4)	0.83(3)	0.75	0.69(4)		1
4212.56(14) 4212.6(4)	4213.0(3)	4212.84	4212.2(3)		0.082(9)	0.082(9)	0.221(24)	0.30(3)	0.27	0.221(24)		
4245.56(18)	4245.5(9)	4245.34			0.020(8)		0.054(22)	0.045(11)	0.04			
4253.3(3) 4269.8(3)	4253.4(3)	4253.24	4252.0(3)		0.032(5)	0.032(5)	0.086(13)	0.134(12)	0.12	0.086(13)		
4275.36(19)	4275.63(21)	4275.47	4274.82(18)	4276.1(20)	0.063(6)	0.063(6)	0.169(16)	0.201(13)	0.18	0.169(16)		0.2
4288.45(18) 4298.13(16)	4288.3(4)	4288.14	4288.3(3)		0.036(5)	0.036(5)	0.097(13)	0.108(11)	0.1	0.097(13)		
4300.88(12)	4300.8(3)	4300.63	4300.11(17)		0.061(6)	0.061(6)	0.164(16)	0.183(15)	0.17	0.164(16)		
4306.3(4)	4307.2(10)	4307.03			0.008(10)		0.02(3)	0.018(14)	0.02			
4312.43(19)	4313.0(4)	4312.83	4312.67(21)		0.046(6)	0.046(6)	0.124(16)	0.143(16)	0.13	0.124(16)		
4329.00(18)	4329.02(15)	4328.85	4328.45(13)	4329.1(20)	0.105(8)	0.105(8)	0.282(22)	0.341(15)	0.31	0.282(22)		0.46
4336.67(20)	4336.7(4)	4336.53	4336.32(23)		0.039(6)	0.039(6)	0.105(16)	0.112(11)	0.1	0.105(16)		
4350.40(12)	4350.49(13)	4350.32	4349.94(22)	4348.8(20)	0.091(13)	0.091(13)	0.24(4)	0.351(14)	0.32	0.24(4)		0.2
4370.46(19)	4370.49(21)	4370.32	4370.32(20)		0.078(12)	0.078(12)	0.21(3)	0.255(15)	0.23	0.21(3)		
4377.29(19)	4377.18(15)	4377.01	4376.56(22)	4376.8(20)	0.119(10)	0.119(10)	0.32(3)	0.385(18)	0.35	0.32(3)		0.25
4395.62(11)	4396.20(15)	4396.03	4395.33(23)	4394.4(20)	0.128(11)	0.128(11)	0.34(3)	0.315(15)	0.29	0.34(3)		0.23
4414.8(3)	4415.1(5)	4414.93	4413.8(6)		0.018(10)	0.018(10)	0.05(3)	0.079(11)	0.07	0.05(3)		
4426.3(4)	4427.6(12)	4427.42			0.014(7)		0.038(19)	0.032(10)	0.03			
4444.47(24)	4444.9(4)	4444.72	4444.31(25)		0.045(7)	0.045(7)	0.121(19)	0.099(11)	0.09	0.121(19)		
4469.71(10)	4469.90(20)	4469.72	4468.98(25)	4471(2)	0.061(8)	0.061(8)	0.164(22)	0.213(13)	0.19	0.164(22)		0.11
4481.98(23)	4482.3(3)	4482.12	4481.9(3)		0.040(7)	0.040(7)	0.108(19)	0.130(11)	0.12	0.108(19)		
4528.35(11)	4528.57(19)	4528.39	4527.9(4)	4527.2(20)	0.071(7)	0.071(7)	0.191(19)	0.200(12)	0.18	0.191(19)		0.19

Energy (keV)					Elemental cross section		Intensity per 100 captures					
Adopted	ENSDF	LANL	Budapest	Lone	Adopted	Budapest	Adopted	ENSDF	LANL	Budapest	BARC	Lone
4547.05(11)	4547.01(11)	4546.82	4546.4(4)	4546.5(20)	0.115(9)	0.115(9)	0.309(24)	0.451(16)	0.41	0.309(24)		0.36
4590.31(11)	4590.2(3)	4590.01	4589.3(4)		0.059(7)	0.059(7)	0.159(19)	0.143(13)	0.13	0.159(19)		
4607.00(7)	4607.03(8)	4606.84	4606.5(3)	4607.1(20)	0.311(13)	0.311(13)	0.84(4)	0.92(3)	0.84	0.84(4)		0.85
4624.29(16)	4623.75(15)	4623.56	4623.1(5)	4622.9(20)	0.104(8)	0.104(8)	0.280(22)	0.334(15)	0.3	0.280(22)		0.2
4646.83(15)	4646.52(18)	4646.33	4645.4(3)	4645.8(20)	0.081(10)	0.081(10)	0.22(3)	0.265(14)	0.24	0.22(3)		0.35
4666.15(10)	4666.18(17)	4665.99	4665.78(19)	4666.8(20)	0.085(8)	0.085(8)	0.229(22)	0.274(14)	0.25	0.229(22)		0.14
4706.11(13)	4706.13(12)	4705.93	4705.8(3)	4705.9(20)	0.137(9)	0.137(9)	0.368(24)	0.395(15)	0.36	0.368(24)		0.19
4719.93(17)	4720.07(25)	4719.87	4718.9(4)		0.045(7)	0.045(7)	0.121(19)	0.155(11)	0.14	0.121(19)		
4731.06(17)	4731.14(15)	4730.94	4730.8(3)	4731.5(20)	0.089(8)	0.089(8)	0.239(22)	0.276(13)	0.25	0.239(22)		0.17
4758.0(6)	4757.4(8)	4757.2	4758.5(4)		0.036(9)	0.036(9)	0.097(24)	0.047(10)	0.04	0.097(24)		
4781.95(17)	4781.9(3)	4781.7	4781.6(4)	4781.4(20)	0.042(9)	0.042(9)	0.113(24)	0.132(10)	0.12	0.113(24)		0.25
4799.75(15)	4799.7(4)	4799.49	4799.2(4)		0.026(7)	0.026(7)	0.070(19)	0.079(9)	0.07	0.070(19)		
4836.00(16)	4835.9(3)	4835.69	4835.83(19)		0.040(5)	0.040(5)	0.108(13)	0.119(9)	0.11	0.108(13)		
4870.06(17)	4870.9(4)	4870.69	4870.4(3)		0.030(6)	0.030(6)	0.081(16)	0.121(13)	0.11	0.081(16)		
4884.30(10)	4884.79(10)	4884.58	4884.22(14)	4884.3(20)	0.237(10)	0.237(10)	0.64(3)	0.783(25)	0.71	0.64(3)	0.668(56)	0.8
4893.76(10)	4893.78(11)	4893.57	4893.23(14)		0.217(11)	0.217(11)	0.58(3)	0.675(23)	0.61	0.58(3)	0.62(11)	
4906.17(7)	4906.16(7)	4905.94	4906.06(17)	4905.4(20)	0.43(3)	0.43(3)	1.16(8)	1.87(4)	1.7	1.16(8)		1.86
4921.85(9)	4922.24(8)	4922.02	4921.74(14)	4921.5(20)	0.285(13)	0.285(13)	0.77(4)	1.01(3)	0.92	0.77(4)		1.01
4946(3)	4946(3)											
4963.11(6)	4963.03(21)	4962.81	4962.84(19)		0.061(7)	0.061(7)	0.164(19)	0.210(13)	0.19	0.164(19)		
5003.24(8)	5003.24(9)	5003.02	5002.70(25)	5002.4(20)	0.264(11)	0.264(11)	0.71(3)	0.799(23)	0.73	0.71(3)		0.55
5040.76(16)	5040.67(17)	5040.44	5040.0(4)	5038.7(20)	0.086(8)	0.086(8)	0.231(22)	0.262(13)	0.24	0.231(22)		0.22
5060.47(9)	5061.9(9)	5061.67			0.020(7)		0.054(19)	0.045(10)	0.04			
5068.69(9)	5068.97(14)	5068.74	5068.5(3)	5069(2)	0.109(10)	0.109(10)	0.29(3)	0.347(14)	0.31	0.29(3)		0.27
5127.84(9)	5127.97(9)	5127.73	5127.4(3)	5128.1(20)	0.205(12)	0.205(12)	0.55(3)	0.527(15)	0.48	0.55(3)		0.35
5140.05(10)	5140.5(4)	5140.26			0.042(6)		0.113(16)	0.096(9)	0.09			
5150.08(9)	5149.89(24)	5149.65	5149.1(3)	5148.3(20)	0.302(13)	0.302(13)	0.81(4)	0.154(10)	0.14	0.81(4)		0.13
5167.5(3)	5168.2(3)	5167.96	5167.4(3)	5166.5(20)	0.068(10)	0.068(10)	0.18(3)	0.304(23)	0.28	0.18(3)		0.38
5181.77(7)	5181.74(7)	5181.5	5181.14(12)	5181.2(20)	0.912(23)	0.912(23)	2.45(6)	2.94(8)	2.67	2.45(6)	2.71(11)	2.65

Energy (keV)					Elemental section	cross	Intensity	per 100	captures			
Adopted	ENSDF	LANL	Budapest	Lone	Adopted	Budapest	Adopted	ENSDF	LANL	Budapest	BARC	Lone
5211.98(6)	5212.7(4)	5212.46	5211.3(3)	5212.6(20)	0.072(11)	0.072(11)	0.19(3)	0.23(3)	0.21	0.19(3)		0.4
5217.09(20)	5217.1(6)	5216.86	5215.76(25)		0.081(10)	0.081(10)	0.22(3)	0.18(3)	0.16	0.22(3)		
5270.15(4)	5270.36(7)	5270.11	5269.92(12)	5269.6(20)	0.404(11)	0.404(11)	1.09(3)	1.15(3)	1.05	1.09(3)	1.58(11)	1.23
5308.80(6)	5308.8(3)	5308.55	5307.8(7)		0.051(9)	0.051(9)	0.137(24)	0.140(12)	0.13	0.137(24)		
5358.44(8)	5358.46(11)	5358.2	5357.98(25)	5357.9(20)	0.160(8)	0.160(8)	0.430(22)	0.488(16)	0.44	0.430(22)		0.44
5370.21(8)	5370.25(10)	5369.99	5369.66(25)	5370.5(20)	0.188(9)	0.188(9)	0.506(24)	0.550(18)	0.5	0.506(24)		0.42
5410.75(16)	5411.3(9)	5411.04			0.015(5)		0.040(13)	0.034(8)	0.03			
5446.36(12)	5446.2(4)	5445.93	5445.7(5)		0.032(7)	0.032(7)	0.086(19)	0.099(10)	0.09	0.086(19)		
5510.56(6)	5510.86(9)	5510.59	5510.29(13)	5509.7(20)	0.163(11)	0.163(11)	0.44(3)	0.544(15)	0.5	0.44(3)		0.54
5567.63(22)	5568.1(5)	5567.82		5567.2(20)	0.048(9)		0.129(24)	0.109(13)	0.1			0.26
5602.97(4)	5602.99(7)	5602.71	5602.39(10)	5602.3(20)	0.434(16)	0.434(16)	1.17(4)	1.30(3)	1.18	1.17(4)	1.29(19)	1.17
5614.67(5)	5614.68(8)	5614.4	5614.04(10)	5613.6(20)	0.399(15)	0.399(15)	1.07(4)	1.14(3)	1.04	1.07(4)	0.829(55)	0.99
5639.03(4)	5639.13(10)	5638.85	5638.55(10)	5638.5(20)	0.379(15)	0.379(15)	1.02(4)	1.06(3)	0.96	1.02(4)	0.96(18)	1.1
5660.93(4)	5660.51(6)	5660.22	5660.68(16)	5659.7(20)	1.89(6)	1.89(6)	5.08(16)	7.85(17)	7.14	5.08(16)	7.35(26)	7.2
5704.28(5)	5704.50(13)	5704.21	5703.67(12)	5702.9(20)	0.177(9)	0.177(9)	0.476(24)	0.516(20)	0.47	0.476(24)		0.51
5742.53(4)	5742.78(6)	5742.48	5742.16(9)	5742.2(20)	0.766(23)	0.766(23)	2.06(6)	2.39(6)	2.17	2.06(6)	2.49(14)	2.1
5782.20(14)	5782.8(10)	5782.5			0.024(9)		0.065(24)	0.054(13)	0.05			
5852.04(5)	5851.99(12)	5851.68	5852.56(23)	5849.5(20)	0.110(10)	0.110(10)	0.30(3)	0.320(12)	0.29	0.30(3)		0.33
5925.89(4)	5925.98(7)	5925.67	5925.39(10)	5925.1(20)	0.643(18)	0.643(18)	1.73(5)	1.99(6)	1.81	1.73(5)	2.43(38)	1.84
5975.98(4)	5976.13(5)	5975.81	5975.60(22)	5975.1(20)	2.9(4)	2.9(4)	7.8(11)	7.59(15)	6.9	7.8(11)	7.28(81)	6.83
6040.60(4)	6040.89(10)	6040.56	6040.05(15)	6039.9(20)	0.166(13)	0.166(13)	0.45(4)	0.576(18)	0.52	0.45(4)		0.56
6110.81(6)	6111.01(8)	6110.68	6110.59(25)	6109.7(20)	0.213(11)	0.213(11)	0.57(3)	0.597(16)	0.54	0.57(3)		0.62
6149.99(7)	6150.06(9)	6149.72	6149.46(13)	6148.9(20)	0.186(9)	0.186(9)	0.500(24)	0.513(14)	0.47	0.500(24)		0.28
6274.84(3)	6275.16(10)	6274.81	6274.7(3)	6275.2(20)	0.222(11)	0.222(11)	0.60(3)	0.708(21)	0.64	0.60(3)		0.68
6283.91(4)	6284.28(10)	6283.93	6283.7(3)	6282.8(20)	0.204(11)	0.204(11)	0.55(3)	0.666(20)	0.61	0.55(3)		0.54
6341.01(6)	6341.3(3)	6340.94	6340.3(12)		0.019(6)	0.019(6)	0.051(16)	0.088(8)	0.08	0.051(16)		
6359.09(4)	6359.9(8)	6359.54			0.014(5)		0.038(13)	0.033(7)	0.03			
6485.99(3)	6486.61(6)	6486.23	6486.17(13)	6485.9(20)	2.32(5)	2.32(5)	6.24(13)	6.88(13)	6.25	6.24(13)	6.68(46)	6.42
6706.01(3)	6706.22(7)	6705.82	6705.52(10)	6705.8(20)	3.02(6)	3.02(6)	8.12(16)	8.29(20)	7.54	8.12(16)	7.1(43)	7.43

Energy (keV)					Elemental cross section		Intensity	per 100	captures			
Adopted	ENSDF	LANL	Budapest	Lone	Adopted	Budapest	Adopted	ENSDF	LANL	Budapest	BARC	Lone
6877.16(3)	6877.40(7)	6876.98	6876.76(11)	6876.8(20)	3.02(6)	3.02(6)	8.12(16)	9.26(20)	8.42	8.12(16)	8.85(84)	8.21
6948.87(3)	6948.97(11)	6948.54	6948.3(4)	6948.1(20)	0.249(11)	0.249(11)	0.67(3)	0.755(25)	0.69	0.67(3)	0.89(17)	0.73
6985.41(3)	6985.61(6	6985.17	6984.9(4)	6984.9(20)	1.05(13)	1.05(13)	2.8(4)	3.04(7)	2.76	2.8(4)	3.35(29)	2.97
7055.92(3)	7056.11(7)	7055.66	7055.43(12)	7055.6(20)	0.666(19)	0.666(19)	1.79(5)	1.94(4)	1.76	1.79(5)	1.942(96)	1.81
7203.22(3)	7203.45(12)	7202.99	7203.02(13)		0.369(16)	0.369(16)	0.99(4)	0.94(3)	0.85	0.99(4)	1.01(16)	
7214.42(3)	7214.79(7)	7214.32	7214.09(12)	7213.7(20)	1.38(3)	1.38(3)	3.71(8)	4.07(9)	3.7	3.71(8)	4.44(16)	4.72
7433.07(3)	7433.34(12)	7432.85	7432.40(22)	7433.6(20)	0.083(7)	0.083(7)	0.223(19)	0.240(9)	0.22	0.223(19)		0.28
7491.54(3)	7491.99(8)	7491.49	7491.29(12)	7490.8(20)	1.16(3)	1.16(3)	3.12(8)	3.17(8)	2.88	3.12(8)	3.26(28)	2.99
No. γ							337	335	333	302	48	113
Σ Iγ							242	252	276	237	171	201
%Sn							87	98	89	85	66	79

4. New binding energies and cross sections

As illustrated in the previous section, the new discrete capture gamma data are fairly complete for light nuclei. Therefore, it was is possible to infer new binding energy and capture cross section values and compare them with recent evaluated data, independent from the present data set. The results are summarised in Table 4 for elements up to calcium, Z=20 [20].

The neutron separation energies S_n were determined from the adopted level schemes, constructed in a way described in this document. They agree well with those from the 1995 mass evaluation by Audi and Wapstra [21], and are generally more precise.

The capture cross sections have been obtained as the sum of partial production cross sections of all gamma rays populating the ground state of the particular nuclide. As the ground state feedings are often fairly complete even for heavier nuclei, it was expected that the procedure would provide more accurate cross sections than available before, at least for light nuclei. In the rightmost column of Table 4 the adopted values from Ref. [20] are compared with the new evaluation by Mughabghab [22].

Inspection of the cross sections shows that the agreement is fairly good, and even the precision has been improved in a number of cases. Significant deviations are observed for nuclides with low capture cross section or low abundance (e.g., ^{40}K). For example, the ^{6}Li value deviates strongly, while the ^{7}Li value coming from the same experiment with a natural target is in excellent agreement with the evaluated value. It should be noted that the ^{6}Li(n,α) reaction has orders of magnitude higher cross section than the ^{6}Li(n,γ) reaction, that might be the cause for the discrepancy. Another notable case is ^{12}C, for which the new value is larger than the evaluated value [22] by 11 %, which is a rather unexpected finding.

In view of the importance of the carbon cross section, new experiments were undertaken at Budapest to test the accuracy of the present adopted value. The cross section can be obtained by summing the partial production cross sections for the 3089 keV, 3684 keV and 4945 keV ground-state transitions. Experiments with 4 different compounds containing carbon with a well-defined stoichiometric ratio yielded 3.87(5) mb for ^{12}C, which is the same as before, with improved precision. From the most recent JAERI k_0-factors for the 3684 keV and 4945 keV gamma rays [19] (with the 0.4 % contribution of the weak 3089 keV gamma ray added) one gets 3.63(13) mb for the cold guide and 4.01(15) mb for the thermal guide measurement. The average of these two values is 3.79(19) mb, in excellent agreement with the Budapest number. The weighted average of all three new values is 3.85(5) mb, which is still larger than the Mughabghab value by 9 %, suggesting reconsideration of the standard cross section for the ^{12}C(n,γ) reaction.

Table 4. Inferred neutron binding energies and capture cross sections for the isotopes of light elements as compared to recent evaluated values

Target isotope	Abundance (%) Rosman [23]	S_n (keV) Audi [21]	New value	σ (mb) Mughabghab [22]	New value
^{1}H	99.9885(70)	2224.5725(22)	2224.576(19)	332.6(7)	standard
^{2}H	0.0115(70)	6257.2482(24)		0.519(7)	0.492(25)
^{3}He	0.000137(3)	20577.62		0.031(9)	
^{4}He	99.999863(3)			0	
^{6}Li	7.59(4)	7249.96(9)	7249.94(4)	38.6(36)	52.6(22)*
^{7}Li	92.41(4)	2033.8(3)	2032.57(4)	45.4(30)	45.7(9)
^{9}Be	100	6812.33(6)	6812.10(3)*	8.77(35)	8.8(6)
^{10}B	19.9(7)	11454.12(20)	11454.15(14)	500(100)	303(20)
^{10}B(n,α)				3837(9)b$^\#$	3820(135)b
^{11}B	80.1(7)	3370.4(14)		5.5(33)	
^{12}C	98.93(8)	4946.310(10)	4946.311(3)	3.53(5)	3.87(6)*
^{13}C	1.07(8)	8176.440(18)	8176.61(18)	1.37(4)	1.22(11)
^{14}N	99.632(7)	10833.230(10)	10833.317(12)*	79.8(14)	79.0(9)
^{15}N	0.368(7)	2490.8(23)		24(8)	
^{16}O	99.757(16)	4143.33(21)	4143.06(10)	0.190(19)	0.189(8)
^{17}O	0.038(1)	8044.4(8)		0.538(65)	
^{18}O	0.205(14)	3957(3)		0.16(1)	
^{19}F	100	6601.31(5)	6601.344(16)	9.6(5)	9.50(11)
^{20}Ne	90.48(3)	6761.11(4)	6761.19(5)	37(4)	
^{21}Ne	0.27(1)			666(110)	
^{22}Ne	9.25(3)	5200.62(12)	5200.64(17)	45.5(60)	
^{23}Na	100	6959.44(5)	6959.592(15)*	530(5)	529(7)
^{24}Mg	78.99(4)	7330.67(4)	7330.53(4)*	53.6(15)	53.7(14)
^{25}Mg	10.00(1)	11093.09(4)	11093.157(21)	200(5)	193(2)
^{26}Mg	11.01(3)	6443.35(4)	6443.35(3)	38.6(60)	37.7(13)
^{27}Al	100	7725.05(6)	7725.170(4)*	231(3)	233.6(16)
^{28}Si	92.2297(7)	8473.56(3)	8473.537(23)	177(5)	186(3)
^{29}Si	4.6832(5)	10609.18(3)	10609.23(3)	119(3)	118(3)
^{30}Si	3.0872(5)	6587.40(5)	6587.39(3)	107(2)	116(3)*
^{31}P	100	7935.65(4)	7935.596(23)	172(6)	163(2)
^{32}S	94.93(31)	8641.58(3)	8641.809(25)*	548(10)	536(8)
^{33}S	0.76(2)	11416.94(5)	11417.219(16)*	454(25)	461(15)
^{34}S	4.29(28)	6985.84(4)	6986.091(15)*	235(5)	279(7)*
^{36}S	0.02(1)	4303.58(9)	4303.608(25)	230(20)	170(40)
^{35}Cl	75.78(4)	8579.70(7)	8579.672(18)	43.55(40) b	43.1(5) b
^{37}Cl	24.22(4)	6107.78(10)	6107.73(9)	430(6)	552(20)*
^{39}K	93.2581(44)	7799.50(8)	7799.558(14)	2.1(2) b	2.19(3) b
^{40}K	0.0117(1)	10095.18(10)	10095.255(15)	30(4)	96(15)*
^{41}K	6.7302(44)	7533.77(15)	7533.822(10)	1.45(3) b	1.64(6) b*
^{40}Ca	96.941(6)	8363.7(3)	8362.86(5)*	410(20)	410(7)
^{42}Ca	0.647(23)	7933.0(3)	7932.65(15)	680(70)	740(40)
^{43}Ca	0.135(10)	11132.0(7)	11131.45(14)	6.2(6) b	7.3(5) b
^{44}Ca	2.09(11)	7414.8(3)	7414.79(15)	880(50)	1053(25)*
^{46}Ca	0.004(3)	7276.1(5)	7276.1(3)	720(30)	
^{48}Ca	0.187(21)	5146.6(4)	5146.48(21)	1.09(7) b	1.05(12) b

$^\#$ Obtained with 0.93722(11) for the γ branching ratio [24].
* More than 2σ deviation.

References

[1]   ACHARYA, R.N., SUDARSHAN, K., NAIR, A.G.C., SCINDIA, Y.M., GOSWAMI, A., REDDY, A.V.R., MANOHAR, S.B., Measurement of k0-factors in prompt gamma-ray neutron activation analysis, J. Radioanal. Nucl. Chem. 250 (2001) 303-307.

[2]   SUDARSHAN, K., ACHARYA, R.N., NAIR, A.G.C., SCINDIA, Y.M., GOSWAMI, A., REDDY, A.V.R., MANOHAR, S.B., Determination of Prompt k0-Factors in PGNAA, in Summary Rept of 2nd Res. Coord. Mtg of CRP on Development of a Database for Prompt Gamma-Ray Neutron Activation Analysis, Report INDC(NDS)-424, International Atomic Energy Agency, Vienna (2001) pp. 39-50.

[3]   SUDARSHAN, K., NAIR, A.G.C., ACHARYA, R.N., SCINDIA, Y.M., REDDY, A.V.R., MANOHAR, S.B., GOSWAMI, A., Capture gamma-rays from Co-60 as multi gamma-ray efficiency standard for prompt gamma-ray neutron activation analysis, Nucl. Instrum. Meth. A 457 (2001) 180-186.

[4]   SUN, G.M., BYUN, S.H., CHOI, H.D., Prompt k0-factors and relative g-emission intensities for the strong non-1/v absorbers 113Cd, 149Sm, 151Eu and !55,157Gd, J. Radioanal. Nucl. Chem. (in press).

[5]   VUONG HUU TAN, NGUYEN CANH HAI, NGUYEN XUAN QUY, LE NGOC CHUNG, Evaluation and Measurement of Prompt k0-Factors to Use in Prompt Gamma-Ray Neutron Activation Analysis, in Summary Rept of 2nd Res. Coord. Mtg of CRP on Development of a Database for Prompt Gamma-Ray Neutron Activation Analysis, Report INDC(NDS)-424, International Atomic Energy Agency, Vienna (2001) pp. 33-38.

[6]   MOLNÁR, G.L., RÉVAY, Z., BELGYA, T., Wide energy range effciency calibration method for Ge detectors, Nucl. Instrum. Meth. A 489 (2002) 140-159.

[7]   KRUSCHE, B., LIEB, K.P., DANIEL, H., VON EGIDY, T., BARREAU, G., BÖRNER,
H.G., BRISSOT, R., HOFMEYR, C., RASCHER, R., Gamma-ray energies and 36Cl level scheme from the reaction 35Cl(n,g), Nucl. Phys. A 386 (1982) 245-268.

[8]   MOLNÁR, G.L., RÉVAY, Z., PAUL, R.L., LINDSTROM, R.M., Prompt-gamma activation analysis using the k(0) approach, J. Radioanal. Nucl. Chem. 234 (1998) 21-26.

[9]   RÉVAY, Z., MOLNÁR, G.L., BELGYA, T., KASZTOVSZKY, Z., FIRESTONE, R.B., A new gamma-ray spectrum catalog for PGAA, J. Radioanal. Nucl. Chem. 244 (2000) 383-389.

[10]   RÉVAY, Z., MOLNÁR, G.L., Characterisation of neutron beam and gamma spectrometer for PGAA, in Summary Rept of 2nd Res. Coord. Mtg of CRP on Development of a Database for Prompt Gamma-Ray Neutron Activation Analysis, Report INDC(NDS)-424, International Atomic Energy Agency, Vienna (2001) pp. 57-68.

[11]   FIRESTONE, R.B., RÉVAY, Z., MOLNÁR, G.L., New capture gamma-ray library and atlas of spectra for all elements, Proc. 11th Int. Symp. on Capture Gamma-Ray Spectroscopy and Related Topics, World Scientific, Singapore (2003).

[12]   MOLNÁR, G.L., RÉVAY, Z., BELGYA, T., FIRESTONE, R.B., The new prompt gamma-ray catalogue for PGAA, Appl. Radiat. Isotopes 53 (2000) 527-533.

[13]   RÉVAY, Z., MOLNÁR, G.L., BELGYA, T., KASZTOVSZKY, Z., FIRESTONE, R.B., A new gamma-ray spectrum catalog and library for PGAA, J. Radioanal. Nucl. Chem. 248 (2001)
395-399.

[14]   RÉVAY, Z., MOLNÁR, G.L., Standardisation of the prompt gamma activation analysis method, Radiochim. Acta (in press).

[15] RÉVAY, Z., MOLNÁR, G.L., BELGYA, T., KASZTOVSZKY, Z., In-beam determination of k0 factors of short-lived nuclides, J. Radioanal. Nucl. Chem. (in press).

[16] LONE, M.A., LEAVITT, R.A., HARRISON, D.A., Prompt Gamma Rays from Thermal-Neutron Capture, Atom. Data Nucl. Data Tables 26 (1981) 511-559.

[17] PAUL, R.L., LINDSTROM, R.M., Measurement of k0-Factors for Prompt Gamma-Ray Activation Analysis, Proc. Second International k0 Users Workshop, Jozef Stefan Institute, Ljubljana, Slovenia (1997) pp. 54-57.

[18] MATSUE, H., YONEZAWA, C., Neutron spectrum correction of k0-factors for k0-based neutron induced prompt gamma-ray analysis, J. Radioanal. Nucl. Chem. 255 (2003) 125-129.

[19] MATSUE, H., YONEZAWA, C., Measurement and evaluation of k0 factors for PGA at JAERI, J. Radioanal. Nucl. Chem. (in press)

[20] MOLNÁR, G.L., RÉVAY, Z., BELGYA, T., FIRESTONE, R.B., New Catalog of Neutron Capture g Rays for Prompt Gamma Activation Analysis, J. Nucl. Sci. Technol. (Japan), Supplement (2002)

[21] AUDI, G., WAPSTRA, A.H., The 1995 update to the atomic mass evaluation, Nucl. Phys. A 595 (1995) 409-480.

[22] MUGHABGHAB, S.F., Thermal neutron capture cross cections, resonance integrals and
g-factors, Report INDC(NDS)-440, International Atomic Energy Agency, Vienna (2003).

[23] ROSMAN, K.J.R., TAYLOR, P.D.P., Isotopic compositions of the elements 1997, J. Phys. Chem. Ref. Data 27 (1998) 1275-1287.

[24] CONDÉ, H., Nuclear Data Standards for Nuclear Measurements, 1991 NEANDC/INDC Nuclear Standards File, Report NEANDC-311 U, INDC(SEC)-101, OECD Nuclear Energy Agency, Paris (1992).